

# **Physical Oceanographic Conditions on the Newfoundland and Labrador Shelf during 2022**

Frédéric Cyr, Jonathan Coyne, Steve Snook, Charlie Bishop, Peter S. Galbraith, Nancy Chen and Guoqi Han

Northwest Atlantic Fisheries Centre  
Fisheries and Oceans Canada  
80 East White Hills Road  
St. John's, NL  
A1C 5X1, Canada

2024

**Canadian Technical Report of  
Hydrography and Ocean Sciences 377**



Fisheries and Oceans  
Canada      Pêches et Océans  
                  Canada

**Canada**

## **Canadian Technical Report of Hydrography and Ocean Sciences**

Technical reports contain scientific and technical information of a type that represents a contribution to existing knowledge but which is not normally found in the primary literature. The subject matter is generally related to programs and interests of the Oceans and Science sectors of Fisheries and Oceans Canada.

Technical reports may be cited as full publications. The correct citation appears above the abstract of each report. Each report is abstracted in the data base *Aquatic Sciences and Fisheries Abstracts*.

Technical reports are produced regionally but are numbered nationally. Requests for individual reports will be filled by the issuing establishment listed on the front cover and title page.

Regional and headquarters establishments of Ocean Science and Surveys ceased publication of their various report series as of December 1981. A complete listing of these publications and the last number issued under each title are published in the *Canadian Journal of Fisheries and Aquatic Sciences*, Volume 38: Index to Publications 1981. The current series began with Report Number 1 in January 1982.

## **Rapport technique canadien sur l'hydrographie et les sciences océaniques**

Les rapports techniques contiennent des renseignements scientifiques et techniques qui constituent une contribution aux connaissances actuelles mais que l'on ne trouve pas normalement dans les revues scientifiques. Le sujet est généralement rattaché aux programmes et intérêts des secteurs des Océans et des Sciences de Pêches et Océans Canada.

Les rapports techniques peuvent être cités comme des publications à part entière. Le titre exact figure au-dessus du résumé de chaque rapport. Les rapports techniques sont résumés dans la base de données *Résumés des sciences aquatiques et halieutiques*.

Les rapports techniques sont produits à l'échelon régional, mais numérotés à l'échelon national. Les demandes de rapports seront satisfaites par l'établissement auteur dont le nom figure sur la couverture et la page de titre.

Les établissements de l'ancien secteur des Sciences et Levés océaniques dans les régions et à l'administration centrale ont cessé de publier leurs diverses séries de rapports en décembre 1981. Vous trouverez dans l'index des publications du volume 38 du *Journal canadien des sciences halieutiques et aquatiques*, la liste de ces publications ainsi que le dernier numéro paru dans chaque catégorie. La nouvelle série a commencé avec la publication du rapport numéro 1 en janvier 1982.

Canadian Technical Report  
of Hydrography and Ocean Sciences 377

2024

Physical Oceanographic Conditions on the Newfoundland and Labrador Shelf during 2022

Frédéric Cyr<sup>1</sup>, Jonathan Coyne<sup>1</sup>, Steve Snook<sup>1</sup>, Charlie Bishop<sup>1</sup>, Peter S. Galbraith<sup>2</sup>,  
Nancy Chen<sup>3</sup>, and Guoqi Han<sup>3</sup>

<sup>1</sup> Northwest Atlantic Fisheries Centre, Fisheries and Oceans Canada, 80 East White Hills Road,  
St. John's, NL, A1C 5X1, Canada

<sup>2</sup> Maurice-Lamontagne Institute, Fisheries and Oceans Canada, 850 Rte de la Mer,  
Mont-Joli, QC, G5H 4Z4, Canada

<sup>3</sup>Institute of Ocean Sciences, Fisheries and Oceans Canada, 9860 West Saanich Road,  
Sidney, BC, V8L 4B2, Canada

© His Majesty the King in Right of Canada, as represented by the Minister of the Department of Fisheries and Oceans, 2024

Cat. No. Fs97-18/377E-PDF

ISBN 978-0-660-71446-2

ISSN 1488-5417

Correct citation for this publication:

Cyr, F., Coyne, J., Snook, S., Bishop, C., Galbraith, P.S., Chen, N., Han, G. 2024. Physical Oceanographic Conditions on the Newfoundland and Labrador Shelf during 2022. Can. Tech. Rep. Hydrogr. Ocean Sci. 377: iv + 53 p.

## **1 Contents**

1	Introduction.....	1
2	Meteorological conditions .....	3
3	Sea ice conditions .....	8
4	Icebergs.....	16
5	Satellite sea-surface temperature .....	17
6	Ocean conditions on the Newfoundland and Labrador shelf.....	20
6.1	Long-term observations at Station 27 .....	20
6.2	Standard hydrographic sections .....	30
6.2.1	Temperature and Salinity Variability.....	30
6.2.2	Cold Intermediate Layer Variability .....	33
6.3	Bottom observations in NAFO sub-areas.....	36
6.3.1	Spring Conditions .....	37
6.3.2	Fall Conditions.....	41
6.3.3	Summary of bottom temperatures.....	44
7	Labrador Current transport .....	45
8	Summary .....	48
8.1	Highlights of 2022.....	50
9	Acknowledgements.....	50
	References.....	51

## ABSTRACT

Cyr, F., Coyne, J., Snook, S., Bishop, C., Galbraith, P.S., Chen, N., Han, G. 2024. Physical Oceanographic Conditions on the Newfoundland and Labrador Shelf during 2022. Can. Tech. Rep. Hydrogr. Ocean Sci. 377: iv + 53 p.

An overview of physical oceanographic conditions in the Newfoundland and Labrador (NL) Region during 2022 is presented in support of the Atlantic Zone Monitoring Program. The winter North Atlantic Oscillation index, a key indicator of the direction and intensity of the winter wind field patterns over the Northwest Atlantic was positive in 2022. Since 2014, all years except 2021 were positive (normally indicative of colder conditions). The large majority of the environmental parameters presented in this report were however above normal in 2022 (normal being defined as the average over the 1991–2020 climatological period), except for sea ice and the cold intermediate layer area that were normal. Sea surface temperatures were at record-warm over the zone in 2022 (beating 2021), also establishing new monthly and seasonal records across the different Northwest Atlantic Fisheries Organization divisions analyzed, while bottom temperatures were the third warmest of time series after 2021 and 2011. The transport on the Scotian Slope was normal for the second time only since 2014 (last time was in 2019). On the NL slope, the transport was back to positive anomalies after three years being normal. The NL Climate index was at +0.7 in 2022.

## RÉSUMÉ

Cyr, F., Coyne, J., Snook, S., Bishop, C., Galbraith, P.S., Chen, N., Han, G. 2024. Physical Oceanographic Conditions on the Newfoundland and Labrador Shelf during 2022. Can. Tech. Rep. Hydrogr. Ocean Sci. 377: iv + 53 p.

Un sommaire des conditions océanographiques physiques pour la région de Terre-Neuve et Labrador (TNL) en 2022 est présenté dans le cadre du Programme de Monitorage de la Zone Atlantique. L'Oscillation Nord-Atlantique, un indicateur clé pour la direction et l'intensité des champs de vents hivernaux au-dessus de l'Atlantique nord-ouest, était positive en 2022 (normalement indicatif de conditions froides). Depuis 2014, seulement 2021 a été négative. La grande majorité des indices environnementaux présentés dans ce rapport étaient au-dessus de la normale en 2022 (la normale étant définie comme la moyenne sur la période climatologique 1991-2021), à l'exception de la glace de mer et de l'aire de la couche intermédiaire froide Les températures de surface de la mer ont établis de nouveaux records chauds pour la zone en 2022 (en battant 2021). Ceci inclus de nombreux records mensuels et saisonniers pour les différentes divisions de l'Organisation des pêches de l'Atlantique nord-ouest analysées. Les températures au fond ont été les troisièmes plus chaudes enregistrées après 2021 et 2011. Le transport le long du talus néo-écossais était normal pour la deuxième fois seulement depuis 2014 (la dernière fois étant en 2019). Sur le talus de TNL, le transport était de retour vers des anomalies positives après avoir été normal durant les trois dernières années. L'indice du climat de TNL était à +0.7 en 2022.

# 1 Introduction

This manuscript presents an overview of the 2022 environmental and physical oceanographic conditions in the Newfoundland and Labrador (NL) Region (Figure 1), in support of the Fisheries and Oceans Canada (DFO) Atlantic Zone Monitoring Program (AZMP; Therriault et al., 1998). This report complements similar reviews of the environmental conditions in the Gulf of St. Lawrence (Galbraith et al., 2023) and the Scotian Shelf and Gulf of Maine (Hebert et al., 2023). Physical oceanographic conditions for the NL region in 2021 were presented in Cyr et al., (2022).

The information presented in this report is derived from various sources:

1. Ice data from the Canadian Ice Service, while meteorological data are from Environment and Climate Change (ECCC) Canada and other sources cited in the text.
2. Sea Surface Temperatures (SSTs) (Galbraith et al., 2021). These correspond to a blend of Advanced Very High Resolution Radiometer (AVHRR) data from Pathfinder version 5.3 (1982–2014), the Maurice Lamontagne Institute (1985–2013) and the GHRSST NOAA/STAR L3S-LEO-Daily (2007–present). See Galbraith et al., (2021, 2023) for a description.
3. Observations made throughout the year at monitoring Station 27 near St. John's, NL;
4. Measurements made along standard AZMP cross-shelf sections (see map Figure 1);
5. Oceanographic observations made during spring and fall multi-species resource assessment surveys;
6. Other multi-source historical data (ships of opportunity, international campaigns, surveys from other DFO regions, the Argo program, etc.);

All vertical profiles of temperature and salinity used in this report (e.g. points 3-6 above) are available at <https://doi.org/10.20383/102.0739> [consulted 2023-09-15] (Coyne et al., 2023).

Time series of temperature, salinity and other climate indices anomalies were constructed by subtracting the average computed over a standard climatological period from 1991 to 2020. When a variable is measured throughout the seasonal cycle (e.g. air temperature, station 27 observations), the annual anomaly is calculated as the average of monthly anomalies. Unless otherwise specified, annual or seasonal anomalies were normalized by dividing the values by the standard deviation (SD) of the data time series over the climatological period. A value of 2, for example, indicates that the index was 2 SD higher than its long-term average. As a general guide, anomalies within  $\pm 0.5$  SD are considered to be normal.

The normalized values of water properties and derived climate indices are presented as “scorecards”, which are color-coded gradations of 0.5 SD (Figure 2). Shades of blue represent cold environmental conditions and red represent warm conditions. In some instances, such as for the North Atlantic Oscillation (NAO), or for ice and cold intermediate layer (CIL) properties, negative anomalies indicate warm conditions, and are therefore colored red. Most of the colormaps used in this report are taken from the *cmocean* colormaps package for oceanography (Thyng et al., 2016).

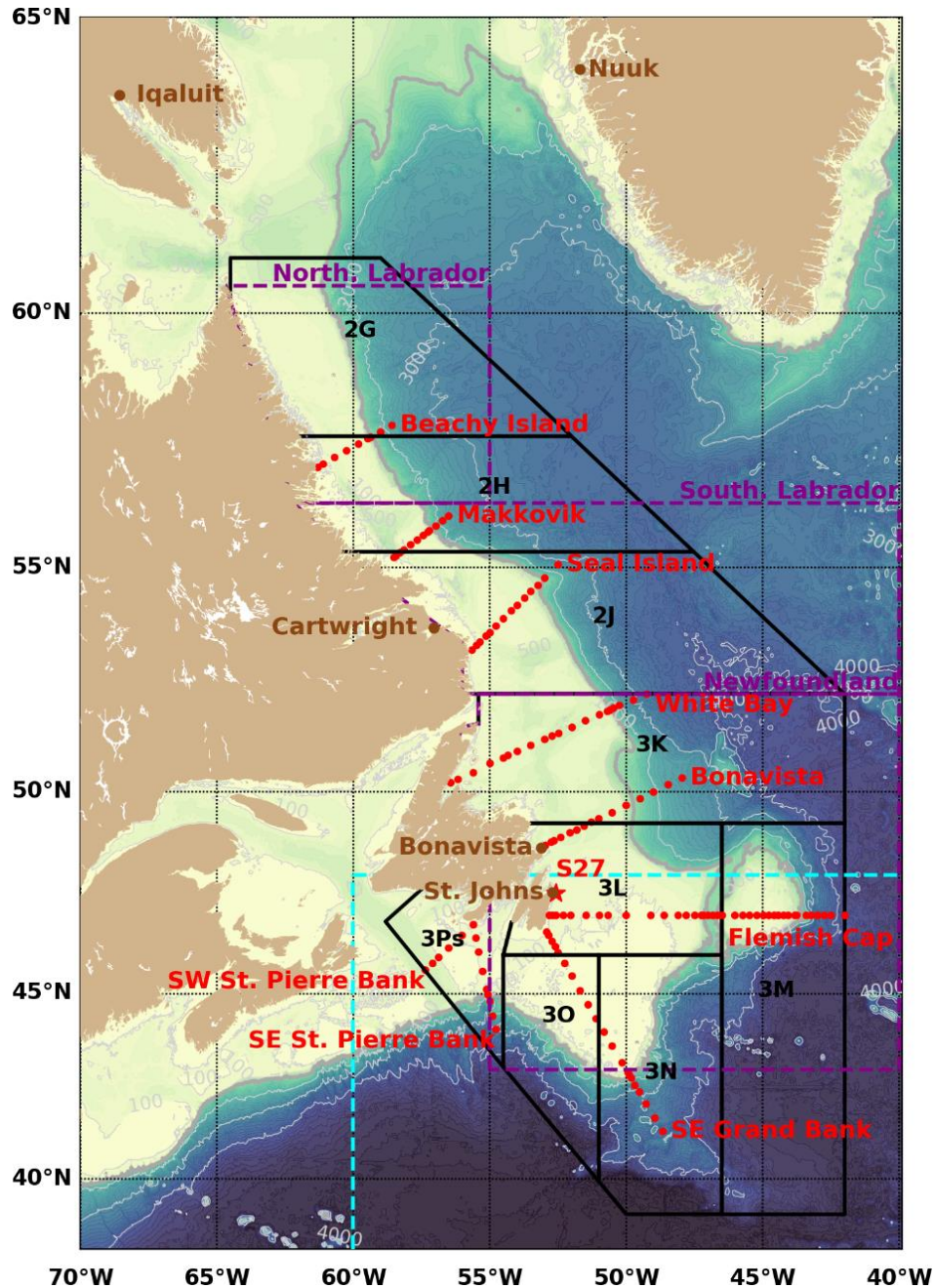


Figure 1: Map of the Northwest Atlantic Ocean, including important bathymetric features (the gray isobaths are identified on the figure). NAFO Divisions (sub-areas 2 and 3) on the Newfoundland and Labrador (NL) shelf are drawn. (black boxes) The AZMP hydrographic sections are shown with red dots, and their names labeled in red text on the figure. Long-term AZMP hydrographic Station 27 is highlighted with a red star. The five stations used for the air temperature time series are shown in brown. The three regions used for sea ice calculations (Northern Labrador shelf, Southern Labrador shelf and Newfoundland shelf) are drawn with dashed magenta lines. The region used by the International Ice Patrol for iceberg sightings south of 48°N is drawn in dashed cyan. The shelf break is delimited by a thicker and darker gray contour corresponding to the isobath 1,000 m (used to clip the SST and bottom temperature).

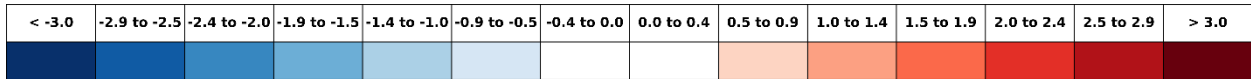


Figure 2: Color scale used for the presentation of normalized anomalies. Color levels are incremented by 0.5 standard deviations (SD), where blue is below normal and red above normal. Values between 0 and  $\pm 0.5$  SD remain white indicating normal conditions. Anomalies are rounded to the nearest tenth.

## 2 Meteorological conditions

The North Atlantic Oscillation (NAO; see Figure 3 for time series since 1951 and Figure 4 for tabulated values since 1980) refers to the anomaly in the sea-level pressure (SLP) difference between the subtropical high (average location near the Azores) and the subpolar low (average location near Iceland). Several definitions of the NAO exist, though the one used here is from the National Center for Environmental Information of the National Oceanic and Atmospheric Administration (NOAA) available [online](#). The winter NAO (defined here as the average of monthly values from December to March) is considered a measure of the strength of the winter westerly and northwesterly winds over the Northwest Atlantic. A high NAO index (positive phase) occurs during an intensification of the Icelandic Low and Azores High. Except for some years for which the SLP patterns are spatially shifted (e.g., 1999, 2000, and 2018), positive winter NAO years favor strong northwesterly winds, cold air and sea surface temperatures (SSTs), and heavy ice conditions on the NL shelves (Colbourne et al., 1994; Drinkwater et al., 1994; Petrie et al., 2007). After being negative for the first time in seven years in 2021 (-0.1), the winter NAO index was back to positive in 2022 (+1.0; first row in Figure 4). While the lowest winter NAO index value was reached in 2010, all years between 2012 and 2020 (except 2013) were positive, including the record high of +1.6 in 2015.

The Arctic Oscillation (AO) is a larger scale index intimately linked with the NAO. During a positive phase, the Arctic air outflow to the Northwest Atlantic increases, resulting in colder winter air temperatures over much of NL and adjacent shelf regions. The AO was slightly positive in 2022 at +0.1 (Figure 4). In 2015, the AO was at its highest value since 1990 at +0.6. A record low was reached in 2010 when it was below normal at -1.5 (warm air temperatures).

The Atlantic Multidecadal Oscillation (AMO) is also provided in Figure 4. This index, based on the Sea Surface Temperature of the Atlantic Ocean, evolves as part of a 65–80 years cycle that influences the regional climate and has consequences on the ocean circulation in the North Atlantic (e.g., Kerr, 2000). The AMO has been in a positive phase since the late 1990s.

Air temperature anomalies (winter and annual values) from five coastal communities around the Northwest Atlantic (Nuuk, Greenland; Iqaluit on Baffin Island, Nunavut; Cartwright, Labrador; Bonavista and St. John's in Newfoundland; see Figure 1) are shown in Figure 4 as normalized anomalies between 1980 and 2022, and in Figure 6 and Figure 5 as annual and monthly (cumulative for all stations) anomalies, respectively. Except for Nuuk for which data are obtained from the Danish Meteorological Institute, the air temperature data from Canadian sites are from the second generation of Adjusted and Homogenized Canadian Climate Data (AHCCD), which accounts for shifts in station location and changes in observation methods (Vincent et al., 2012). Because the AHCCD product was not ready for the year 2022, historical data from the Government of Canada Monthly Climate Summaries have been used for that year.

In 2022, the air temperature was normal or close to normal in northern sites (Cartwright, Iqaluit and Nuuk) and above normal in Newfoundland (Bonavista and St. John's), both during the winter and for the

annual average (Figure 4). Temperatures were especially cold at the northern sites in February and warm at all sites in December (Figure 5). Averaged over the year, the air temperatures were above normal, making 2022 the 5<sup>th</sup> warmest year since 1950 at +0.8 SD (Figure 5). 2010 was the warmest year at +2.1 SD, and all of the warmest 5 years have happened since 2005.

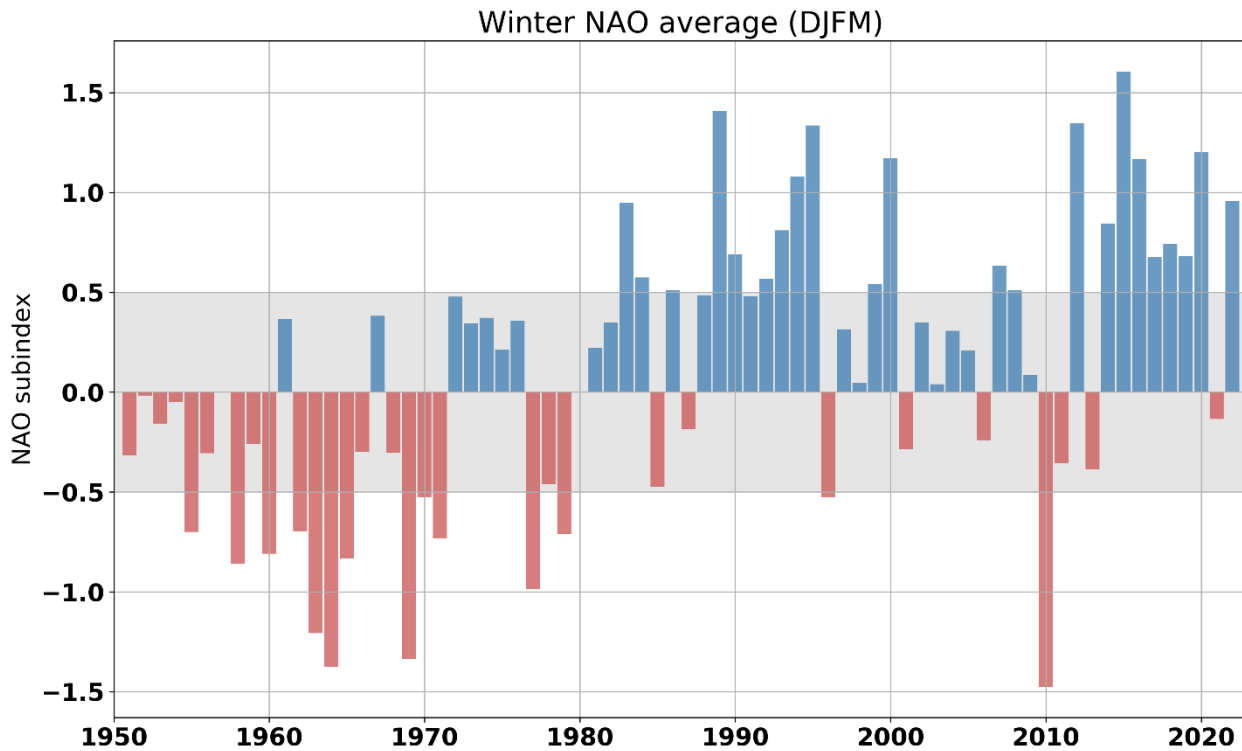
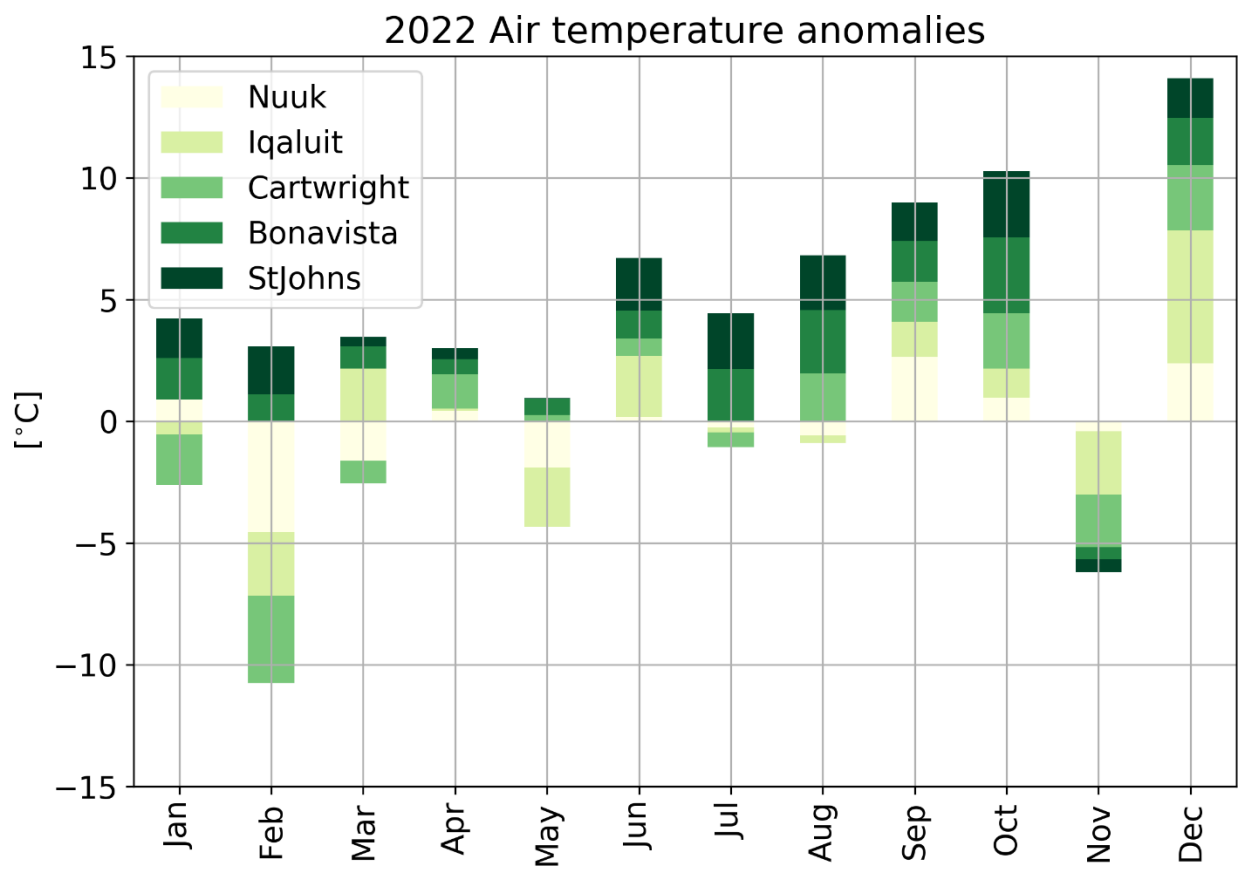


Figure 3: Winter North Atlantic Oscillation (NAO) Index calculated by averaging the December to March values since 1951 (which correspond to the average of December 1950 and January-March 1951). The NAO Index used here is from the National Center for Environmental Information of the NOAA. This index is used as part of the NL climate index mentioned in the summary (Figure 39).

	-- Climate indices --																								$\bar{x}$	sd																			
	80	81	82	83	84	85	86	87	88	89	90	91	92	93	94	95	96	97	98	99	00	01	02	03	04	05	06	07	08	09	10	11	12	13	14	15	16	17	18	19	20	21	22	$\bar{x}$	sd
NAO <sub>winter</sub>	0.0	0.2	0.3	0.9	0.6	0.5	0.5	-0.2	0.5	1.4	0.7	0.5	0.6	0.8	1.3	1.3	0.5	0.2	0.0	0.5	1.2	0.3	0.4	0.0	0.3	0.2	0.2	0.6	0.5	0.1	1.5	0.4	1.3	0.4	0.8	1.6	1.2	0.7	0.7	0.7	1.2	0.1	1.0		
AO	-0.6	-0.4	0.3	0.0	-0.2	-0.5	0.1	-0.5	0.0	1.0	1.0	0.2	0.4	0.1	0.5	-0.3	-0.5	0.0	0.3	0.1	0.0	-0.2	0.1	0.2	-0.2	-0.4	0.1	0.3	0.2	-0.3	-1.0	0.5	-0.2	0.0	-0.1	0.6	-0.1	0.3	0.2	0.1	0.8	-0.1	0.1		
AMO	0.0	-0.1	-0.2	-0.1	-0.2	-0.3	-0.3	0.0	0.0	-0.1	-0.1	-0.2	-0.3	-0.2	-0.2	-0.1	-0.1	0.0	0.3	0.1	0.0	0.0	0.2	0.0	0.2	0.1	0.3	0.1	0.0	0.1	0.3	0.0	0.0	0.1	0.3	0.0	0.2	0.2	0.2						
	-- Winter Air Temperature --																																												
Nuuk	0.8	0.2	0.0	-3.0	-3.6	0.4	2.2	-0.4	0.4	-1.4	-1.4	-2.5	-0.7	-1.3	0.4	0.1	-0.1	-0.3	0.1	0.2	0.1	0.9	1.3	0.3	0.6	1.0	-1.5	0.6	2.3	1.3	-0.1	0.5	0.1	-1.0	0.1	0.1	-0.5	1.1	-0.5	0.9	0.0	-7.2	2.2		
Iqaluit	0.4	0.8	0.9	-2.3	-2.0	0.6	1.7	-1.3	-0.4	-1.7	-1.1	-1.7	-0.9	-2.1	-0.8	-0.2	0.2	0.1	-1.9	-0.3	0.2	0.4	-0.2	0.3	0.8	-0.6	0.4	1.1	-1.0	-0.1	2.2	2.1	0.6	0.6	0.5	-1.2	0.2	0.4	0.1	0.6	0.3	2.7	0.3	23.9	3.0
Cartwright	0.4	0.8	0.1	-1.3	-1.0	-0.2	0.0	-0.2	-0.1	-1.3	-1.4	-1.6	-1.5	-1.1	-0.8	0.4	0.1	0.7	0.3	0.2	-0.1	0.3	0.1	1.8	-0.1	0.6	0.8	-0.9	0.1	2.7	2.0	0.0	0.8	-0.8	-1.2	0.3	-0.2	0.2	-0.3	-0.9	2.2	-0.6	12.0	2.6	
Bonavista	-0.3	0.6	0.2	-0.3	-0.4	-1.0	-0.5	-0.9	-0.2	-1.5	-2.4	-1.5	-1.8	-2.1	-1.7	-1.0	0.4	-0.2	0.1	0.8	1.0	-0.3	0.1	-0.9	0.9	0.4	1.9	0.2	-0.5	0.4	1.0	1.9	0.8	-1.2	0.1	0.6	0.0	1.1	-0.7	0.0	2.0	0.8	-3.2	1.3	
St.Johns	-0.6	0.6	-0.4	0.6	0.4	-0.8	-0.3	-1.3	-0.4	-1.7	-2.4	-1.3	-1.9	-1.9	-1.5	-1.0	0.1	-0.1	-0.1	1.1	1.2	-0.8	0.0	-1.0	0.7	0.5	1.4	-0.1	-0.4	0.9	0.9	2.0	0.7	0.4	-1.0	0.5	0.6	-0.1	1.2	-0.8	0.0	2.1	1.0	-3.0	1.2
	-- Annual Air Temperature --																																												
Nuuk	0.4	-0.2	-1.6	-2.4	-2.7	1.0	-0.2	-0.4	0.0	-1.7	-1.2	-0.7	-2.0	-2.2	-1.1	-0.6	0.1	-0.2	0.0	-0.3	0.1	0.5	-0.1	1.1	0.4	1.0	0.6	0.4	-0.1	0.3	2.8	-0.6	0.9	0.5	0.1	-1.5	1.0	0.2	-0.9	1.0	-0.6	0.8	-0.1	-1.0	1.3
Iqaluit	0.4	1.2	-1.3	-2.1	-1.6	0.9	-1.1	-1.2	-0.4	-1.6	-1.7	-0.9	-2.3	-2.3	-0.7	0.3	0.3	0.6	-0.2	-0.5	0.2	0.4	-0.5	0.6	-0.2	0.7	1.3	-0.1	-0.4	0.2	2.9	0.3	0.4	0.0	0.2	-1.7	0.1	0.5	-0.6	0.9	0.5	2.3	0.2	-8.3	1.5
Cartwright	-0.2	0.9	-1.3	-0.6	-1.1	-0.7	-1.0	0.3	-0.4	-0.6	-1.2	-1.5	-1.3	-1.3	-0.6	-0.5	0.3	0.4	0.5	0.8	0.4	0.5	-0.4	0.3	0.8	0.7	1.5	0.0	0.0	0.3	2.2	0.5	1.1	0.4	-0.1	-3.0	-0.4	0.1	-0.2	-1.1	0.4	1.5	0.2	0.2	1.4
Bonavista	-1.1	0.6	-1.0	0.1	-0.4	-1.3	-0.9	-0.3	0.2	-0.2	-0.7	-1.7	-1.7	-1.6	-0.6	-0.7	0.5	-0.9	0.6	0.5	0.9	0.5	-0.2	0.2	0.7	0.8	1.2	0.6	0.4	0.2	1.3	-1.6	1.4	0.7	-0.1	0.7	0.3	0.9	-2.1	-0.5	0.9	1.6	1.6	5.0	1.0
St.Johns	-1.6	0.8	-1.3	0.3	0.1	2.0	-1.3	-0.9	-0.1	-0.9	-0.8	-1.8	-2.2	-1.8	-0.7	-1.0	0.1	-1.4	0.4	1.8	0.8	0.1	-0.7	0.1	0.3	0.5	1.4	-0.4	0.6	0.7	1.3	0.1	1.5	0.7	0.1	-1.0	0.2	0.1	0.2	-0.7	0.8	1.4	1.8	5.5	0.8

Figure 4: Scorecard of large-scale indices (winter NAO, AO and AMO) and normalized air temperature anomalies (winter and annual) for five cities between 1980 and 2022. Means and standard deviations for the air temperatures during the 1991–2020 period are provided in the last column (in °C). No means or standard deviations are provided for the large-scale indices (grayed boxes).



*Figure 5: Cumulative monthly air temperature anomalies at Nuuk, Iqaluit, Cartwright, Bonavista and St. John's for 2022.*

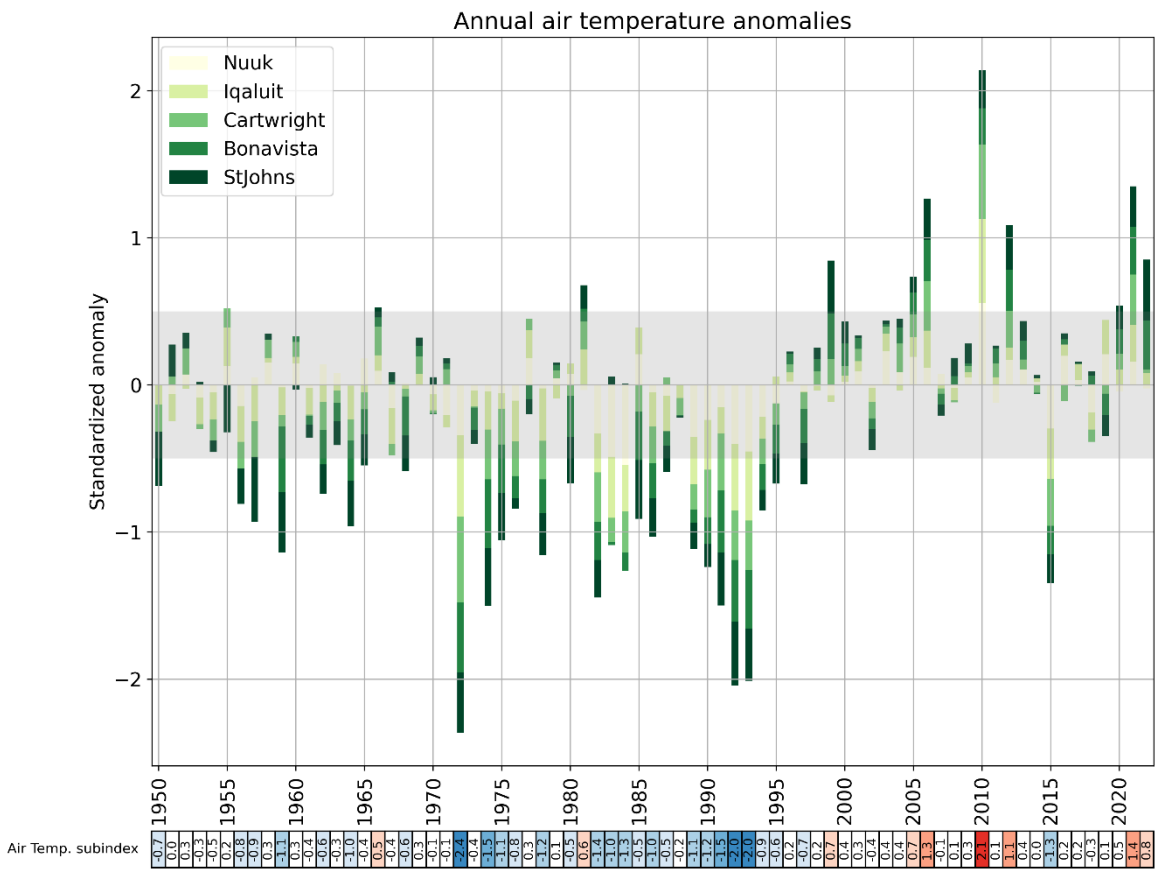


**Figure 6:** Normalized annual air temperature anomalies for Nuuk, Iqaluit, Cartwright, Bonavista and St. John's. This figure shows the average of the five stations, in which the length of each bar corresponds to the relative contribution of the individual station to the average. The shaded area corresponds to the 1991–2020 average  $\pm 0.5$  SD, a range considered normal. The numerical values of this time series are reported in a colour-coded scorecard at the bottom of the figure. The bottom scorecard is the average of these five time series, and is used to construct the NL climate index presented in the summary (Figure 39).

### 3 Sea ice conditions

Ice cover area, volume and seasonal duration are estimated from ice cover products obtained from the Canadian Ice Service (CIS). These products consist of Geographic Information System (GIS) charts covering the East Coast and Hudson Bay system, the latter providing coverage of the Northern Labrador Shelf. The East Coast region has weekly charts available for 1969–2022 and daily charts for 2009–2022 while only weekly charts are available for the Hudson Bay system for 1980–2022. All vector charts were further converted into regular  $0.01^{\circ}$  latitude by  $0.015^{\circ}$  longitude grids (approximately 1 km resolution), with ice concentrations and growth stages attributed to each grid point. Average thicknesses (and therefore regional volumes) are estimated from standard thicknesses associated with each stage of ice growth from new ice and nilas (5 cm), grey ice (12.5 cm), grey-white ice (22.5 cm), thin first year ice (50 cm), medium first year ice (95 cm) and thick first year ice (160 cm). Prior to 1983, the CIS reported ice categories with fewer classifications, where a single category of first year ice ( $\geq 30$  cm) was used with a suggested average thickness of 65 cm. We have found this value leads to underestimates of the seasonal maximum thickness and volume based on high interannual correlations between the estimated volume of the weekly seasonal maximums and its area or sea-ice season duration. The comparisons of the slope of these correlations pre- and post-1983 provided estimates of first-year ice thickness of 85 cm in the Gulf of St. Lawrence and 95 cm on the Newfoundland and Labrador Shelf for this single first year ice category, which were used instead of the suggested 65 cm.

Several products were computed to describe the sea-ice cover inter-annual variability. The day of first and last occurrence, ice season duration (Figure 7) and the distribution of ice thickness during the week of maximum volume (Figure 8) are presented as maps. These two figures combine information from the East Coast sea ice charts and Hudson Bay system charts, leading to a slight jump in the climatology maps of first occurrence and duration. This occurs because there are often missing weeks in the Hudson Bay charts around the period of first occurrence on the northern Labrador Shelf. Therefore, anomalies of these two parameters have more uncertainty than the rest. Regional scorecards of anomalies for the first and last day of ice, duration of the sea ice season and maximum ice volume are presented in Figure 9 for the Labrador and Newfoundland shelves. Here, the areas defined as the Northern and Southern Labrador shelves and the Newfoundland Shelf are depicted in Figure 1, with the Newfoundland Shelf and Gulf of St. Lawrence delimited at the Eastern end of the Strait of Belle Isle. Evolution of the ice volume during the 2022 ice season is presented in Figure 9 for the three regions in relation to the climatology and historical extremes. The Northern Labrador Shelf progression is shown using weekly data extracted from Hudson Bay charts, while the others are shown using daily data extracted from East Coast charts. Time series of seasonal maximum ice volume, area (excluding thin new ice) and ice season duration are presented for the Northern (top) and Southern (middle) Labrador Shelf and for the Newfoundland Shelf (bottom) in Figure 10. The December-to-April air temperature anomaly at Cartwright showed the best correlation with sea ice properties and is included with reversed scale in the Newfoundland Shelf panel. The durations shown in Figure 9 and Figure 11 are different products. The first corresponds to the number of weeks where the volume of ice anywhere within the region exceeded 5% of the climatological maximum, while the second is the average duration at every pixel of Figure 7, which is much shorter than the first.

Ice typically starts forming in December along the Labrador coast and only by late February at the southernmost extent of sea-ice presence (Figure 7). The last occurrence is usually in late June to early July on the Labrador coast, leading to sea-ice season durations of 23 weeks or more. There has been a declining trend in ice cover severity since the early 1990s, reaching the lowest values in 2010 and 2011, with a rebound in 2014 and third lowest value in 2021 (Figure 9 and Figure 11). On the Newfoundland Shelf, the sea ice metrics of annual maximum ice area, volume, and ice cover duration are all well-correlated with each other ( $R^2 = 0.71$  to  $0.74$ ; Figure 11). The strongest correlation with air temperature

was found between the December–April air temperature anomaly at Cartwright and the sea-ice metrics of the Newfoundland Shelf ( $R^2 = 0.62\text{--}0.78$ ), indicative of the advective nature of the Newfoundland shelf sea ice; i.e. strong ice cover is associated with cold air temperatures in the source area. Sensitivity of the Newfoundland Shelf ice cover to increases in air temperature (e.g. through climate change) can thus be estimated using 1969–2022 co-variations between winter air temperature at Cartwright and sea-ice parameters, which indicate losses of 14 km<sup>3</sup>, 26,000 km<sup>2</sup> and eight days of sea-ice season for each 1°C increase in winter air temperature.

In 2022, the sea-ice cover first appeared at a near-normal date to a later-than-normal date except offshore on the Northern Labrador Shelf (Figure 7). Regional thresholds of 5% were crossed later than normal (Figure 9). The last occurrence on the Labrador Shelf was a mix of earlier than normal inshore and later than normal offshore, and mostly earlier than normal on the Newfoundland Shelf (Figure 7). Sea ice volumes progressed mostly below to near normal throughout the season in the three regions (Figure 10). The maximum ice volumes reached during the season were below normal in the three regions, at 85 km<sup>3</sup> (-1.0 SD), 81 km<sup>3</sup> (-0.5 SD) and 39 km<sup>3</sup> (-0.8 SD) north to south, while the December-to-June seasonal averages were near normal at 46 km<sup>3</sup> on the Northern Labrador Shelf and below normal at 30 km<sup>3</sup> (-0.7 SD) and 8 km<sup>3</sup> (-0.8 SD) on the Southern Labrador and Newfoundland Shelves (Figure 9). The pixel average durations were 112 (-0.8 SD), 87 (-0.4 SD) and 32 days (-0.6 SD), respectively (Figure 7 and Figure 11). The maximum area reached within each region (excluding ice less than 15 cm thick) was above normal on the Northern Labrador Shelf (131 000 km<sup>2</sup>, +1.0 SD) and near normal in the Southern Labrador and Newfoundland Shelves (129 000 km<sup>2</sup>, +0.5 SD and 101 000 km<sup>2</sup>, -0.3 SD). An overview of sea ice conditions (area and season duration) for NL since 1969 is presented in Figure 12 as the average of normalized anomalies. In 2022, this index was normal at -0.1 SD.

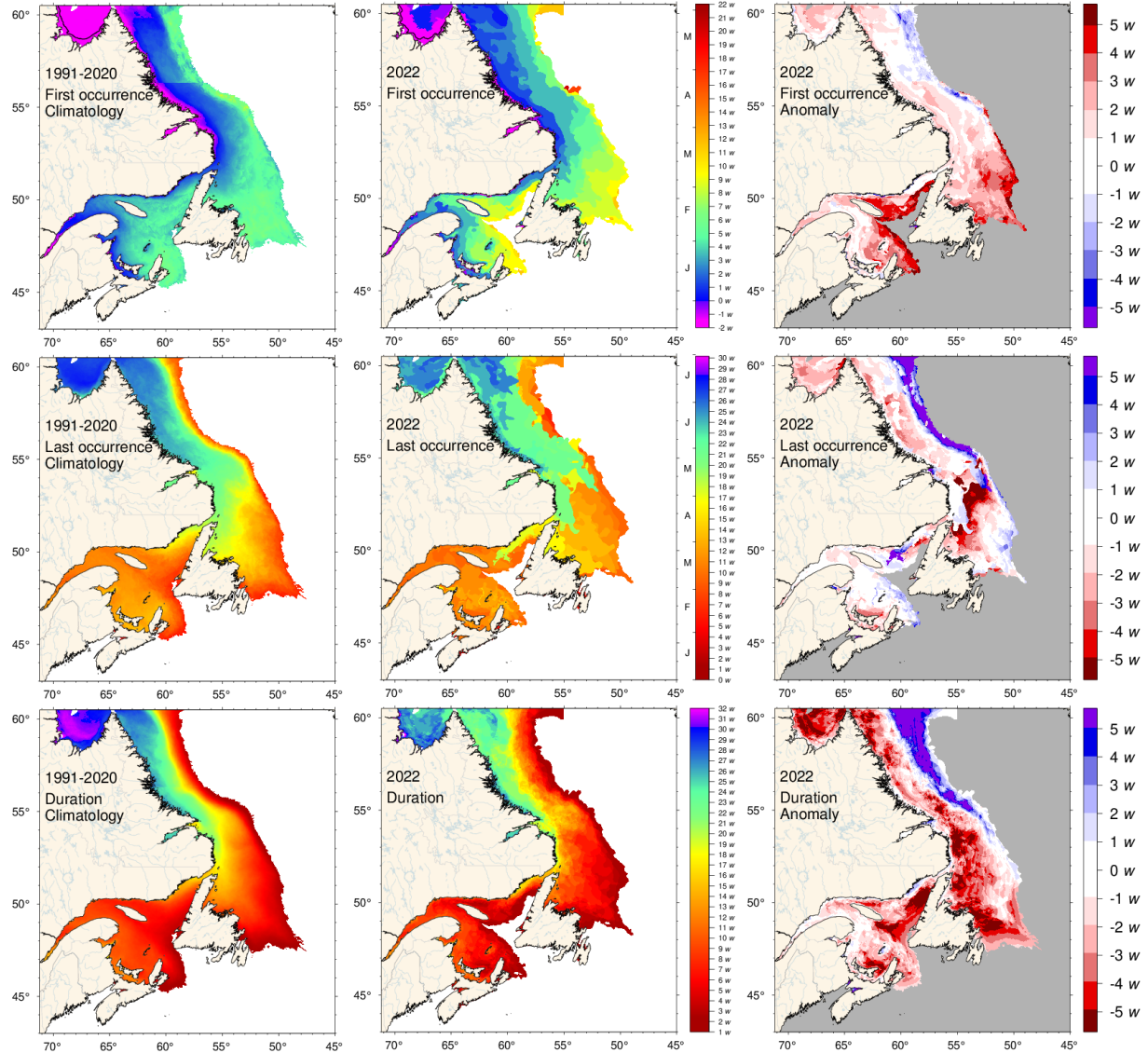


**Figure 7:** First (top) and last (middle) occurrence of ice and ice season duration (bottom) based on weekly data. The 1991–2020 climatologies are shown (left) as well as the 2022 values (middle) and anomalies (right). First and last occurrences are defined here as the first and last weekly chart in which any amount of ice is recorded for each pixel and are illustrated as day-of-year. Ice duration sums the number of weeks with ice cover for each pixel. Climatologies are shown for pixels that had at least 15 years out of 30 with occurrence of sea-ice, and therefore also show the area with 50% likelihood of having some sea-ice at any time during any given year. The duration anomaly map includes pixels with no ice cover where some was expected based on the climatology.

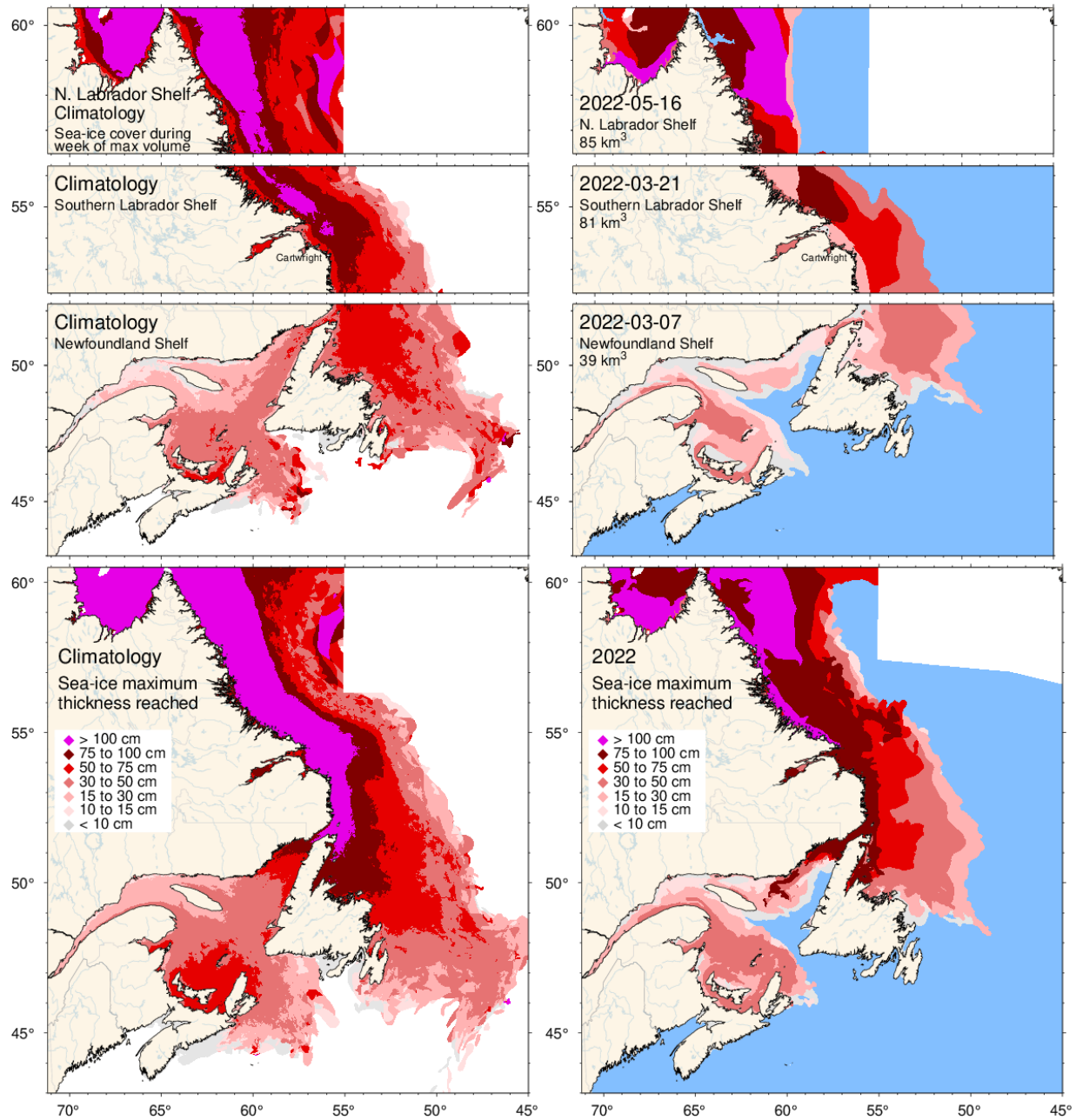


*Figure 8: Ice thickness map for 2022 for the week with the maximum annual volume on the Newfoundland and Labrador Shelf (three upper right panels) and similarly for the 1991–2020 climatology of the weekly maximum (three upper left panels). Note that these maps reflect the ice thickness distribution on that week. The maximum ice thickness observed at any given location during the year is presented in the lower panels, showing the 1991–2020 climatology and 2022 distribution of the thickest ice recorded during the season at any location.*

			Mean ± S.D.
First	Northern Labrador Shelf	102	-2 ± 14
	Southern Labrador Shelf	102	5 ± 12
	Newfoundland Shelf	102	26 ± 18
Last	Northern Labrador Shelf	153	186 ± 14
	Southern Labrador Shelf	153	175 ± 16
	Newfoundland Shelf	153	144 ± 20
Duration	Northern Labrador Shelf	521	189 ± 22
	Southern Labrador Shelf	521	171 ± 23
	Newfoundland Shelf	521	118 ± 36
Max volume	Northern Labrador Shelf	220	108 km³ ± 33
	Southern Labrador Shelf	220	93.3 km³ ± 23.6
	Newfoundland Shelf	220	70.9 km³ ± 42.0
Seasonal volume	Northern Labrador Shelf	5	154 km³ ± 63
	Southern Labrador Shelf	5	54.6 km³ ± 18.0
	Newfoundland Shelf	5	40.0 km³ ± 14.8
1970	Northern Labrador Shelf	24	29 ± 10
	Southern Labrador Shelf	24	29 ± 10
	Newfoundland Shelf	24	29 ± 10
1975	Northern Labrador Shelf	63	44 ± 15
	Southern Labrador Shelf	63	44 ± 15
	Newfoundland Shelf	63	44 ± 15
1980	Northern Labrador Shelf	28	48 ± 10
	Southern Labrador Shelf	28	48 ± 10
	Newfoundland Shelf	28	48 ± 10
1985	Northern Labrador Shelf	13	39 ± 6
	Southern Labrador Shelf	13	39 ± 6
	Newfoundland Shelf	13	39 ± 6
1990	Northern Labrador Shelf	43	79 ± 11
	Southern Labrador Shelf	43	79 ± 11
	Newfoundland Shelf	43	79 ± 11
1995	Northern Labrador Shelf	54	55 ± 56
	Southern Labrador Shelf	54	55 ± 56
	Newfoundland Shelf	54	55 ± 56
2000	Northern Labrador Shelf	58	74 ± 94
	Southern Labrador Shelf	58	74 ± 94
	Newfoundland Shelf	58	74 ± 94
2005	Northern Labrador Shelf	58	71 ± 111
	Southern Labrador Shelf	58	71 ± 111
	Newfoundland Shelf	58	71 ± 111
2010	Northern Labrador Shelf	38	47 ± 55
	Southern Labrador Shelf	38	47 ± 55
	Newfoundland Shelf	38	47 ± 55
2015	Northern Labrador Shelf	29	40 ± 54
	Southern Labrador Shelf	29	40 ± 54
	Newfoundland Shelf	29	40 ± 54
2020	Northern Labrador Shelf	8	30 ± 46
	Southern Labrador Shelf	8	30 ± 46
	Newfoundland Shelf	8	30 ± 46

*Figure 9: First and last day of ice occurrence, ice duration, maximum seasonal ice volume and average seasonal (DJFMAMJ) ice volume by region. The moment when ice was first and last observed in days from the beginning of each year is indicated for each region, and the color code expresses the anomaly based on the 1991–2020 climatology, with blue (cold) representing earlier first occurrence and later last occurrence. The threshold is 5% of the climatological average of the seasonal maximum ice volume. Numbers in the table are the actual day of the year or volume, but the color coding is according to normalized anomalies based on the climatology of each region. Duration is the numbers of days that the threshold was exceeded. Seasonal average volumes (lowermost scorecard) are reported in the ICES Report on Ocean Climate (e.g., Cyr & Galbraith, 2022).*

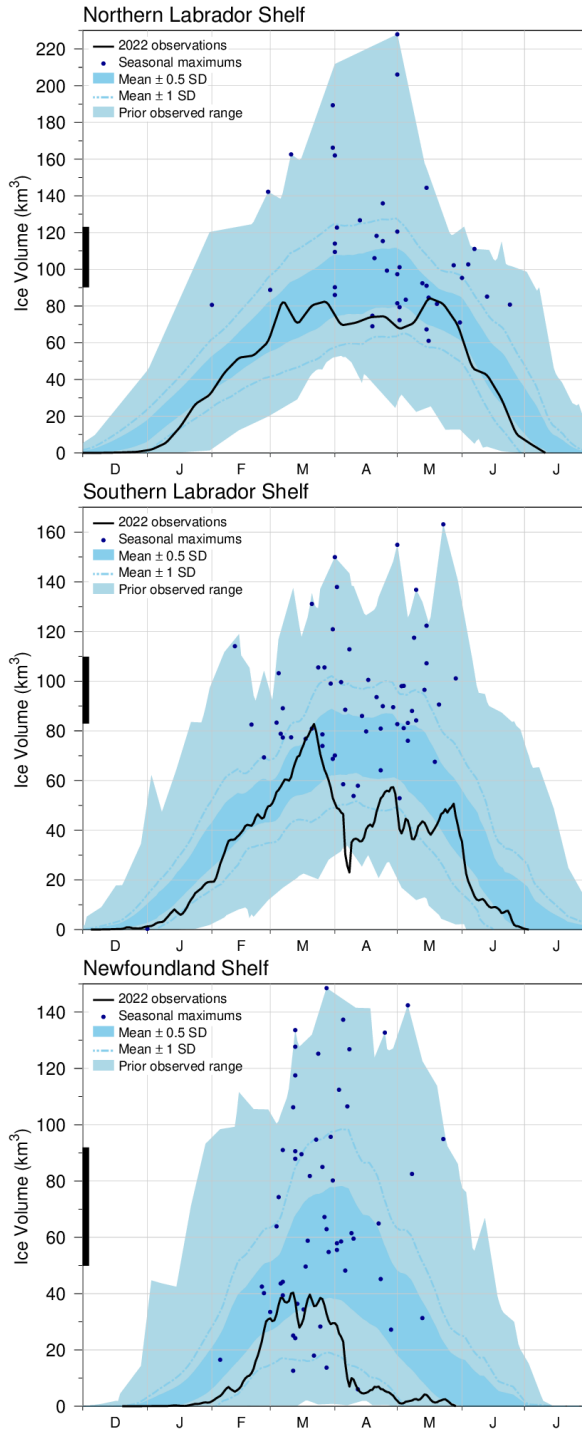


*Figure 10: Time series of the 2021–22 mean ice volume (black lines) for the Northern Labrador Shelf (top), Southern Labrador Shelf (middle), and Newfoundland Shelf (bottom), the 1991–2020 climatological mean volume  $\pm 0.5$  and  $\pm 1 \text{ SD}$  (dark blue area and dashed line respectively), the minimum and maximum span of 1969–2021 observations (light blue), and the date and volumes of 1969–2021 seasonal maximums (blue dots). The black thick line on the left indicates the mean volume  $\pm 0.5 \text{ SD}$  of the annual maximum ice volume, which is higher than the peak of the mean daily ice volume distribution.*

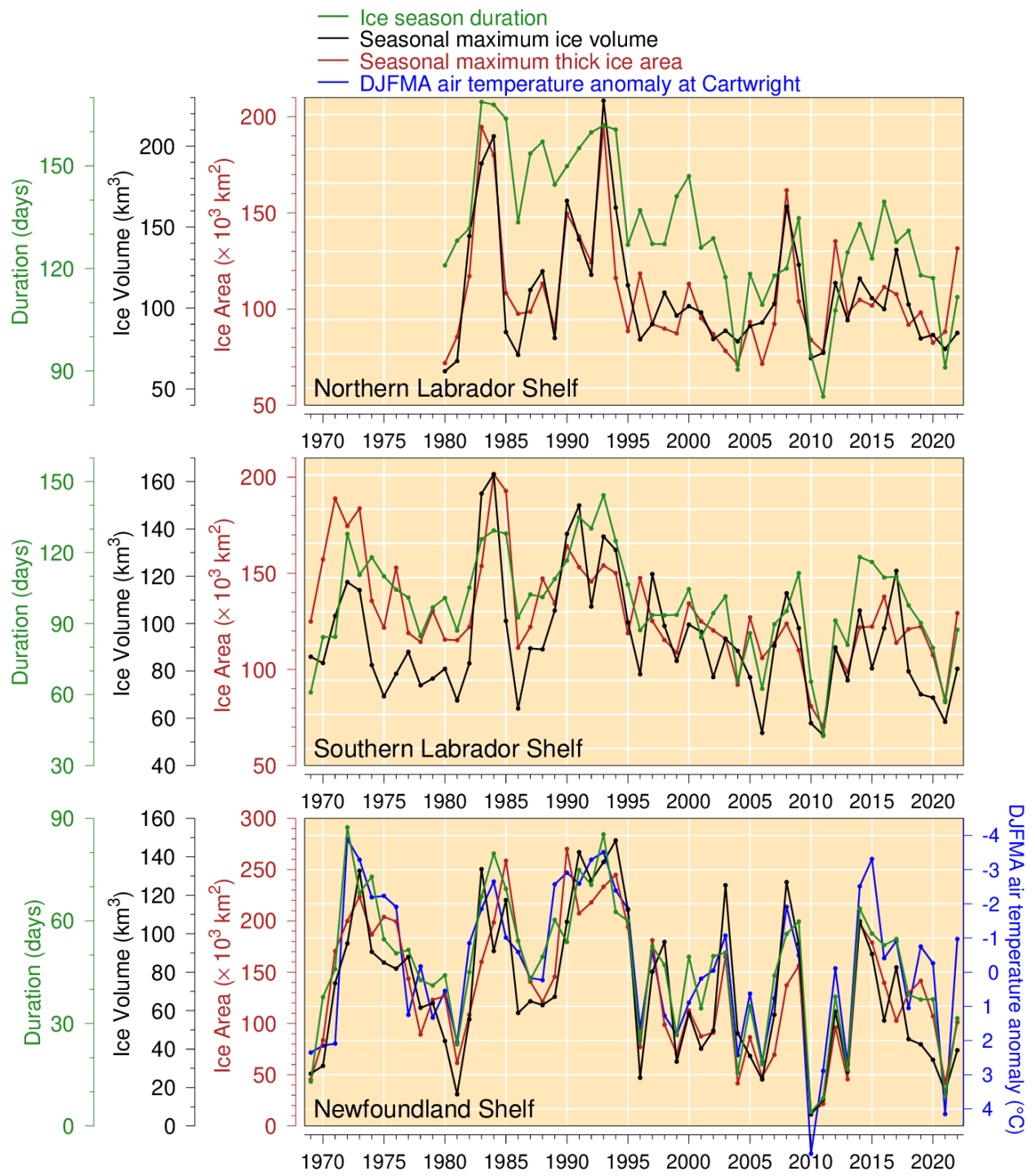
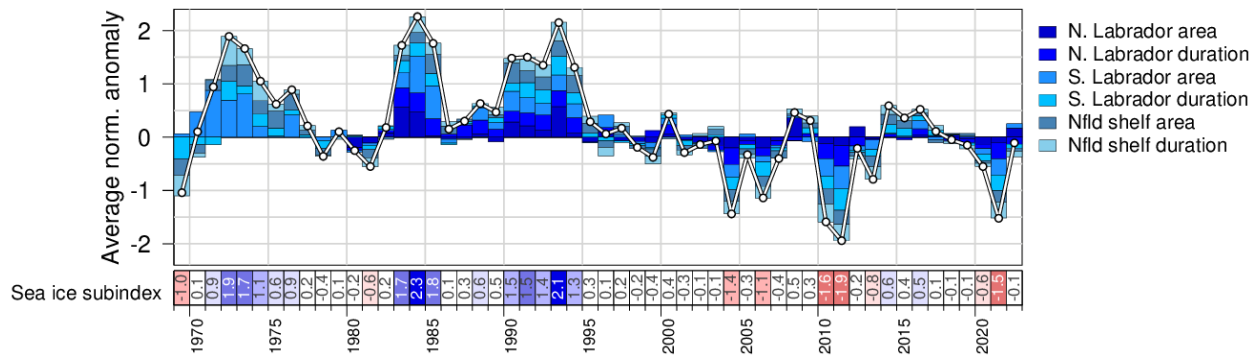


Figure 11. Regional average sea ice metrics and NL sea ice index. Seasonal maximum ice volume (black lines) and area (excluding ice less than 15 cm thick; red lines), and ice season duration (green lines) for the Northern and Southern Labrador Shelf (first and second panels, respectively) and the Newfoundland Shelf (third), and December-to-April air temperature anomaly at Cartwright (blue line).



*Figure 12. Newfoundland and Labrador sea ice index established by averaging the normalized anomalies of volume and duration of sea ice for Newfoundland and Labrador shelves (black and green time series in Figure 11). This sea ice index contributes to the NL climate index described in the summary (Figure 39).*

## 4 Icebergs

Iceberg counts obtained from the International Ice Patrol of the US Coast Guard indicate that only 58 icebergs drifted south of 48°N onto the Northern Grand Bank during 2022 (Figure 13). This number is much lower than the climatological (1991–2020) average of 771. Other years have also seen similarly low numbers. For example, only one iceberg was observed in 2010 and 2021, two in 2011 and 13 in 2013. Only two years (1966 and 2006) in the 120-year time series have reported no icebergs south of 48°N. More than 1,500 icebergs have been observed in some years during the cold periods of the early 1980s and 1990s, including the all-time record of 2,202 in 1984, along with a recent high number of 1,515 in 2019. Years with low iceberg numbers on the Grand Banks generally correspond to higher-than-normal air temperatures, lighter-than-normal sea-ice conditions, and warmer-than-normal ocean temperatures on the NL Shelf. As such, the normalized anomaly of the number of icebergs (scorecard at the bottom of Figure 13) is used as one component of the NL climate index presented in the summary.

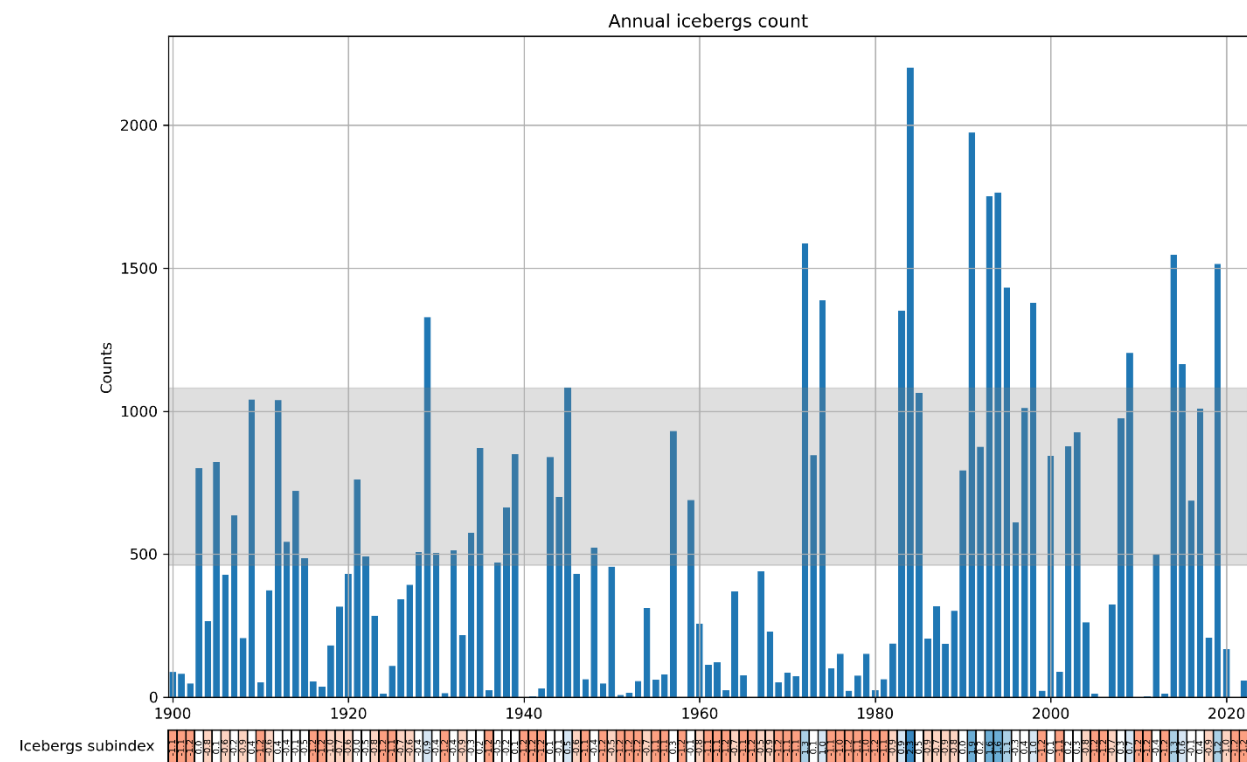


Figure 13: Annual iceberg count crossing south of 48°N on the northern Grand Bank. The shaded area corresponds to the 1991–2020 average  $\pm 0.5$  SD. The data are from the International Ice Patrol (International Ice Patrol, 2020). The normalized anomaly of this time series is color-coded in the bottom scorecard. This iceberg sub-index contributes to the NL climate index described in the summary (Figure 39).

## 5 Satellite sea-surface temperature

The satellite-based sea surface temperature product used in the previous two years' reports blends data from Pathfinder version 5.3 (4 km resolution for 1982–2020; Casey et al. 2010), Maurice Lamontagne Institute (MLI; 1.1 km resolution for 1985–2013) and Bedford Institute of Oceanography (BIO; 1.5 km resolution for 1997–2022) as detailed in Galbraith et al. (2021). The process selects the products with the best percent coverage for every averaging area and period (week or month). Monthly (and weekly) temperature composites are calculated from averaged available daily anomalies to which monthly (or weekly) climatological average temperatures are added.

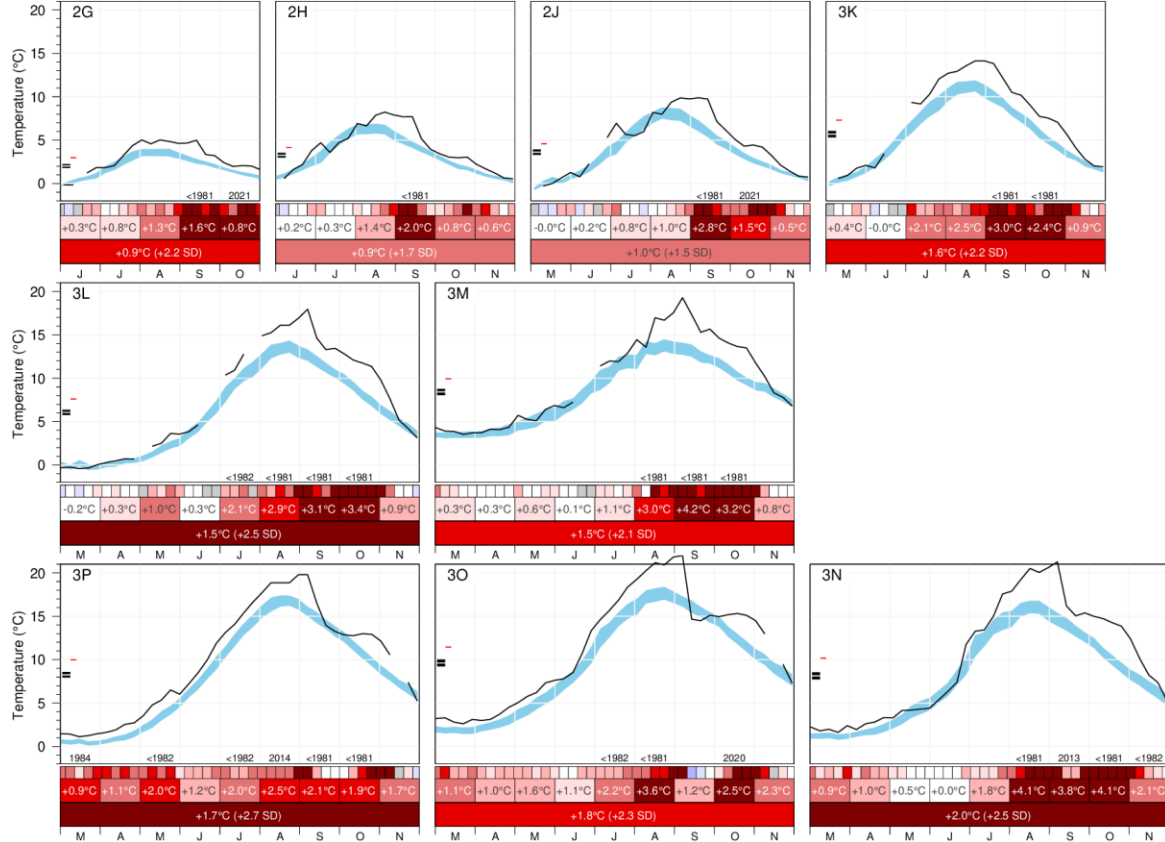
The BIO data stopped being produced in June 2022 and so two NOAA operational products were investigated to continue our operational coverage of the Atlantic Zone. The GHRSST NOAA/STAR L3S-LEO-Daily “super-collated” product was retained (0.02 degree resolution for 2007 to current; NOAA/STAR 2021). Day and night composites for each day are used to create a daily composite as the average of both values if available for a pixel, or using the available day or night pixel value minus or plus half of the average diurnal variation in the Atlantic Zone ( $0.22^{\circ}\text{C}$ ). Daily pixel values were then compared against the daily range of observations at four offshore thermograph stations (Mont-Louis, Havre-Saint-Pierre, Beaugé, La Romaine) as well as at all oceanographic Viking buoys. This initially consisted of 10165 days of observations, from which are excluded from the comparison all thermograph and buoy daily data that had diurnal temperature variations greater than the mean diurnal range, leaving 6691 days of observations. This filtering is done because the difference between in-situ and satellite observations is greater when diurnal range is high and may bias the calibration. A linear regression was performed of the average daily temperature at thermographs against the NOAA/LEO daily composite values at corresponding pixels and used as a calibration ( $\text{SST} = 1.01 \text{ LEO} - 0.41$ ). This calibration cools the NOAA/LEO daily composite values by  $0.41^{\circ}\text{C}$  at  $0^{\circ}\text{C}$  and by  $0.19^{\circ}\text{C}$  at  $20^{\circ}\text{C}$ . Before calibration, 69% of NOAA/LEO observations were within the 10165 thermograph/buoy diurnal ranges. After calibration, this increased to 95.4%. The calibrated NOAA/LEO daily composites were added to our blend method (Galbraith et al. 2021) and the BIO product was removed. The new blend has significantly higher temperatures for 2021 than were reported last year; the weighted seasonal average reported last year (+0.8 SD) is now +1.6 SD for 2021 and would have been reported as warmest with the new product.

Figure 14 shows the weekly evolution of the SSTs (black lines in each panel) for NAFO divisions 2GHJ3KLMNOP cropped at the shelf break (see Figure 1) in relation to the 1991–2020 climatology (blue shades). The color-coded anomalies are shown below each panel as weekly, monthly and seasonal scorecards. Only SST measurements during the ice-free periods of the year are considered. These seasonal windows range from as short as June to September on the northern Labrador Shelf (NAFO division 2H), to as long as March to November on the south coast of Newfoundland (NAFO division 3P).

In 2022, monthly average SSTs were largely above normal in ice-free areas across the region with the warmest anomalies found between August and October (Figure 14, middle scorecards at the bottom of panels). Several new monthly warm records were established across the different NAFO divisions and for the different months. The largest departures to the average temperature ( $+4^{\circ}\text{C}$  above average) were reached on Flemish Cap (Division 3M) in September and on the tail of the Grand Banks (3N) in August and October.

Seasonal SSTs averaged over the ice-free months were also significantly above normal across the NL Shelf (between +1.5 to +2.7 SD above average for the different NAFO division; Figure 14, bottom scorecards at the bottom of panels). It is thus not surprising that the spatially weighted average over the NL region also established a new warm record at +2.2 SD above average (Figure 15), easily beating the previous record established last year (+1.6 SD). Note that the last three years are among the 5 warmest on record.

Note that air temperature has been found to be a good proxy of sea surface temperature. The warming trend observed in air temperature since the 1870s of about 1°C per century is also expected to have occurred in surface water temperatures across Atlantic Canada (Galbraith et al. 2021).



*Figure 14: Weekly evolution of AVHRR Sea surface temperature evolution in 2022 for NAFO divisions 2GHJ3KLMNOP (black lines) during the ice-free season (season-length variable). Broken lines indicate that the threshold for the number of good pixels was not reached during these weeks (no data). The blue area represents the 1991–2020 climatological weekly mean  $\pm 0.5$  SD. Scorecards representing the weekly, monthly and seasonal averages (in °C) appear at the bottom of each panel and are colour-coded according to the normalized anomalies (top, middle and bottom row, respectively), with data gaps in grey. The two black ticks along the y-axis correspond to the seasonal climatological average  $\pm 0.5$  SD, while the red tick represents the 2022 seasonal average.*

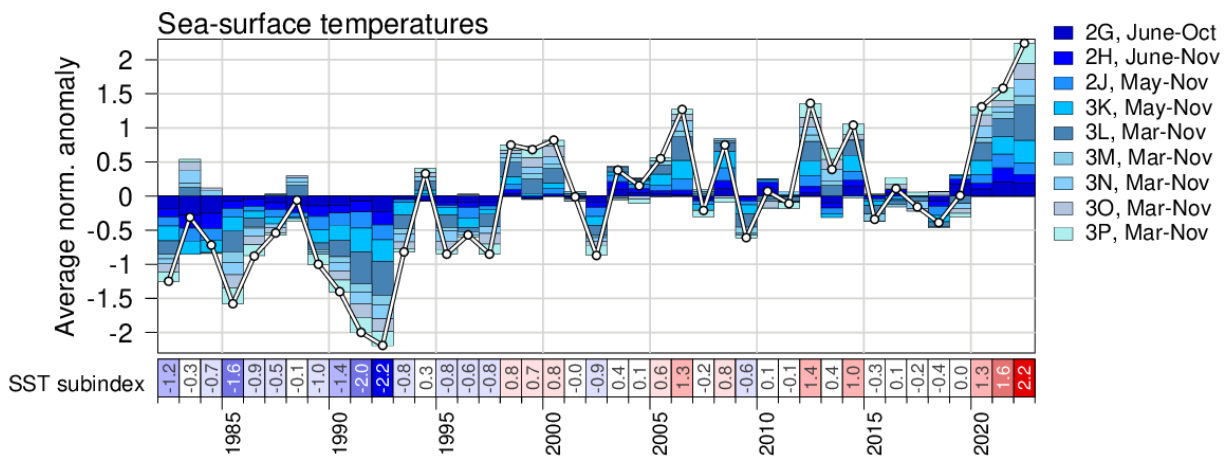


*Figure 15: Northwest Atlantic SST index built from the average of the seasonal anomalies for all NAFO divisions (bottom rows of panels in Figure 14). This index contributes to the NL climate index described in the summary (Figure 39).*

# 6 Ocean conditions on the Newfoundland and Labrador shelf

The following section presents observations of various ocean parameters (long-term monitoring Station 27, standard hydrographic sections, bottom ocean conditions, etc.).

## 6.1 Long-term observations at Station 27

Station 27 ( $47^{\circ}32.8'N$ ,  $52^{\circ}35.2'W$ ), is located in the Avalon Channel off Cape Spear, NL (Figure 1). It is one of longest hydrographic time series in Canada with frequent, near-monthly, occupations since 1948. In 2022, the station was occupied 37 times including 16 Conductivity-Temperature-Depth (CTD)-only casts, 20 full AZMP physical-biogeochemical samplings and 1 Expendable Bathythermograph (XBT) measurement.

Since 2017, an automatic profiling system installed on a surface buoy (type Viking) usually provides extended temporal coverage of temperature (T) and salinity (S) at Station 27. Unfortunately, in 2022, the system was deployed in early July and was recovered shortly thereafter due to a water leak in the main controller. Due to delays experienced while repairing the buoy it was not redeployed in 2022. 4 CTD profiles were collected in 2022 by the buoy, but the CTD data suffered electronic spikes that have not been corrected at the time this report was written.

Station occupations were used to obtain the annual evolution of temperature and salinity at Station 27, as well as the anomaly compared to the 1991–2020 climatology, shown in Figure 16 and Figure 17. These figures demonstrate the seasonal warming of the top layer (~20 m), with temperature peaking in August before being mixed during the fall. The CIL (Petrie et al., 1988), a remnant of the previous winter cold layer and defined as temperature below  $0^{\circ}C$  (thick black line in Figure 16) is also evident below 100 m throughout the summer. Interestingly, the coldest water body within the CIL (darkest shades of blue in the middle panel of Figure 16) is generally found in the summer between mid-June and mid-August, suggesting advection of cold waters from the Labrador Shelf and the Arctic to the Newfoundland Shelf. The surface layer is generally freshest between early-September and mid-October, with salinities below 31 (Figure 17). These low near-surface salinities, generally from early summer to late fall, are a prominent feature of the salinity cycle on the Newfoundland Shelf and is largely due to the melting of coastal sea-ice. This presence of large volume of freshwater late in the summer season also points out towards advection from northern areas (Labrador and the Arctic).

The water column was warmer and fresher than average during the winter in 2022 (Figure 16 and Figure 17, top and bottom panels). This is probably due to the milder winter conditions experienced in Newfoundland in 2022 (e.g. Figure 5). At depth, the rest of the year was relatively normal as a result of the advection of colder water from the Labrador shelf. Consistent with record warm SSTs experienced throughout the region (see Section on Sea Surface Temperature), a thick, warmer-than-average layer developed near the surface (Figure 16). This layer was also fresher than average (Figure 17).

Over 2022, the annual temperature anomaly (defined as the average of monthly anomalies) for the vertically averaged (0–176 m) temperature was slightly above average (+0.8 SD), while the vertically-averaged salinity was slightly fresh (Figure 18). The fresh anomaly of the early 1970s (Figure 18, bottom panel) is commonly referred to as the Great Salinity Anomaly in the North Atlantic (Dickson et al., 1988). Normalized anomalies of temperature and salinity for all years since 1980 and for different depth ranges (0–176 m, 0–50 m and 150–176 m) are reported in scorecards in Figure 19.

The summer (May-July) CIL statistics at Station 27 since 1951 are presented in Figure 20. Here the CIL mean temperature corresponds to the average of all temperatures below 0°C. The CIL thickness as well as the CIL core temperature (the minimum temperature of the CIL) and its depth are also presented in Figure 20. This year, the discovery of a set of problematic casts associated with Mechanical Bathythermographs collected in the 1960s and 1970s, where the negative temperatures were converted into positive values, has slightly reduced the warm anomalies during these decades. While the warm early 1960s to the mid-1970s for the CIL mean and core temperatures (coldest temperature within the CIL) remains (top and middle panels, respectively), these anomalies have reduced compared to the previous assessment (Cyr et al., 2022). After the prevalence of a warm CIL in the early 2010s (with some of the warmest years since the mid-1970s), there has been a cooler period between about 2014 and 2017. The CIL was warmer than normal between 2018 and 2022, except in 2020 when it was normal. The SD of these metrics are reported in a scorecard in Figure 19.

The monthly mean mixed layer depth (MLD) at Station 27 was also estimated from the density profiles as the depth of maximum buoyancy frequency (N) calculated from the monthly averaged density profiles ( $\rho[z]$ ):

$$N^2 = \frac{-g}{\rho_0} \frac{\Delta\rho(z)}{\Delta z};$$

with  $g = 9.8 \text{ ms}^{-2}$  as the gravitational acceleration,  $z$  the depth and  $\rho_0$  the mean density. Here  $N^2$  is calculated using the Gibbs-SeaWater (GSW) Oceanographic Toolbox (McDougall & Barker, 2011).

Climatological monthly MLD values, as well as monthly MLDs during 2022, are presented in Figure 21. The climatological annual cycle shows a gradual decrease of the MLD between late fall and summer (mixed layer thickest in December-January and shallowest in July-August). Overall, the MLD was close to normal for most of the months, except deeper in January and September and shallow in March and October. The transition from a shallow to a deep MLD from September to October is likely the result of hurricane Fiona that hit the Maritimes region in late September. No MLD data was available for February and December. Figure 22 shows a time series of the annual mean values of the MLD (solid gray line) and its 5-year moving average (dashed-black line). In general, there is a strong interannual and decadal oscillation in MLD, but the striking feature is a step-like increase since the 1990s. A scorecard of annual and seasonal MLD anomalies since 1980 can be found in Figure 19.

Stratification is an important characteristic of the water column since it influences, for example, the transfer of solar heat to lower layers and the vertical exchange of biogeochemical tracers between the deeper layers and the surface. The seasonal development of stratification is also an important process influencing the formation and evolution of the CIL on the shelf regions of Atlantic Canada. It insulates the lower water column from the upper layers, thus slowing vertical heat flux from the seasonally heated surface layer.

Stratification at Station 27 is calculated from monthly average density profiles ( $\rho$ ) using discrete differences between two depths ( $z$ ). Unlike in previous reports (e.g., Cyr et al., 2021), two definitions of the stratification indices are calculated for Station 27. The first one uses the density difference (i.e.  $\Delta\rho/\Delta z$ ) between 0 and 50 m and the second one between 10 and 150 m (see bottom two scorecards in Figure 19). The reason for these two definitions is that historical near-surface measurements in the 1950s and 1960s were made at discrete depths of  $z=[0, 25, \text{and } 50]\text{m}$ . In the 1970s and 1980s, these discrete depths were changed to  $z=[0, 10, 20, 30, 50]\text{m}$ . Finally, since the widespread use of electronic measurements using CTD mounted on rosettes started in the 1980s, near-surface ( $z=0$ ) measurements of density are usually discarded, and each high-resolution cast usually starts at  $z\sim[2-5]\text{m}$  to avoid electronic noise contamination or damage to the rosette by surface waves or ship motion. There is thus no simple definition that can ensure continuity of the metric from the 1950s to present. Here the definition 0-50 m will mostly focus on the 1950-1990 period, while the definition 10-150m will be representative of the period 1960-present.

Note that the 0-50 m definition is also calculated until present, but it considers the average [0-5]m as the surface measurement, making it difficult to directly compare with historical data.

The 2022 and climatological evolution of the 0-50m stratification throughout the year are shown in Figure 23. The stratification is generally weakest between December and April, before rapidly increasing at the onset of spring until it peaks in August. While the stratification was close to normal for the first part of 2022, a notable observation is the high stratification in the late summer- early fall, especially in October (Figure 23). This increase in stratification is a direct consequence of the warm SST observed during these months.

The interannual evolution of the stratification anomaly since 1950 is shown in Figure 24. Strong decadal variations exist in the two different definitions of stratification. For the 0-50m range, an increase in stratification from the 1950s to about 2000 is observed, followed by a slight decrease since then. For the 10-150m definition, no real trends are discernable. In 2022, the annual stratification was slightly above normal. A scorecard of annual and seasonal stratification anomalies since 1980 can be found in Figure 19.

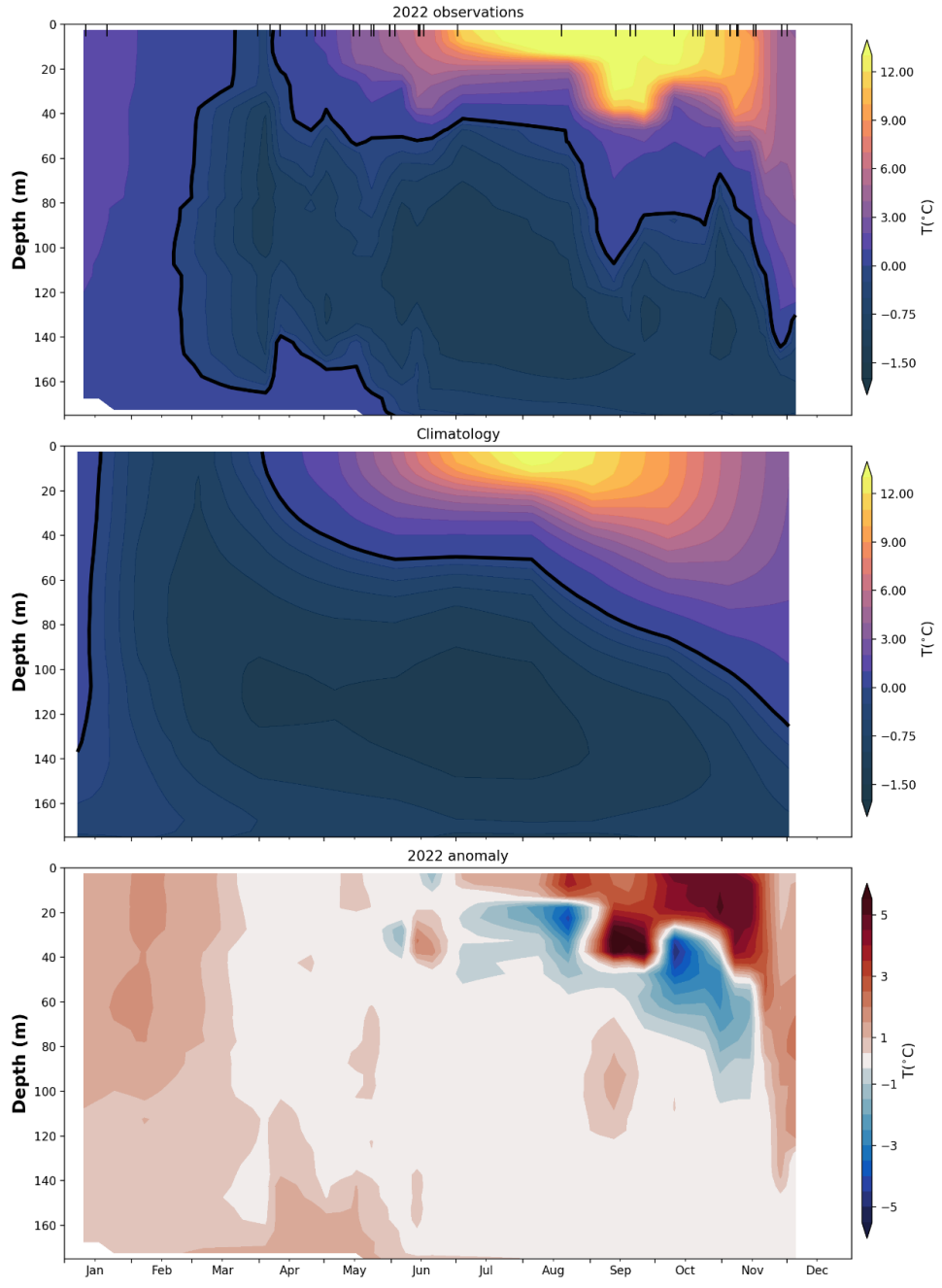


*Figure 16: Annual evolution of temperature at Station 27. The 2022 contour plot (top panel) is generated from weekly averaged profiles from all available data, including station occupations and Viking buoy casts (indicated by black tick marks on top of panel). The solid black contour delineates the cold intermediate layer (CIL), defined as water below 0°C. The 1991–2020 weekly climatology is plotted in the middle panel. Note the uneven colorbar used in the two first panels: below 0°C, 0.25°C increments are used, while 1°C increments are used above 0°C. The anomaly (bottom panel) is the difference between the 2022 field and the climatology.*

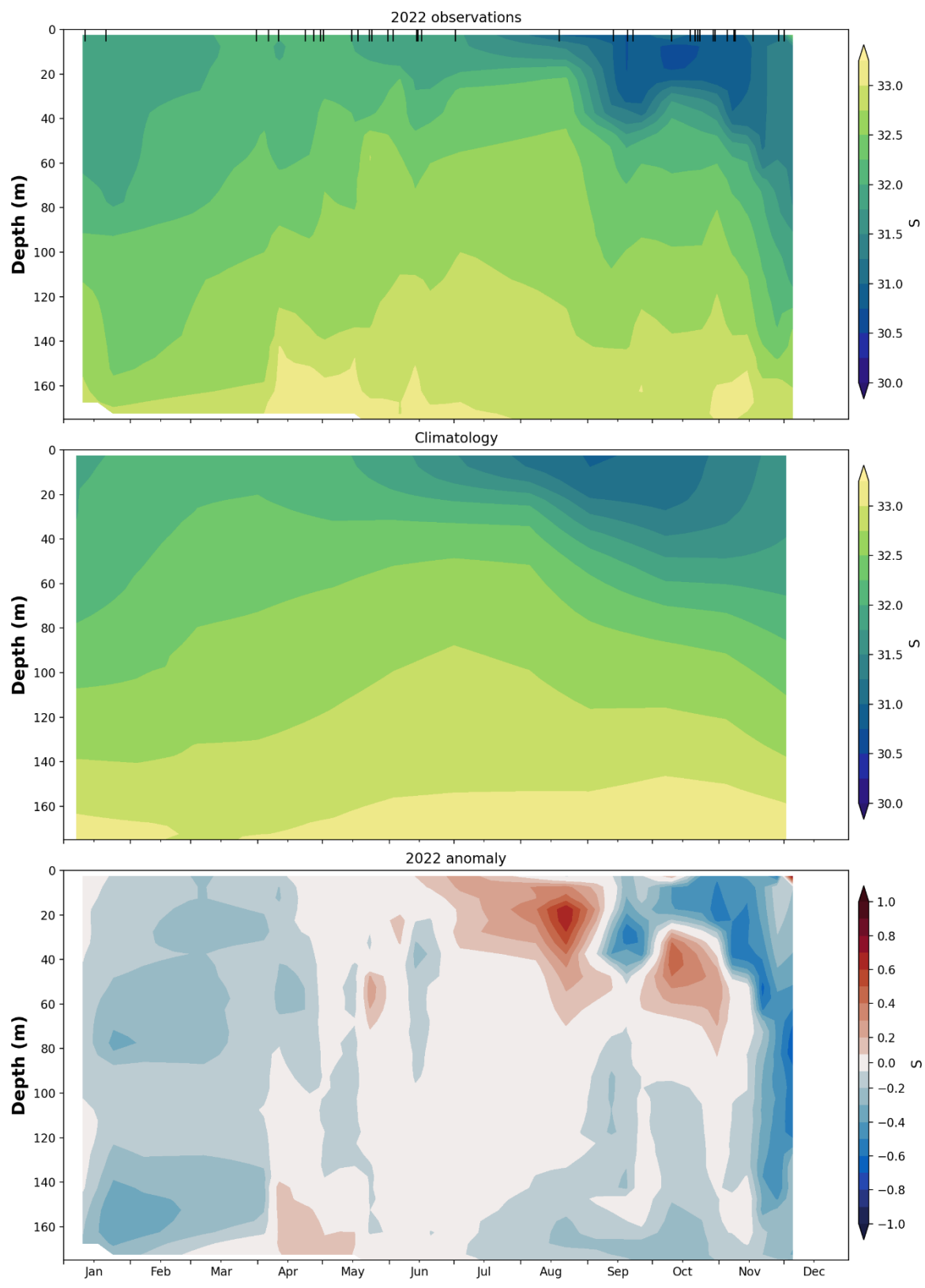
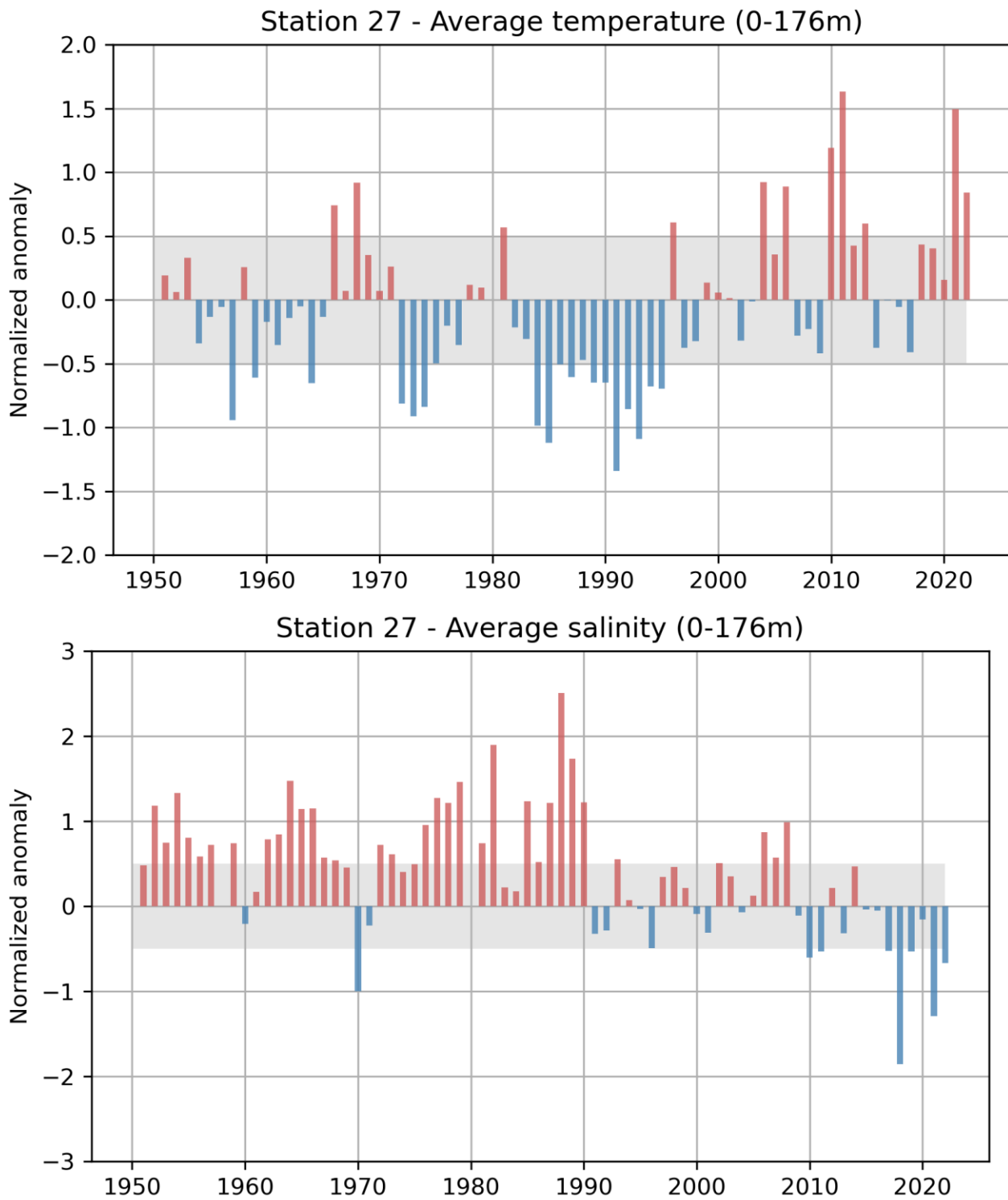
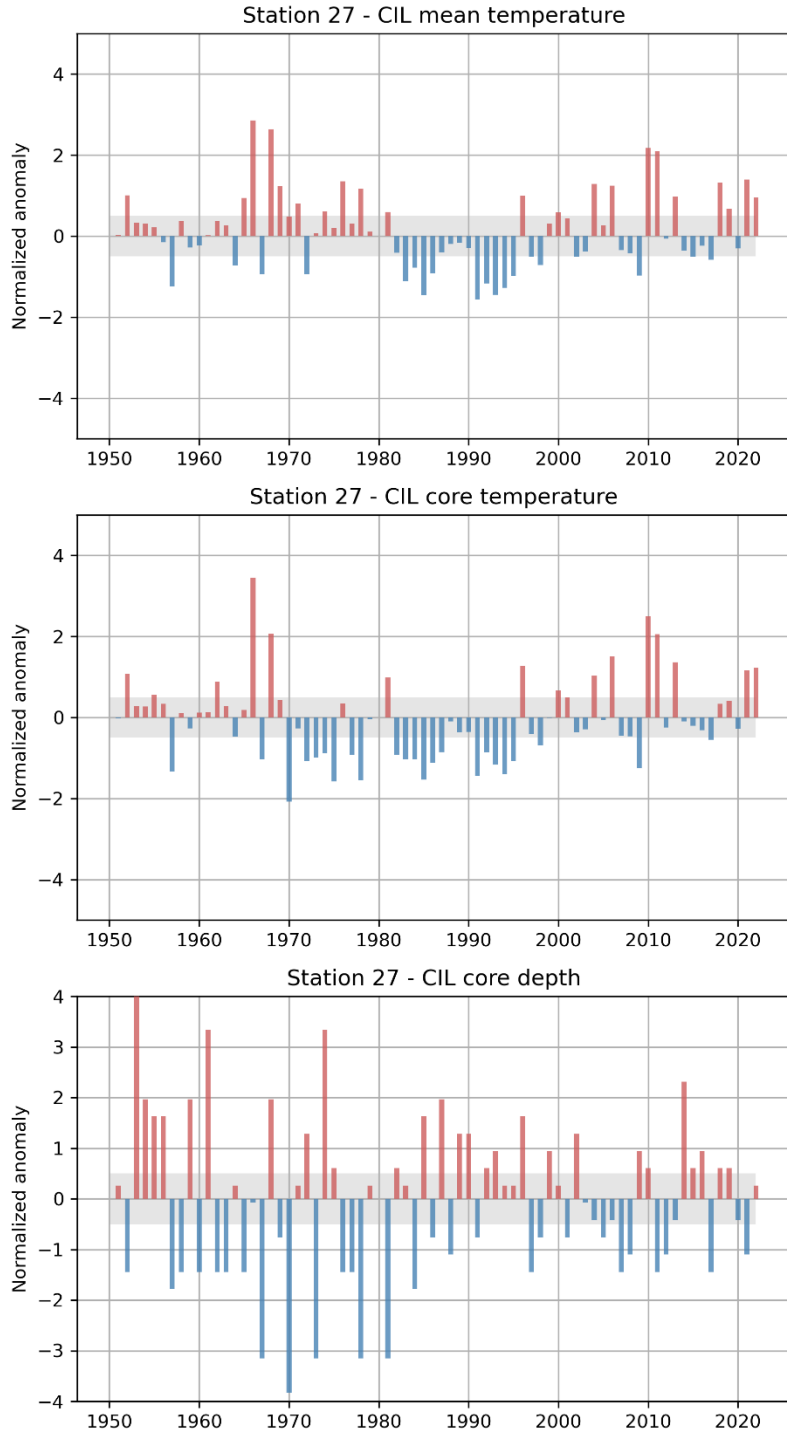


Figure 17: Same as in Figure 16, but for salinity.



*Figure 18: Annual normalized anomaly of vertically averaged (0–176 m) temperature (top) and salinity (bottom) at Station 27 calculated from all occupations since 1951. Only years where at least 8 months of the year are sampled are presented. Shaded gray areas represent the climatological (1991–2020) average  $\pm 0.5$  SD range considered “normal”. These two time series contribute to the NL climate index described in the summary (Figure 39).*

	81	82	83	84	85	86	87	88	89	90	91	92	93	94	95	96	97	98	99	00	01	02	03	04	05	06	07	08	09	10	11	12	13	14	15	16	17	18	19	20	21	22	x	sd
Temp 0-176m	<b>2.1</b>	1.2	0.9	-1.1	-1.0	-0.4	-0.6	-0.7	-0.5	-0.9	<b>-2.0</b>	-1.0	-1.3	-0.6	-0.8	0.7	-0.6	-0.5	0.2	0.0	0.0	-0.4	0.2	<b>1.0</b>	0.5	<b>1.1</b>	-0.5	-0.2	-0.5	<b>1.3</b>	<b>1.8</b>	0.7	0.7	-0.4	0.3	0.1	-0.5	0.4	0.4	0.1	<b>2.4</b>	1.0	0.6	0.5
Temp 0-50m	0.8	0.1	0.2	-1.3	-1.1	-0.4	-0.5	-0.7	-0.9	-0.9	<b>-1.7</b>	-0.8	-1.0	-0.3	-0.7	0.5	-0.6	-0.2	0.2	0.0	0.2	-0.6	0.2	0.6	0.5	1.2	-0.6	0.4	-0.8	0.9	1.1	0.8	0.6	-0.2	0.1	0.4	-0.4	0.0	-0.1	0.1	<b>2.1</b>	1.1	3.4	0.8
Temp 150-176m	0.7	-0.2	-0.8	-1.0	-1.4	-0.6	-0.5	-0.5	-0.7	-1.1	<b>-1.4</b>	-1.0	-1.4	-1.2	-0.8	0.1	-0.1	0.2	0.3	0.1	0.3	-0.2	-0.3	<b>1.3</b>	0.9	<b>1.1</b>	0.1	-0.2	-0.6	<b>1.1</b>	<b>2.5</b>	0.5	0.6	-0.7	-0.7	-0.6	0.4	0.1	0.9	<b>1.8</b>	1.0	-0.8	0.4	
<b>-- Vertically averaged temperature --</b>																																												
Sal 0-176m	0.1	1.4	-1.1	-0.6	0.7	-0.3	0.9	<b>2.4</b>	2.5	1.5	-0.6	-0.3	0.7	0.2	-0.1	-0.5	0.3	0.5	0.2	-0.2	-0.4	0.3	<b>0.6</b>	-0.1	0.2	<b>1.1</b>	0.7	<b>1.2</b>	0.0	-0.8	-0.6	0.3	-0.3	0.5	-0.2	0.0	-0.8	<b>-2.2</b>	-0.4	0.0	<b>-1.5</b>	-0.8	32.5	0.1
Sal 0-50m	0.3	1.7	-1.1	1.2	0.7	1.3	2.3	2.2	1.4	<b>-1.4</b>	-0.3	0.2	0.0	-0.9	-0.2	0.0	0.0	0.0	-0.4	-0.5	<b>1.0</b>	1.1	0.4	0.3	0.6	0.4	0.8	0.4	-0.9	-0.4	0.3	0.0	0.1	0.0	0.3	-0.9	-1.1	0.4	0.2	-0.7	-0.5	31.9	0.1	
Sal 150-176m	<b>1.8</b>	<b>2.3</b>	0.8	0.9	0.8	0.0	0.9	<b>2.5</b>	0.8	0.8	-0.3	-0.5	0.8	0.1	0.3	-0.6	0.3	0.7	0.2	0.2	0.0	0.0	-0.5	0.1	0.3	1.3	0.6	0.9	-0.3	0.1	0.1	0.3	-0.6	0.3	-0.4	-0.6	-0.5	-1.7	-1.1	0.1	-1.2	-0.9	33.0	0.1
<b>-- Vertically averaged salinity --</b>																																												
CIL temp	0.6	-0.4	-1.1	-0.8	-1.5	-0.9	-0.4	-0.2	-0.2	-0.3	<b>-1.6</b>	-1.2	-1.5	-1.3	-1.0	1.0	-0.5	-0.7	0.3	0.6	0.4	-0.5	-0.4	1.3	0.3	1.2	-0.3	-0.4	-1.0	<b>2.2</b>	<b>2.1</b>	-0.1	1.0	-0.4	-0.5	-0.2	-0.6	1.3	0.7	-0.3	1.4	0.9	-1.1	0.2
CIL core T	<b>1.0</b>	-0.9	-1.0	-1.0	-1.5	-1.1	-0.9	-0.1	-0.4	-0.4	<b>-1.4</b>	-0.9	-1.2	-1.4	-1.1	1.3	-0.4	-0.7	0.0	0.7	0.5	-0.4	-0.3	1.0	-0.1	<b>1.5</b>	-0.5	-0.5	-1.3	<b>2.5</b>	<b>2.1</b>	-0.2	1.4	-0.1	-0.2	-0.3	-0.6	0.3	0.4	-0.3	1.2	1.2	-1.4	0.2
CIL thickness	<b>1.1</b>	-0.6	0.3	<b>1.6</b>	0.3	0.3	-0.2	<b>1.1</b>	<b>-0.6</b>	-0.2	<b>2.0</b>	0.3	0.3	1.1	0.7	<b>-1.0</b>	0.7	0.7	-0.2	-0.2	-0.2	-0.7	0.1	0.7	<b>-2.3</b>	<b>-1.9</b>	<b>-1.5</b>	-0.2	0.3	-0.2	-0.6	0.7	<b>-1.5</b>	-1.0	0.7	126.8	11.6							
<b>-- Mixed layer depth (MLD) --</b>																																												
MLD winter	-0.9	0.1		<b>1.1</b>		-0.1	-0.3			<b>0.6</b>			<b>-0.9</b>	<b>0.9</b>	-0.9	0.5	0.3	0.5	-0.6	0.0	-0.5	-0.2	-0.5	0.7	0.2	0.4	0.4	-0.5	-1.3	-1.3	0.2	0.4	<b>1.7</b>	0.5	<b>0.9</b>	-0.8		-0.9		0.2	58.3	7.7		
MLD spring	-0.8	-1.3	-1.3	-1.8	-1.7	<b>1.1</b>	<b>-1.9</b>		<b>1.1</b>	<b>2.6</b>	0.2	-0.5	0.1	0.3	-0.8	-0.5	-0.7	-0.5	0.1	-0.1	0.0	0.1	-0.5	0.3	-0.2	-0.4	0.4	-0.3	-0.6	-0.2	-0.7	1.3	0.1	0.6	0.2	-0.2	0.3	<b>0.6</b>	<b>1.2</b>	-0.5	-0.2	38.1	10.3	
MLD summer	-0.2	-0.5	-0.1	-0.8	-0.1	-1.0	0.7	<b>-1.0</b>		-0.1	-0.3	1.2	<b>1.5</b>	0.3	0.5	1.3	-0.1	-0.5	-0.4	-0.4	-0.1	-0.9	0.6	-0.8	-0.7	0.1	-0.8	0.8	-0.6	<b>1.0</b>	-1.1	-0.2	-0.7	1.0	0.4	-0.4	0.8	-0.1	-0.6	0.4	0.2	23.2	5.5	
MLD fall				-0.5	-1.7		-0.3		<b>-3.6</b>	0.6	0.1	-0.5	-0.8	0.4	0.3	-0.3	-0.8	-0.6	0.2	-0.3	-0.8	-0.3	-0.4	0.5	0.3	-0.4	0.8	-0.6	0.3	0.5	0.2	1.2	-0.3	0.4	<b>1.0</b>	-1.2	0.4	0.6	0.7	0.0	-1.0	-1.2	58.2	10.0
MLD annual	-0.7	-0.8	-0.6	-1.1	-0.8	-0.1	-0.4	<b>-2.3</b>	0.8	0.6	-0.2	0.0	0.3	0.4	-0.3	0.1	-0.4	-0.1	-0.2	-0.2	-0.3	-0.4	-0.3	0.2	-0.1	-0.1	-0.5	-0.5	0.2	0.5	0.1	0.8	-0.4	0.2	0.6	0.4	-0.3	-0.4	44.5	17.1				
<b>-- Stratification (0-50m) --</b>																																												
strat winter		-0.5	0.4	-0.6	-0.6		0.1	<b>-1.5</b>	<b>1.2</b>	<b>1.3</b>	<b>-1.1</b>	1.3	0.2	0.3	-0.8	0.2	0.0	0.3	0.9	0.0	-0.4	0.3	-0.1	-0.4	0.6	0.4	-0.1	0.1	<b>-0.9</b>	<b>-1.3</b>	-0.6	-0.2	-0.7		-0.3		-0.4	0.008	0.001					
strat spring	<b>1.0</b>	0.0	<b>2.9</b>	1.3	-1.1		<b>-1.1</b>		-1.6	0.1	0.2	0.6	-0.4	<b>2.4</b>	-0.8	0.2	<b>1.2</b>	1.2	0.0	0.2	-1.0	0.0	0.3	0.7	0.1	-0.1	<b>1.0</b>	-0.3	0.0	0.0	-0.4	-0.7	-0.2	-0.5	0.0	-1.2	-1.4	<b>2.3</b>	0.5	0.015	0.008			
strat summer	<b>0.1</b>	<b>1.6</b>	-0.4	-0.2	<b>-2.6</b>				-0.9	-0.6	-0.5	-1.0	0.7	<b>-1.1</b>	0.0	0.5	1.0	0.7	1.0	0.0	0.5	0.1	-0.5	-0.1	0.3	0.2	0.8	0.2	0.3	-0.5	<b>-1.6</b>	0.0	<b>2.2</b>	-1.0	0.4	-1.2	-1.4	-1.5	0.7	-0.2	0.5	0.054	0.009	
strat fall	<b>-2.2</b>	-0.9	1.4		<b>-1.4</b>		<b>4.9</b>	-0.7	0.0	<b>1.6</b>	-0.3	-0.6	-0.8	1.0	-0.1	0.3	0.4	-0.2	0.7	<b>1.0</b>	<b>-0.8</b>	0.3	-0.6	-0.2	1.0	<b>0.0</b>	<b>1.1</b>	-1.0	0.8	-0.6	0.0	-0.3	-1.1	1.2	-0.1	-0.7	0.4	0.6	<b>1.4</b>	0.018	0.001			
strat annual	<b>1.0</b>	-0.5	0.4	1.3	-0.7	-0.7	<b>-1.3</b>	<b>1.9</b>	-0.7	-0.5	0.3	0.1	-0.1	<b>-0.3</b>	1.3	-0.5	0.2	0.5	0.6	0.2	0.5	-0.3	-0.3	-0.3	0.1	0.5	0.1	0.4	0.1	0.0	-0.6	-0.1	0.3	-1.3	-1.1	0.6	0.5	0.024	0.002					
<b>-- Stratification (10-150m) --</b>																																												
strat winter	0.0	-1.1		<b>0.6</b>	-0.2	0.2		<b>-1.0</b>	<b>-2.0</b>	-1.2	0.6	-0.6	0.1	0.0	-0.1	0.9	-0.1	<b>1.0</b>	0.1	-0.5	-0.1	-0.7	-0.2	0.2	-0.3	0.7	0.0	0.5	<b>1.3</b>	0.8	<b>-1.2</b>	<b>1.0</b>	0.0	-1.2		-0.6		-0.6	0.009	0.001				
strat spring	<b>1.1</b>	-0.7	<b>1.2</b>	<b>1.6</b>	<b>-1.4</b>				<b>1.5</b>	-0.9	0.5	-0.7	<b>2.2</b>	-0.5	-0.1	<b>1.0</b>	1.2	0.2	0.3	-1.1	-1.7	-0.4	0.3	<b>1.0</b>	0.2	-0.2	0.6	0.8	-0.2	0.6	-0.4	-0.8	-0.1	-1.1	0.3	-0.7	-1.3	<b>2.6</b>	0.7	0.011	0.003			
strat summer	<b>1.7</b>	-0.5	0.6	1.0	-0.4	-0.7	<b>-1.1</b>		-0.8	-0.4	-0.4	-0.9	<b>1.3</b>	1.0	-0.3	0.0	0.0	<b>1.0</b>	-0.4	0.5	0.9	-0.5	-0.5	0.3	0.2	0.0	-0.6	0.7	0.4	-1.4	-1.2	0.0	0.2	0.4	0.024	0.004								
strat fall		<b>1.4</b>	0.7				<b>0.5</b>	-0.8	0.0	<b>1.5</b>	-0.3	-0.7	0.1	-0.2	-0.2	0.1	-0.1	<b>0.8</b>	<b>1.3</b>	<b>-1.6</b>	-0.3	0.0	-0.2	0.8	-0.1	<b>1.1</b>	<b>-1.7</b>	<b>1.1</b>	-0.3	0.0	0.4	0.4	-0.7	0.6	-0.3	-0.8	-0.8	0.7	<b>1.3</b>	<b>1.8</b>	0.018	0.005		
strat annual	<b>1.0</b>	-0.8	1.0	1.0	-0.8	-0.4	-0.5	0.5	-0.8	-0.6	0.7	-0.7	-0.1	0.1	0.8	-0.3	0.0	0.4	0.5	0.4	0.6	-0.7	-0.4	0.1	0.5	-0.1	0.2	0.2	0.3	-0.3	-0.3	0.3	-0.7	-1.1	0.3	1.0	0.5	0.016	0.007					



*Figure 20: Normalized anomalies of summer (May–July) cold intermediate layer (CIL) statistics at Station 27 since 1951. Only years where at least 8 months of the years are sampled are presented. The top panel shows the CIL mean temperature, the middle the CIL core temperature (minimum temperature of the CIL) and the bottom panel the depth of the CIL core. Shaded gray areas represent the climatological (1991–2020) average  $\pm 0.5$  SD range considered “normal”. The CIL core temperature anomalies (middle panel) contribute to the NL climate index described in the summary (Figure 39).*

### Station 27 - Mixed layer depth

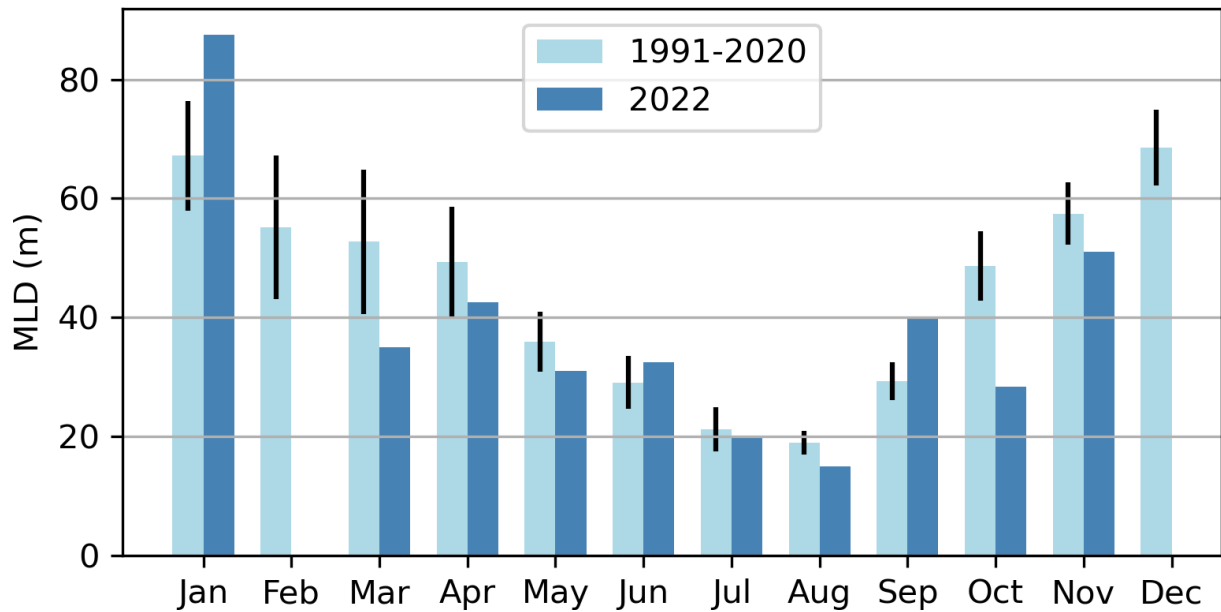


Figure 21: Bar plot of the monthly averaged mixed layer depth (MLD) at Station 27. The 1991–2020 climatology is shown in light blue while the update for 2022 is shown in dark blue. The black lines represent 0.5 SD above and below the climatology. No observations were made in February and in December.

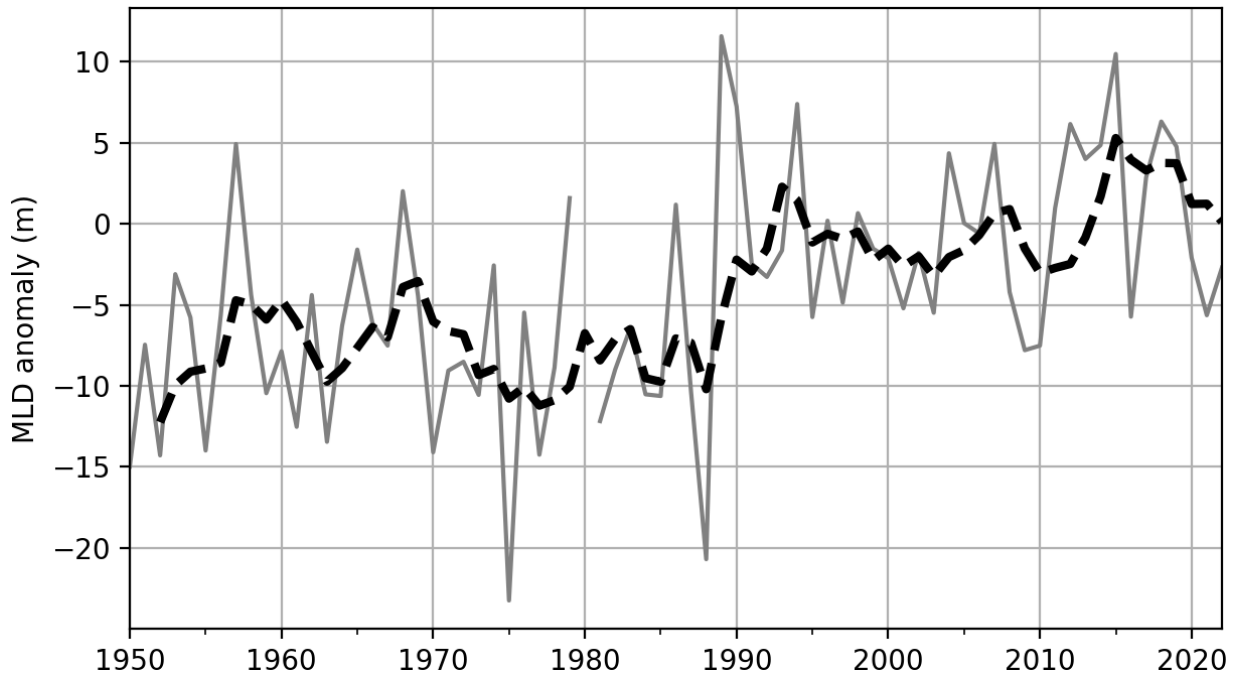


Figure 22: Time series of the annual mixed layer depth (MLD) average at Station 27 since 1950 (gray solid line) and its 5-year running mean (dashed-black line).

## Station 27 - Stratification

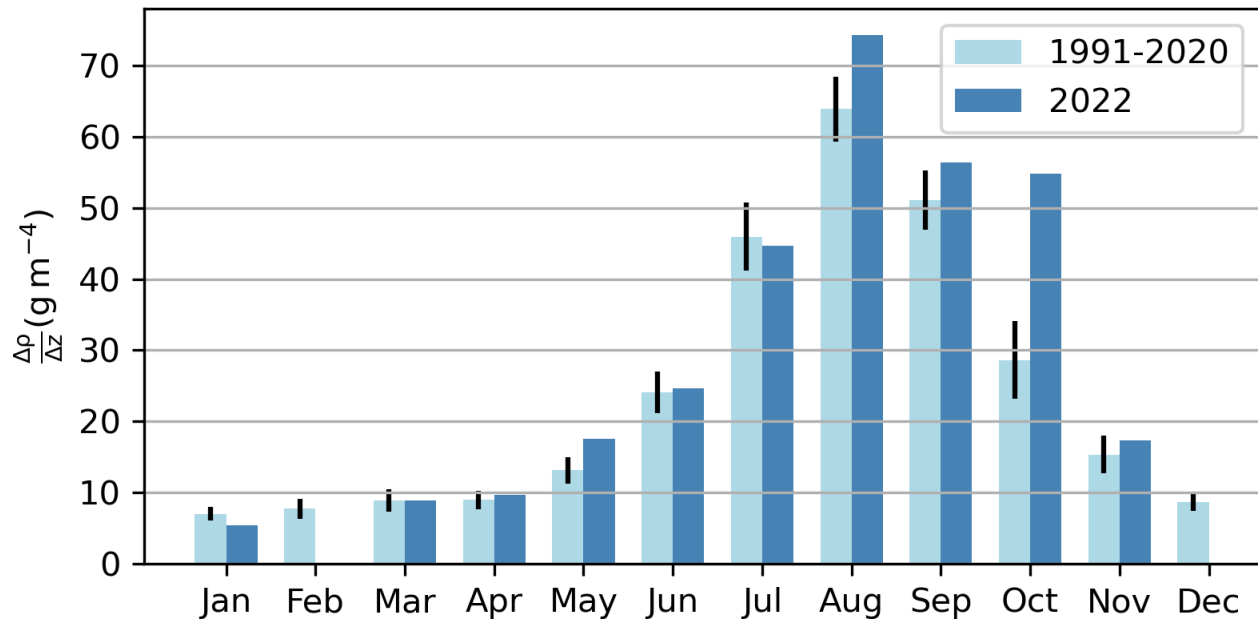


Figure 23: Bar plot of the monthly average stratification (defined as the density difference between 0 and 50 m) at Station 27. The 1991–2020 climatology is shown in light blue while the update for 2022 is shown in dark blue. The black lines represent 0.5 SD above and below the climatology. No observations were made in February and in December.

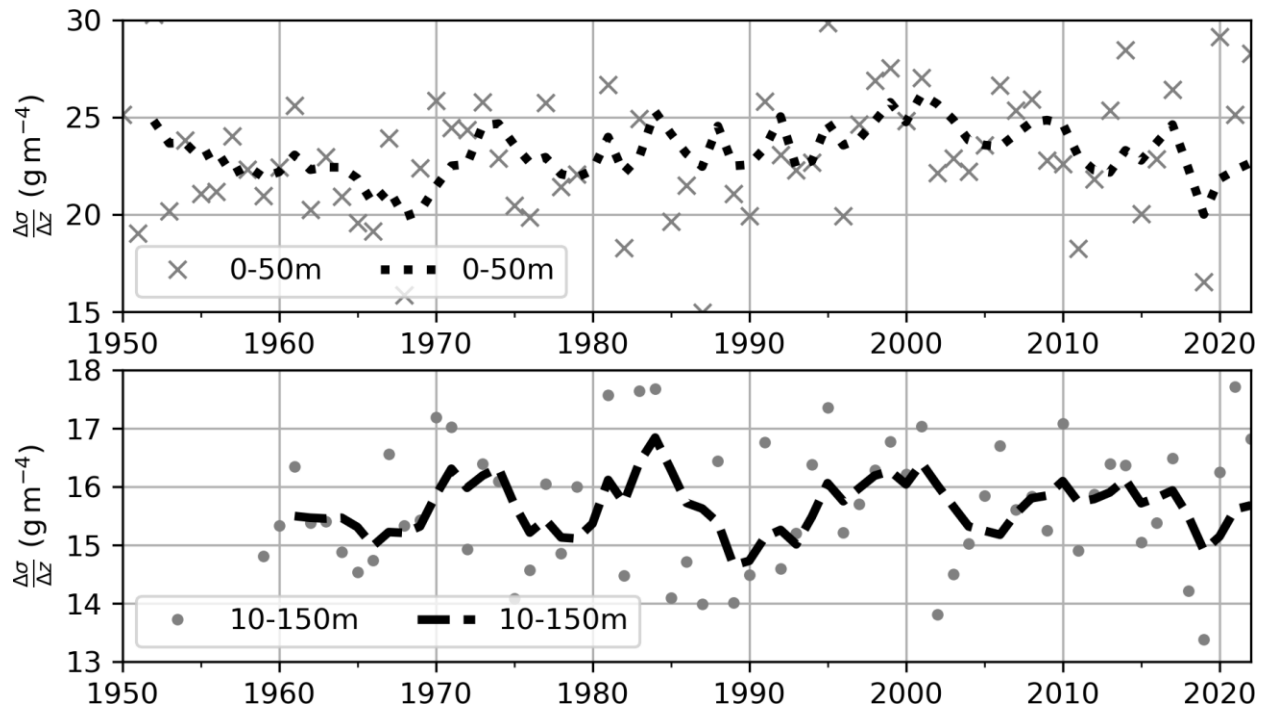


Figure 24. Time series of the annual average stratification at Station 27 between 0 and 50m (gray crosses; top) and 10 and 150m (gray dots; bottom) since 1950. For each panel, the 5-year running mean is shown as a dotted/dashed black line. Note the different vertical axis for the two panels.

## 6.2 Standard hydrographic sections

In the early 1950s, several countries under the auspices of the International Commission for the Northwest Atlantic Fisheries (ICNAF) carried out systematic monitoring along hydrographic sections in NL waters. In 1976, ICNAF normalized a suite of oceanographic monitoring stations along sections in the Northwest Atlantic Ocean from Cape Cod (USA) to Egedesminde (West Greenland) (ICNAF, 1978). In 1998 under the AZMP, the Seal Island (SI), Bonavista Bay (BB), Flemish Cap (47°N) (FC) and Southeast Grand Bank (SEGB) historical stations were selected as core monitoring sections. The White Bay section (WB) continued to be sampled during the summer as a long time series ICNAF/NAFO section (see Figure 1).

Two ICNAF sections on the mid-Labrador Shelf, the Beachy Island (BI) and the Makkovik Bank (MB) sections, were selected to be sampled during the summer if survey time permitted. Starting in the spring of 2009, a section crossing south-west over St. Pierre Bank (SWSPB) and one crossing south-east over St. Pierre Bank (SESPB) were added to the AZMP surveys.

In 2022, the summer survey was canceled. During the spring 2022 survey (April 9-May 1 onboard RV Atlantis), sections SWSPB, SESPB, SEGB, FC, and BB were sampled and during the fall 2022 survey (October 21-November 8 onboard RRS James Cook), sections SEGB, FC, BB and SI were sampled. In this manuscript we present the fall cross sections of temperature and salinity and their anomalies along the SI, BB and FC sections to represent the vertical temperature and salinity structure across the NL Shelf during 2022.

### 6.2.1 Temperature and Salinity Variability

The water mass characteristics observed along the standard sections crossing the NL Shelf are typical of Arctic-origin waters with a subsurface temperature range of -1.5°C to 2°C and salinities from 31.5 to 33.5. Labrador Slope water flows southward along the shelf edge and into the Flemish Pass and Flemish Cap regions. With temperatures in the range of 3°C to 4°C and salinities in the range of 34 to 34.75, this water mass is generally warmer and saltier than the shelf waters. Surface temperatures normally warm to between 10°C and 12°C during late summer, while bottom temperatures remain <0°C over much of the Grand Banks, increasing to between 1°C and 3.5°C near the shelf edge below 200 m and in the deep troughs between the banks. In the deeper (>1,000 m) waters of the Flemish Pass and across the Flemish Cap, bottom temperatures generally range from 3°C to 4°C. In general, the near-surface water mass characteristics along the standard sections undergo seasonal modification from annual cycles of air-sea heat flux, wind-forced mixing, and the formation and melting of sea ice. These mechanisms cause intense vertical and horizontal temperature and salinity gradients, particularly along the frontal boundaries separating the shelf and slope water masses. The seasonal changes in the temperature and salinity fields along the Bonavista section are presented in Colbourne et al. (2015).

Summer temperature and salinity structures along the SI, BB and FC (47°N) hydrographic sections are normally presented in this report. In the absence of summer survey, fall sections are presented in Figure 25 to Figure 27. The dominant thermal feature along these sections is associated with the cold and relatively fresh CIL overlying the shelf. This water mass is separated from the warmer and denser water of the continental slope region by strong temperature and salinity fronts. The cross-sectional area (or volume) of the CIL is bounded by the 0°C isotherm and highlighted as a thick black contour in the temperature panels. The CIL parameters are regarded as robust indicators of ocean climate conditions on the eastern Canadian Continental Shelf. While the CIL area undergoes significant seasonal variability, the changes are highly coherent from the Labrador Shelf to the Grand Banks. The CIL remains present throughout most of the summer until it gradually decays during the fall as increasing winds and storm episodes deepen the surface mixed layer.

The extent of the record-warm fall SSTs during 2022 can be appreciated from the section plots extending from Labrador shelf (section SI) to the Newfoundland shelf (BB) and to the Grand Banks (FC) with the presence of a relatively thin (>50m) and very warm (+3.5°C above normal) layer near the surface across the shelf (Figure 25 to Figure 27, bottom left). Interestingly, in the sub-surface (~50-200m, the depth range of the CIL), the water was colder than average, possibly because this water is a remnant of winter water advected from the north where the winter was relatively cold. In addition, a more stratified water column due to warmer SST may also imply less vertical mixing and a slower seasonal warming of the CIL due to limited heat transfer (Cyr et al., 2011).

The corresponding salinity cross sections show a relatively fresh (<33) upper water layer over the shelf with sources from Arctic outflow on the Labrador Shelf, in contrast to the saltier Labrador Slope water further offshore with values >34 (Figure 25 to Figure 27, right panels). In 2022, salinities were slightly fresh at the surface and slightly higher than normal at the depths of the CIL.

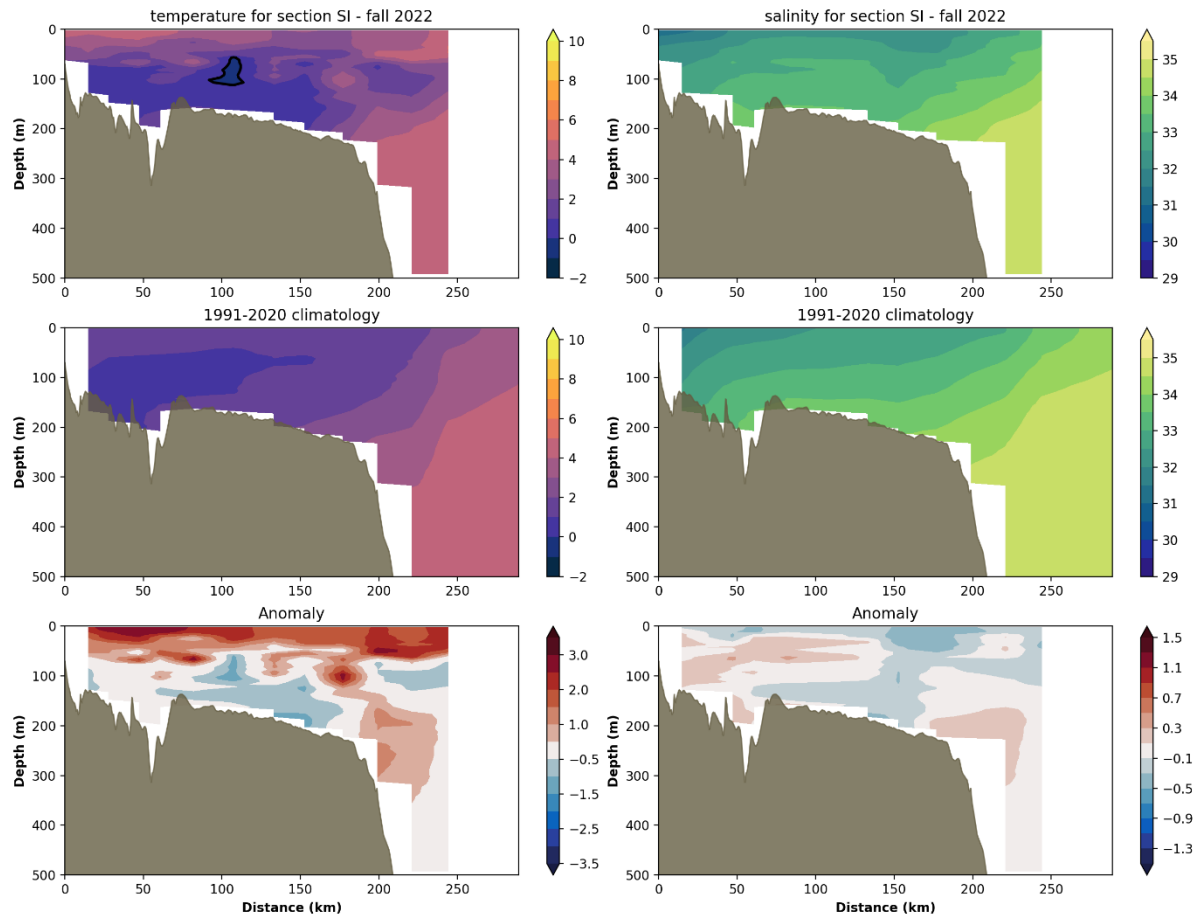


*Figure 25: Contours of temperature (°C), left column, and salinity, right column, during fall 2022 (top row), with climatological averages (middle row) for the Seal Island (SI) hydrographic section (see map Figure 1 for location). Their respective anomalies for 2022 are plotted in the bottom panels.*

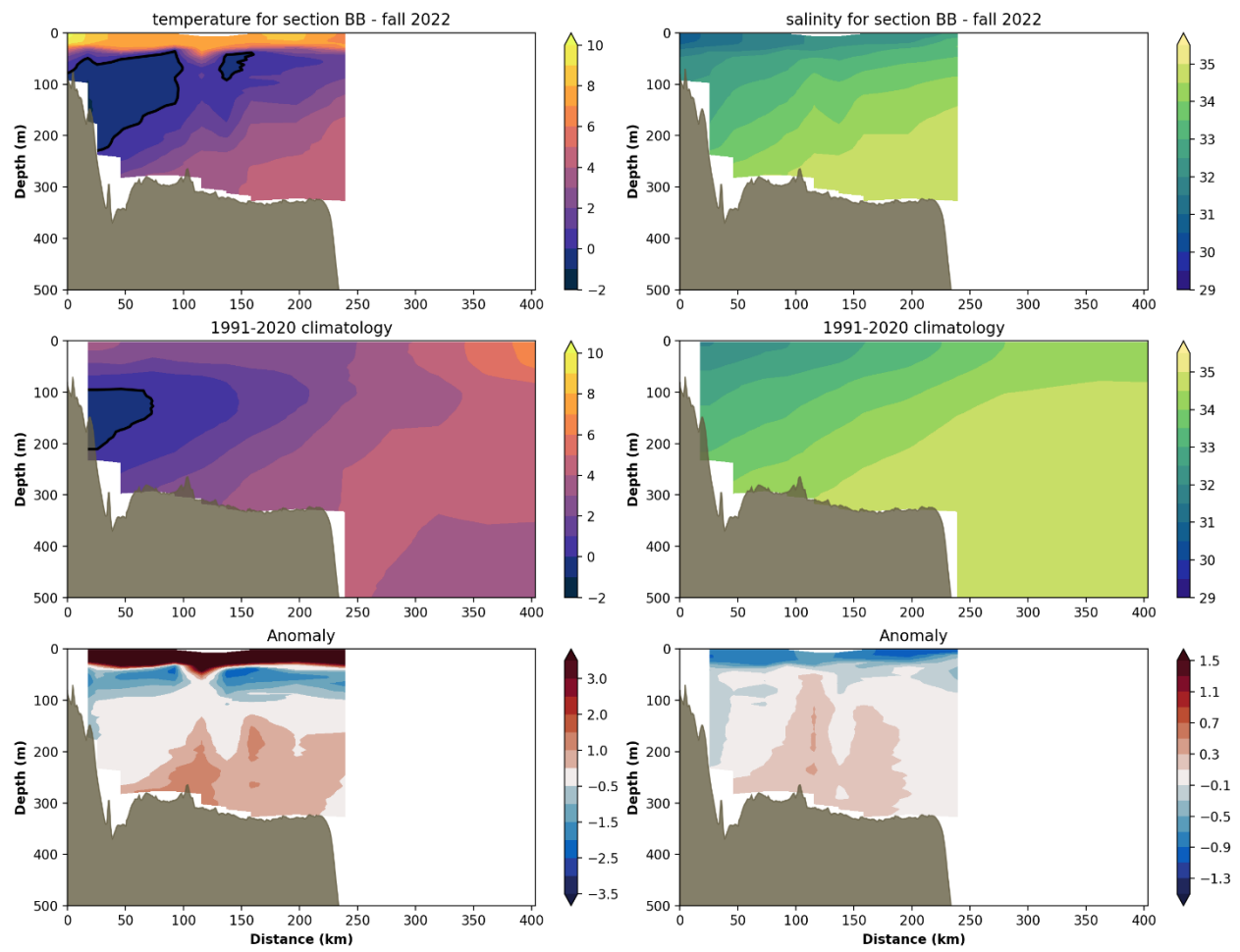


Figure 26: Same as in Figure 25, but for the Bonavista (BB) hydrographic section (see map Figure 1 for location).

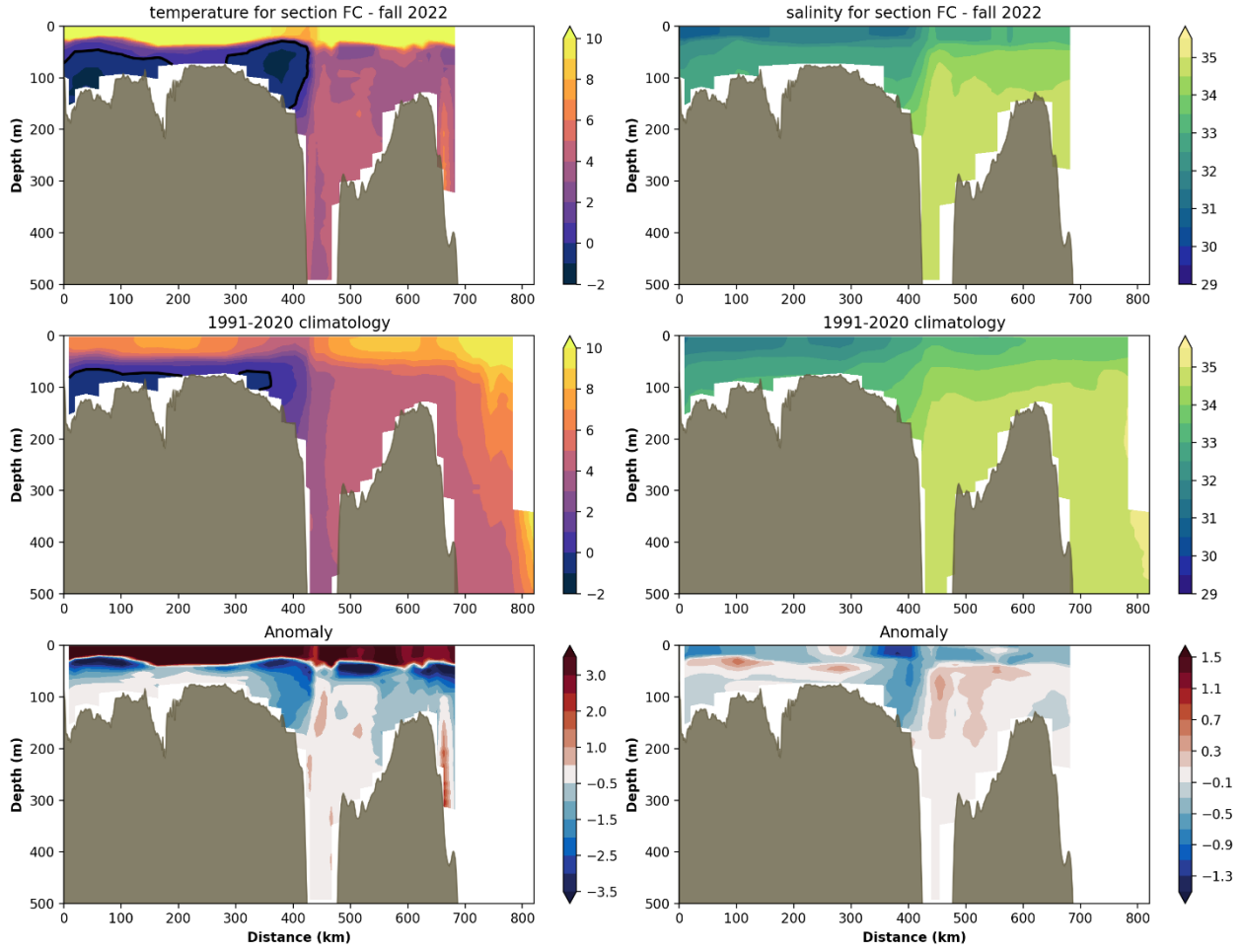


Figure 27: Same as in Figure 25, but for the Flemish Cap (FC) hydrographic section (see map Figure 1 for location).

## 6.2.2 Cold Intermediate Layer Variability

Statistics of summer CIL anomalies (CIL area, CIL core temperature and CIL core depth) for the three sections discussed above (SI, BB and FC) are presented in a scorecard in Figure 28. The climatological average cross-sectional areas of the summer CIL along these sections are  $19.9 \pm 4.1 \text{ km}^2$ ,  $22.9 \pm 7.6 \text{ km}^2$  and  $16.5 \pm 6.4 \text{ km}^2$ , respectively. The averaged anomalies of the CIL cross-sectional area for these three sections are summarized in Figure 29 as a time series going back to 1950. In general, the summer CIL has been predominantly warmer and smaller than average since the mid-1990s, with a cooling trend emerging since about 2012 or 2014 to 2017. However, the most striking aspect of this long time series is the warm conditions that prevailed in the mid-1960s and mid-1970s, followed by a cold period that lasted from the mid-1980s to the mid-1990s.

Unfortunately, due to ship unavailability, no hydrographic survey was realized along sections SI, BB and FC in 2022. We therefore re-constructed the temperature fields by using all available casts from Coyne et al. (2023) in a radius of  $0.1 \times 0.1$  (latitude x longitude) surrounding the nominal position of each station on a section. After visual inspection of the re-constructed section, we provide an update for the CIL when

the re-construction is satisfactory. In 2022, this led to the determination of the CIL area for sections BB and FC (Figure 28). A similar interpolation procedure was done in previous years when section occupations were lacking or before AZMP when stations were not standardized. The years where data are re-constructed are identified in the bottom row of the scorecards with small black dots (Figure 28). Because this method uses the average between June and August, the core CIL temperature is not derived.

In 2022, this led to near-normal CIL area (-0.6 SD for BB and +0.4 SD for FC). Averaged together, this leads to a normal CIL subindex for 2022 of +0.1 SD for 2022 (Figure 29). The normal CIL is likely the result of the relatively cold winter that occurred in Labrador and in the Eastern Arctic in 2022. This is because summer CIL properties are a remnant of the previous winter's conditions that are advected from the north during the rest of the year.

	-- Seal Island section --																												x	sd																	
CIL area (km <sup>2</sup> )	-0.3	-1.3	0.6	0.0	2.2	1.0	-1.8	0.5	-2.7	-1.9	1.7	2.0	0.9	1.2	1.0	-0.7	0.2	-0.4	-0.2	-1.0	0.4	-0.3	0.1	-1.7	-0.1	-0.1	-0.2	0.5	0.6	-0.8	-1.2	0.2	-0.6	0.6	1.4	-0.5	1.1	-1.7	-0.6	-1.9	2.1	21.7	4.9				
CIL core (°C)																			-1.6	-0.9	1.3	-0.6	-0.9	1.0	0.9	-0.8		0.8	1.0	0.1	-1.0	-0.6	1.0	1.3	-0.7	1.0	-1.3	-0.1	-0.8	-0.9	1.3	-0.8	1.3	1.3	-1.5	0.2	
June-Aug. ave.	•	•	•	•	•	•	•	•	•	•	•	•	•	•	•	•	•	•	•	•	•	•	•	•	•	•	•	•	•	•	•	•	•	•	•	•	•	•									
	-- Bonavista section --																																														
CIL area (km <sup>2</sup> )	0.0	0.3	1.7	1.5	3.1	1.8	0.0	-0.2	1.1	0.6	2.2	2.6	1.0	1.1	0.1	-0.3	0.1	-0.4	-1.2	-0.6	-0.5	-0.4	-1.1	-0.1	0.0	-0.5	-0.7	-0.1	-0.7	0.5	-0.2	-2.0	-0.1	-0.5	1.8	1.0	0.7	0.5	-0.3	-0.9	-1.1	-1.3	-0.6	23.0	7.9		
CIL core (°C)																			-1.3	-0.8	-0.5	0.1				-0.5	1.0	1.0	1.2	0.8	-0.3	-0.9	0.8	2.2	-1.0	0.3	-1.2	-0.8	-1.1	0.7	0.4	1.1	1.5		-1.6	0.1	
June-Aug. ave.	•	•	•	•	•	•	•	•	•	•	•	•	•	•	•	•	•	•	•	•	•	•	•	•	•	•	•	•	•	•	•	•	•	•	•	•	•	•	•	•	•	•	•	•	•	•	
	-- Flemish Cap section --																																														
CIL area (km <sup>2</sup> )	-2.0	-1.3	0.0	2.8	1.4	1.5	0.0	-0.4	-0.1	1.2	0.4	1.8	0.0	1.6	-0.3	0.2	-0.3	-0.9	-0.6	0.3	-1.7	-1.5	-1.5	0.5	0.1	0.1	-0.6	-1.1	0.3	0.8	-1.2	-1.1	0.4	-0.6	0.5	1.4	2.3	-0.5	0.3	1.0	0.1	-1.5	0.4	17.8	6.9		
CIL core (°C)																			-1.1	-1.0	-0.6	0.7				0.2	1.1	0.1		-0.2	-1.0	1.9	1.6	-1.1	1.8	-0.9	-1.1	-0.3	0.0	-0.5	0.1	-0.8	-0.4		-1.5	0.2	
June-Aug. ave.	•	•	•	•	•	•	•	•	•	•	•	•	•	•	•	•	•	•	•	•	•	•	•	•	•	•	•	•	•	•	•	•	•	•	•	•	•	•	•	•	•	•	•	•	•	•	•

Figure 28: Scorecards of the cold intermediate layer (CIL) summer statistics along the Seal Island, Bonavista and Flemish Cap hydrographic sections. The CIL area is defined as all water below 0°C (see black contours in Figure 25 to Figure 27) and the CIL core temperature as the minimum temperature of the CIL. Color codes for the CIL area have been reversed (positive is blue and negative is red) because a large CIL represents cold conditions, and vice-versa. Grayed cells indicate an absence of data. When possible, the AZMP station labeled in the data files are used, but in some instances (indicated here by black dots in the last row of each table) the average June-August profile of all available casts in at 0.1x0.1 (lat x lon) box around the nominal station locations are used to reconstruct the section.

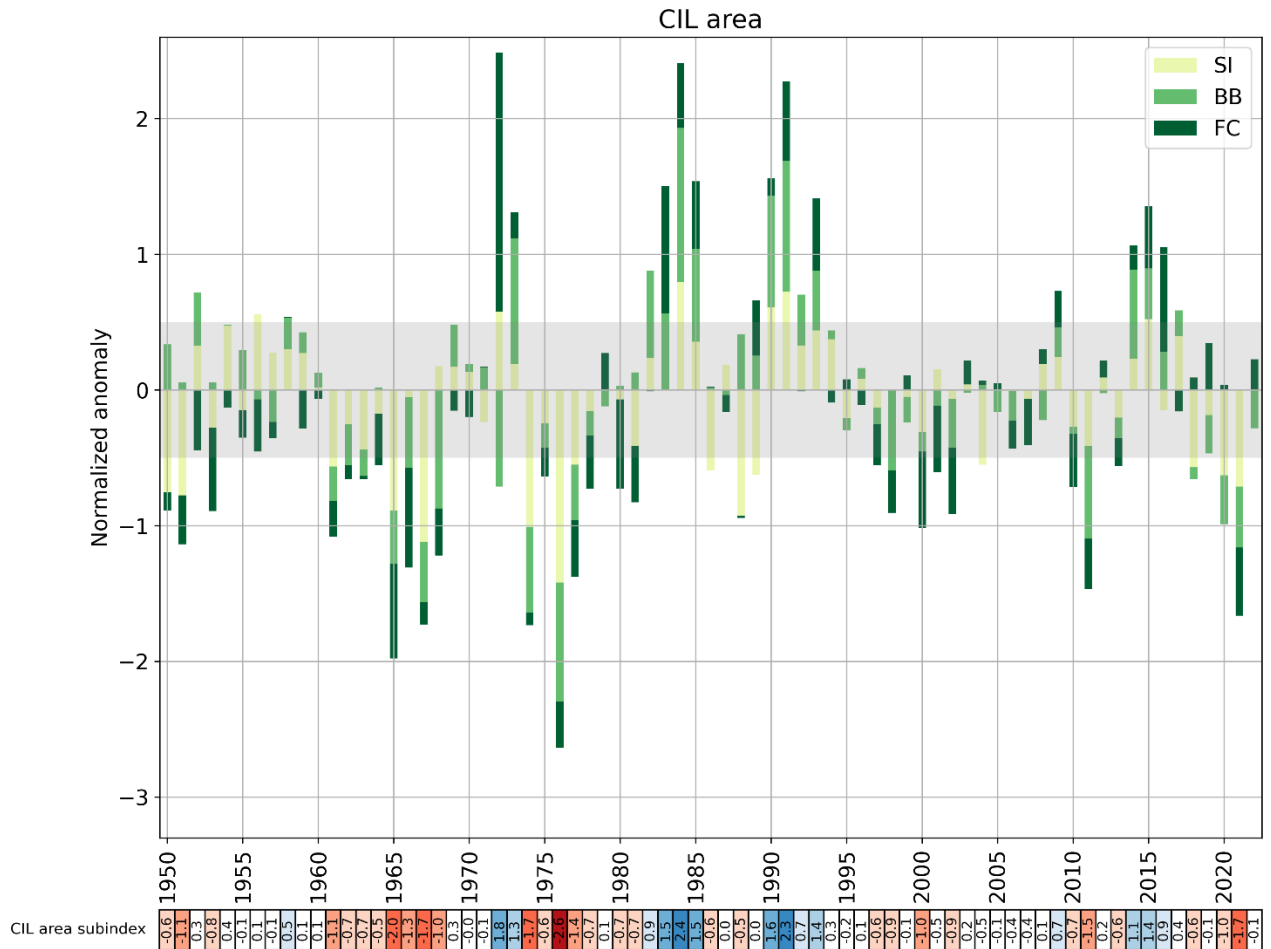


Figure 29: Normalized anomalies of the mean CIL area for hydrographic sections Seal Island (SI), Bonavista Bay (BB) and Flemish Cap (FC). This time series corresponds to the average of the three sections, in which the contribution of each section is represented (values for each separate section since 1980 can be found in Figure 28). The shaded area corresponds to the 1991–2020 average  $\pm 0.5$  SD, a range considered “normal”. The numerical values of this time series are reported in a color-coded scorecard at the bottom of the figure. Here negative anomalies (generally corresponding to warmer conditions) are colored red and positive anomalies blue. This time series is one component of the NL climate index (Figure 39).

## 6.3 Bottom observations in NAFO sub-areas

Canada has been conducting stratified random bottom trawl surveys in NAFO Sub-areas 2 and 3 on the NL Shelf since 1971. Areas within each division, with a selected depth range, were divided into strata, and the number of fishing stations in an individual stratum was based on an area-weighted proportional allocation (Doubleday, 1981). Temperature profiles (and since 1990, salinity profiles) are available for most fishing sets in each stratum. These surveys provide large spatial-scale oceanographic data sets for the Newfoundland and Labrador Shelf. NAFO Subdivision 3Ps on the Newfoundland south coast and Divisions 3LNO on the Grand Banks are surveyed in the spring, and Divisions 2HJ off Labrador in the north, 3KL off eastern Newfoundland, and 3NO on the southern Grand Bank are surveyed in the fall. The hydrographic data collected on these surveys are routinely used to assess the spatial and temporal variability in the thermal habitat of several fish and invertebrate species. Many products based on the data are used to characterize the oceanographic bottom habitat. Among these are contour maps of the bottom

temperatures and their anomalies, the area of the bottom covered by water in various temperature ranges, etc. In addition, species-specific ‘thermal habitat’ indices are often used in marine resource assessments for snow crab and northern shrimp.

The current method to derive the bottom temperature originally introduced by Cyr et al. (2019) was slightly modified this year to restrict the horizontal distance of the interpolation between observations. First, all available annual profiles of temperature and salinity from the CASTS dataset (Coyne et al., 2023) are vertically averaged in 5 m bins and linearly interpolated to fill missing bins. Then, for each season (April-June for spring and September-December for fall), all data are averaged on a regular  $0.1^\circ \times 0.1^\circ$  (latitudinal x longitudinal) grid to obtain one seasonal profile per grid cell. Since this grid has missing data in many cells, each depth level is horizontally linearly interpolated. New from this year, the horizontal interpolation is limited to points that are less than 2 degrees (latitude or longitude) apart. Then for each grid point, the bottom observation is considered as the data at the closest depth to the GEBCO\_2014 Grid bathymetry ([version 20141103](#)), to a maximum 50 m difference. For areas where the interpolation is not possible (for example when the distance between observations is more than 2 degrees apart), missing values for bottom temperature are filled with the climatology. Lastly, bottom observations deeper than 1,000 m are clipped as they are down the continental slope in a depth range with much lower data coverage. This method is applied for all years between 1980 and 2022 from which the 1991–2020 climatology is derived. Anomalies for 2022 are calculated as the difference between annual observations and the climatology.

### 6.3.1 Spring Conditions

Maps of spring climatological temperature and salinity, together with 2022 observations and anomalies for NAFO divisions 3LNOPs, are presented in Figure 30 and Figure 31, respectively (with the center panel for station occupation coverage). It is the first time since 2019 that spring bottom observations are complete for this region. Due to the COVID-19 pandemic, the area was not surveyed during the spring of 2020, while in 2021 only the division 3Ps was properly sampled.

Except for the eastern half of the Grand Banks, widespread warmer-than-average temperatures were found in 3Ps and 3LNO (Grand Banks) in 2022. Temperatures were above  $0^\circ\text{C}$  over the shallower St. Pierre Bank (eastern 3Ps) and above  $6^\circ\text{C}$  in the deep Laurentian Channel, leading to widespread warm anomalies over this division, especially in the shallower part where temperatures were  $0.5^\circ\text{C}$  to  $2.5^\circ\text{C}$  above the climatological mean and in the Halibut channel where temperatures were as warm as  $3.5^\circ\text{C}$  above the climatological mean (Figure 30, right panel). The warmest anomalies were however in 3O (western Grand Banks), where most of the division was  $3.5^\circ\text{C}$  above the climatological mean, including in the Avalon channel.

Spring bottom salinities in 3LNO generally range from 32 to 33 over the central Grand Bank, and from 33 to 35 closer to the shelf edge (Figure 31, left panel). In 2022, salinities were close to normal to slightly fresh in most of the shallower areas of 3Ps and 3LNO (Figure 31, right panel). High salinity anomalies were however found in the deeper areas, such as the 3PS slope and in the Avalon and Halibut channels.

Climate indices based on normalized spring bottom temperature anomalies (mean temperature and temperature in areas shallower than 200 m), as well as the area of the sea floor covered by water above  $2^\circ\text{C}$  and below  $0^\circ\text{C}$  between 1980 and 2022 are shown in a color-coded scorecard in Figure 32. Overall, the colors visually highlight two contrasting periods of this time series: the cold period of the late 1980s / early 1990s (mostly blue cells) and the warm period of the early 2010s (mostly red cells). This warm period lasted between 2010 and 2013 (2011 being the warmest at  $2.1 \text{ SD}$  above normal in 3LNO) before returning towards to normal values between 2015 and 2019 (2014 was slightly cold). Between 2016 and 2019 the bottom area that was covered by  $<0^\circ\text{C}$  water was also normal. No information was available for 2020 and 2021.

Division 3Ps bottom temperatures exhibit some similarities to those from 3LNO, with two periods of warm years, 1999–2000 and 2005–06, separated by a colder period (2003 is the coldest year on record since 1991 at -1.9 SD). With the exception of 2017 (which was normal, and possibly 2020 for which there is no data), all years between 2010 and 2022 were warmer than normal. 2021 and 2022 are the warmest years on record since 1980 at +2.5 SD and +2.8 SD, respectively. 2022 also established a new record for the area of the seafloor covered with water  $>2^{\circ}\text{C}$  at +4.4 SD, beating the 2021 record of +3.6 SD.

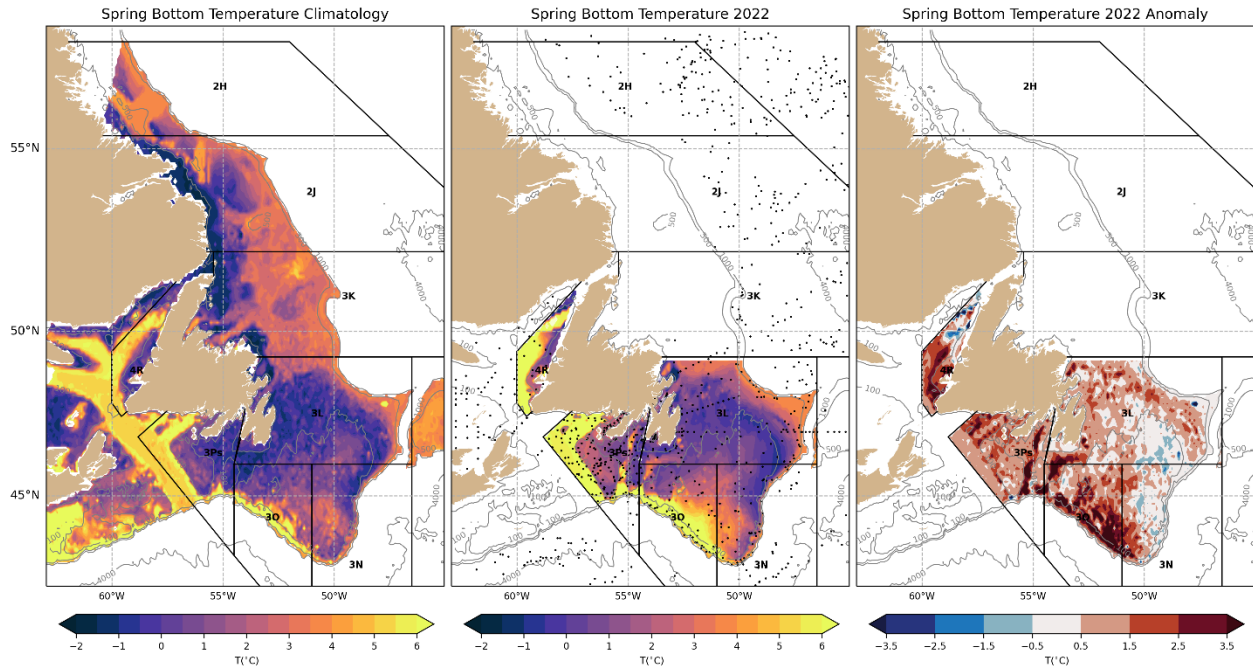


*Figure 30: Maps of the climatological (1991–2020) mean spring bottom temperature (left), and spring 2022 bottom temperature (center) and anomalies (right) for NAFO Divisions 3LNOPs only. The location of observations used to derive the temperature field is shown as black dots in the center panel. When applicable, portion of the shelf where missing bottom temperature were filled with the climatology (see methodology) are left semi-transparent.*

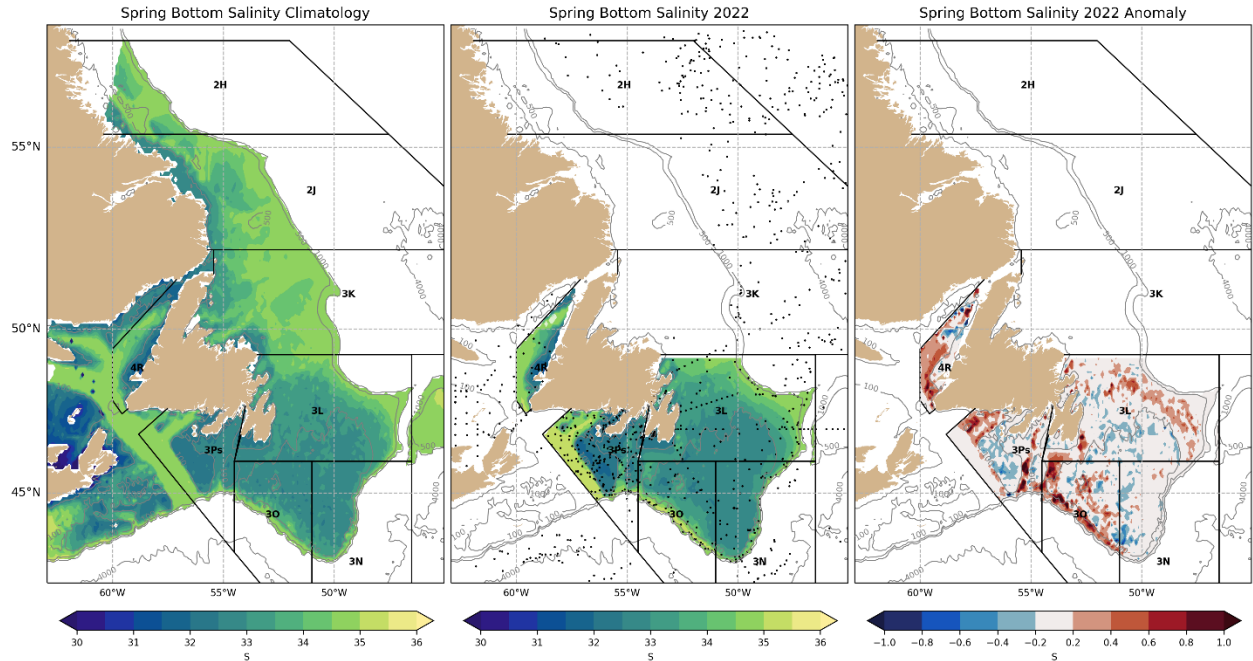


*Figure 31: Maps of the climatological (1991–2020) mean spring bottom salinity (left), and spring 2022 bottom salinity (center) and anomalies (right) for NAFO Divisions 2J3KLNO only. The location of observations used to derive the salinity field is shown as black dots in the center panel. When applicable, portion of the shelf where missing bottom salinity were filled with the climatology (see methodology) are left semi-transparent.*

		-- NAFO division 3LNO --																																												
		80	81	82	83	84	85	86	87	88	89	90	91	92	93	94	95	96	97	98	99	00	01	02	03	04	05	06	07	08	09	10	11	12	13	14	15	16	17	18	19	20	21	22	$\bar{x}$	sd
T <sub>bot</sub>		-0.1	1.3	-0.6	1.2	-1.0	-1.6	-1.3	-0.5	-0.3	-1.3	-2.0	-2.0	-1.8	-1.3	-1.7	-0.9	-0.1	-0.9	0.7	1.2	0.5	-0.1	-0.2	-1.1	1.2	0.6	0.4	0.2	0.2	0.2	0.8	2.1	1.4	1.1	-0.6	-0.1	-0.3	-0.1	0.2	0.2	1.6	1.1	0.6		
T <sub>bot &lt; 200m</sub>		-0.2	1.5	-0.4	1.7	-0.9	-1.5	-1.3	-0.4	-0.1	-1.0	-1.9	-2.0	-1.6	-1.2	-1.7	-0.9	0.0	-1.1	0.8	1.4	0.6	-0.1	-0.1	-1.2	1.2	0.5	0.4	0.2	0.0	0.1	0.7	2.1	1.5	1.1	-0.6	-0.1	-0.3	-0.1	0.2	0.2	1.6	0.7	0.6		
Area > 2°C		-0.2	1.2	-1.3	1.2	-0.8	-1.6	-1.2	-0.4	-0.4	-1.6	-1.9	-1.7	-1.8	-1.1	-1.6	-0.5	-0.2	-0.8	0.7	1.2	0.3	-0.7	-0.3	-1.0	1.7	0.4	0.1	0.4	0.4	0.6	0.2	2.6	1.5	0.3	-0.7	0.4	-0.5	0.1	-0.3	0.1	1.7	70.822.6			
Area < 0°C		-0.4	-1.0	0.0	0.0	1.0	1.3	1.2	0.8	0.6	1.0	1.6	1.9	1.4	1.3	1.4	0.9	0.0	1.0	-0.6	-1.1	-0.1	0.0	0.2	1.0	-1.6	-0.7	-1.4	0.2	0.1	0.4	-1.6	-1.9	-0.9	-1.0	0.8	0.5	0.2	0.1	-0.2	-0.1	-1.1	90.143.8			
T <sub>bot</sub>		-0.7	0.1	1.1								-1.2	-1.4	-0.9	-0.3	-1.3	-0.4	0.7	1.1	-1.2	-0.6	1.9	-0.3	0.6		-1.3	-0.5	0.3	0.7	1.2	1.2	0.9	0.5	0.5	1.6	0.2	1.1	0.8		2.5	2.8	2.3	0.5			
T <sub>bot &lt; 200m</sub>		-0.1	0.5	1.1								-1.7	-1.5	-0.9	-0.1	-1.3	0.1	1.0	1.3	-1.0	-0.7	-1.9	0.0	1.0		-0.9	-0.1	0.6	0.6	1.5	1.0	1.1	0.2	0.3	1.1	-0.4	0.9	0.0		2.0	2.2	0.8	0.6			
Area > 2°C		1.3	1.8	2.8								-0.7	-1.0	0.0	-0.5	-1.1	-0.2	2.0	1.9	-1.4	-1.1	-1.6	-0.7	0.4		-1.3	0.3	0.3	0.2	1.5	0.6	0.9	0.1	0.2	0.6	-0.8	1.3	0.0		3.6	4.4	29.8	3.2			
Area < 0°C		0.2	-0.3	-0.6								1.5	1.3	1.2	-0.2	1.5	0.0	-0.6	-0.8	0.9	0.4	2.1	-1.0	-1.1		0.8	0.5	-0.2	-0.8	-1.5	-1.1	-1.2	-0.1	-0.4	-1.0	0.3	-0.9	0.5		-1.5	-1.3	16.3	11.1			

Figure 32: Scorecards of normalized spring bottom temperature anomalies (mean temperature, mean temperature for area shallower than 200 m, and area of sea floor covered by water above 2°C and below 0°C, respectively) for 3LNO and 3Ps.

### 6.3.2 Fall Conditions

Maps of fall climatological temperature and salinity, together with 2022 observations and anomalies for NAFO Divisions 2HJ3KLNO, are presented in Figure 33 and Figure 34 respectively (see center panel for station occupation coverage). In the fall of 2022, the regular multi-species survey sampling was quite limited and the data presented rely on horizontal interpolation over large distances. The results presented must therefore be interpreted with caution.

Bottom temperatures are generally cold ( $<0^{\circ}\text{C}$ ) in shallow areas of 2HJ3KLNO and warmer on the slopes and the different troughs. In 2022, anomalies are slightly warm across the zones. It is important to note that the marked very warm anomalies around the Grand Banks in 3LNO (Figure 33, right panel) correspond to areas without good observational coverage and should not be trusted.

Bottom salinities in divisions 2HJ and 3K generally display an inshore-offshore gradient between  $<33$  close to the coast and 34 to 35 at the shelf edge (Figure 34, left panel). The Grand Banks (3LNO) bottom salinities range from  $<33$  to 35, with the lowest values on the southeast shoal. In 2022 the bottom salinities were close to normal in most of the region, except for some high salinity anomalies that correspond to the region with little observational coverage (Figure 34, right panel). The latter should not be trusted.

Normalized bottom temperature anomalies (mean temperature and temperature in areas shallower than 200 m), as well as area of the sea floor covered by water above  $2^{\circ}\text{C}$  and below  $1^{\circ}\text{C}$  between 1980 and 2022 are shown in a color-coded scorecard in Figure 35. A clear cold period is visible from the early 1980s to the mid-1990s, with the coldest anomalies reached in NAFO Divisions 2J and 3K. This was followed by a warmer period peaking in 2010 and 2011, the warmest years on records for these divisions. After a slight return to normal-to-cold anomalies between 2012 and 2017, bottom temperatures have been generally above normal since. In 2022, these metrics were not derived for 2H and 2J, and they were slightly above average for 3K and 3LNO, although caution should be taken when interpreting these values.

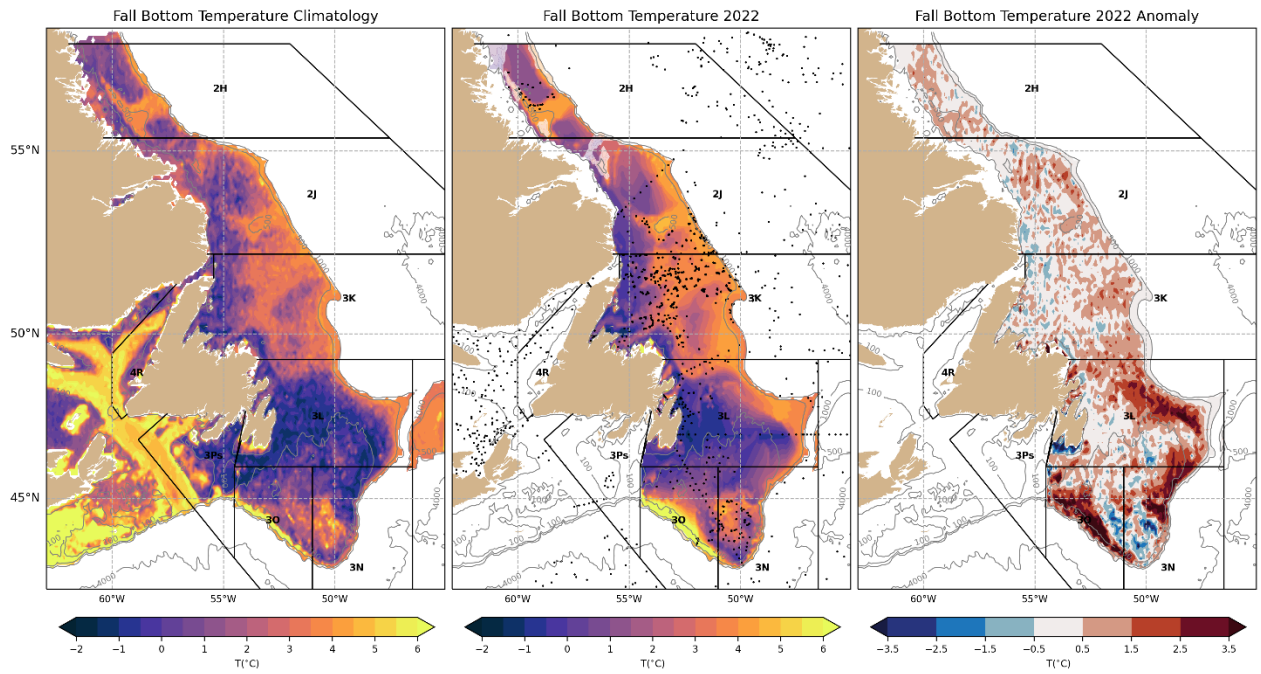


**Figure 33:** Maps of the climatological (1991–2020) mean fall bottom temperature (left), and fall 2022 bottom temperature (center) and anomalies (right) for NAFO Divisions 2HJ3KLNO only. The location of observations used to derive the temperature field is shown as black dots in the center panel. When applicable, portion of the shelf where missing bottom temperature were filled with the climatology (see methodology) are left semi-transparent.

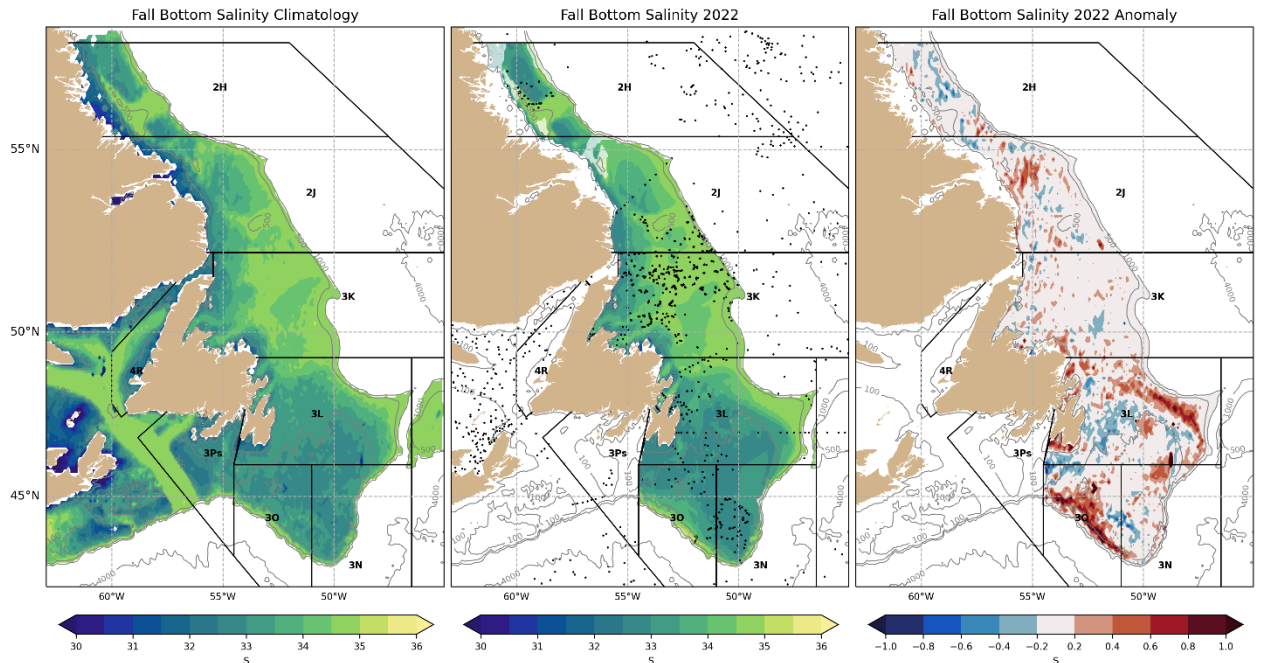


**Figure 34:** Maps of the climatological (1991–2020) mean fall bottom salinity (left), and fall 2022 bottom salinity (center) and anomalies (right) for NAFO Divisions 2HJ3KLNO only. The location of observations used to derive the salinity field is shown as black dots in the center panel. When applicable, portion of the shelf where missing bottom salinity were filled with the climatology (see methodology) are left semi-transparent.

	-- NAFO division 2H --																																												
	80	81	82	83	84	85	86	87	88	89	90	91	92	93	94	95	96	97	98	99	00	01	02	03	04	05	06	07	08	09	10	11	12	13	14	15	16	17	18	19	20	21	22	$\bar{x}$	sd
T <sub>bot</sub>	-0.2	-3.2								-2.0					0.0	-0.2	0.5	-1.0		1.3	-0.4	0.2	1.7	2.1	0.4	-0.6	-0.2	-0.7	-0.4	-1.4	0.2	0.2	0.4	1.0		2.3	0.4								
T <sub>bot&lt;200m</sub>	0.5	-2.8								-1.8					0.5	-0.2	0.5	-1.5		1.1	-0.6	-0.8	1.6	1.9	0.1	-0.9	-0.3	0.1	0.0	-1.3	0.2	0.4	0.8	0.6		1.1	0.5								
Area <sub>&gt;2°C</sub>	-0.3	-1.5								-1.2					0.3	0.0	0.4	-1.0		1.6	0.0	-0.2	2.2	1.9	-0.5	-0.5	-1.6	-0.5	-0.9	0.0	0.1	0.5	0.5		21.2	4.3									
Area <sub>&lt;1°C</sub>	-1.0	2.2								1.8					-0.9	0.6	-0.7	0.7		-0.8	1.2	1.1	-1.4	-1.4	-0.2	1.1	0.3	-0.2	0.1	1.3	-0.4	-0.9	-1.1	-1.1		10.1	7.0								
	-- NAFO division 2J --																																												
T <sub>bot</sub>	-0.9	-0.1	-1.8	-1.8	-3.0	-2.5	-0.3	-2.2	-0.4	-1.4	-1.9	-1.5	-2.3	-2.2	-1.6	0.3	-0.1	-0.1	0.3	-0.6	0.5	0.3	0.6	1.0	1.1	-0.4	1.2	-0.1	0.1	1.7	1.7	-0.1	-0.1	-0.6	-0.7	0.1	-0.3	0.7	0.8	0.0	0.9		2.3	0.5	
T <sub>bot&lt;200m</sub>	-0.6	0.1	-1.2	2.0	-2.7	1.8	0.0	-1.8	-0.3	-1.0	1.5	-1.5	-2.2	-2.0	-1.4	0.5	-0.2	-0.2	0.4	-0.5	0.7	0.2	0.6	0.8	1.2	-0.7	1.2	-0.1	0.0	1.6	1.8	-0.2	-0.4	-0.9	-0.8	0.7	-0.3	0.6	1.2	0.0	0.7		1.0	0.7	
Area <sub>&gt;2°C</sub>	-0.8	-0.3	-1.8	-1.4	-2.3	-2.1	-0.2	-1.9	-0.7	-1.5	-1.9	-1.3	-1.7	-2.0	-1.3	0.7	0.1	-0.3	-0.3	-0.6	0.5	0.1	0.4	0.8	1.3	-0.2	1.4	-0.7	-0.3	1.8	2.2	-0.5	-0.3	-0.7	-0.5	0.2	-0.4	0.5	1.2	0.0	0.6		54.7	12.9	
Area <sub>&lt;1°C</sub>	0.6	0.0	1.9	2.0	2.2	2.1	-0.1	2.1	-0.1	1.1	1.8	1.6	2.0	2.0	1.5	-0.4	-0.1	0.3	-0.9	0.6	-0.7	-0.4	-0.5	-0.6	-1.3	0.6	-1.2	0.5	0.0	-1.3	-1.3	0.6	0.4	0.8	0.7	-1.0	0.4	-0.7	-1.3	-0.2	-0.9		19.1	14.2	
	-- NAFO division 3K --																																												
T <sub>bot</sub>	-0.3	-0.3	-0.9	-1.3	1.8	-2.7	-0.5	-1.5	-0.9	-0.9	-2.1	-1.3	-2.1	-2.2	-1.9	-1.1	-0.4	0.3	0.2	0.6	0.2	-0.2	0.4	0.5	1.3	0.7	0.0	0.8	0.6	0.1	1.4	2.1	0.1	0.3	-0.5	0.3	-0.5	-0.9	0.6	0.6	0.5	1.2	0.4	2.6	0.4
T <sub>bot&lt;200m</sub>	-0.1	-0.5	-1.9	-1.9	-2.1	-2.0	0.0	-1.7	-0.9	-0.9	-1.6	-1.7	-1.8	-2.0	-1.5	0.1	0.4	-0.3	-0.6	0.4	-0.6	0.1	0.6	-0.1	1.2	0.7	-0.3	1.0	-0.5	-0.2	1.8	1.5	-0.2	-0.4	-1.0	-0.2	0.9	-0.5	0.8	1.5	0.9	0.7	-0.8	0.5	0.7
Area <sub>&gt;2°C</sub>	-0.2	-0.1	-0.7	-1.3	-1.7	-2.8	-0.2	-1.5	-1.1	-1.0	-2.1	-0.9	-2.0	-2.1	-2.1	-1.5	-0.4	0.5	0.5	0.6	0.4	-0.2	0.7	0.3	0.9	0.9	0.0	0.8	0.6	-0.5	1.5	1.3	0.1	0.5	-0.6	-0.1	-0.8	-0.8	0.8	0.9	0.8	1.0	0.5	78.9	13.0
Area <sub>&lt;1°C</sub>	0.0	0.1	0.6	1.3	1.4	2.6	-0.4	0.8	0.2	0.3	2.6	1.3	1.9	2.5	2.1	0.2	-0.4	0.1	0.2	-0.3	0.4	0.1	-0.6	0.2	-1.2	-0.9	0.4	-1.0	0.1	0.3	-1.3	-1.5	0.2	-0.2	0.5	0.1	-0.6	0.8	-0.9	-1.4	-1.0	-0.6	0.2	13.2	8.7
	-- NAFO division 3LNO --																																												
T <sub>bot</sub>	0.6	-0.4	-0.5	-0.7	-2.0	-1.3	-0.2	-1.0	-0.4	-0.5	-1.1	-1.5	-1.4	-2.2	-1.7	-0.6	0.0	-0.3	0.5	1.5	-0.4	-0.3	-0.1	-0.4	0.8	0.0	0.3	-0.2	-0.7	0.4	1.0	2.2	0.3	0.5	0.1	0.0	0.0	-0.9	0.5	0.4	2.2	1.1	1.2	0.5	
T <sub>bot&lt;200m</sub>	1.0	-0.3	-0.2	-0.6	-2.0	-1.0	0.0	-0.9	-0.2	-0.2	-0.9	-1.4	-1.2	-2.1	-1.6	-0.4	0.2	-0.4	0.5	1.5	-0.6	-0.3	-0.2	-0.5	0.7	0.0	0.3	-0.4	-1.1	0.4	1.0	2.1	0.3	0.5	0.2	-0.1	0.1	-0.9	0.5	0.4	2.4	0.9	0.8	0.5	
Area <sub>&gt;2°C</sub>	0.7	-0.3	-1.0	-0.4	-1.5	-1.7	0.0	-1.0	-0.8	0.1	-1.2	-1.1	-1.3	-1.9	-1.5	-0.8	-0.2	-0.3	0.7	2.0	-0.4	-0.6	-0.5	-0.7	0.4	-0.3	-0.1	-0.4	-0.7	0.2	1.0	2.1	0.5	0.6	0.4	0.0	0.2	-0.8	0.6	0.4	2.4	1.0	78.8	22.6	
Area <sub>&lt;0°C</sub>	-0.5	0.7	0.0	0.9	2.0	0.5	0.2	0.7	0.0	0.3	0.7	1.4	1.2	2.2	1.7	-0.1	0.1	0.6	-0.2	-1.1	0.7	0.2	-0.4	0.1	-1.6	-0.4	-0.9	0.0	0.7	0.0	-1.1	-2.4	0.1	-0.2	0.0	-0.1	0.3	1.1	-0.3	-0.1	-1.6	-0.9	88.5	32.1	

Figure 35: Scorecards of normalized fall bottom temperature anomalies (mean temperature, mean temperature for area shallower than 200 m, and area of sea floor covered by water above 2°C and below 0°C, respectively) for 2H, 2J, 3K and 3LNO.

### 6.3.3 Summary of bottom temperatures

When standardized anomalies of spring and fall bottom temperatures (first row of all scorecards in Figure 32 and Figure 35) are combined in a bar plot, the low frequency patterns of the bottom temperature on the NL shelf become apparent (Figure 36). The coldest period encompasses the mid-1980s to the mid-1990s. Such cold anomalies are not observed later in the time series. For example, despite a winter NAO index leading to colder conditions between about 2012 and 2017 (see section on meteorological conditions), the bottom temperature during these years was just back to normal, following the rather warm period of the mid-1990s to the mid-2010s. While 2021 is the warmest year on record for the bottom temperature (+2.8 SD), 2022 ranked third warmest at +1.2 SD.

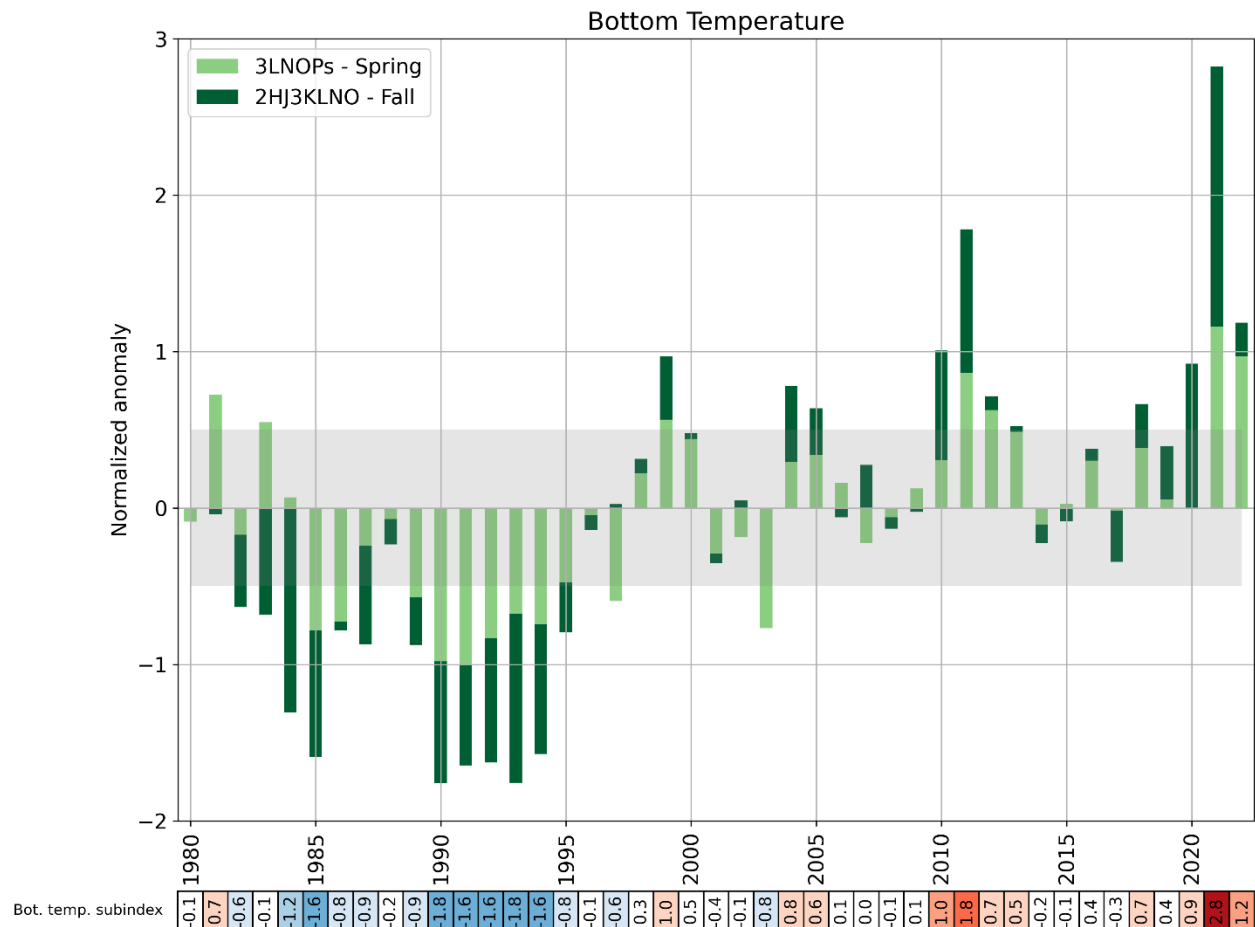


Figure 36: Normalized anomalies of bottom temperature in NAFO Divisions 3LNOPs (spring) and 2HJ3KLNO (fall). This time series corresponds to the average of the two seasons, in which each contribution is represented. The shaded area corresponds to the 1991–2020 average  $\pm 0.5$  SD, a range considered “normal”. The numerical values of this time series are reported in a color-coded scorecard at the bottom of the figure. This time series is one component of the NL climate index (Figure 39).

## 7 Labrador Current transport

The circulation in the NL region is dominated by the south-eastward flowing Labrador Current system, which floods the eastern shelf areas with cold and relatively fresh subpolar waters (Figure 37). This flow can significantly affect physical and biological environments off Atlantic Canada on seasonal and interannual time scales. On the shelf, the Coastal Labrador Current (Florindo-López et al., 2020) originates near the northern tip of Labrador where the outflow from the Hudson Strait combines with the eastern Baffin Island Current and flows southeastward along the Labrador coast. During its southward journey on the Labrador shelf, it is strongly influenced by the seabed topography, following the various cross shelf saddles and inshore troughs. A separate offshore branch of the Labrador Current flows southeastward along the western boundary of the Labrador Sea. This current is part of the large-scale Northwest Atlantic circulation consisting of the West Greenland Current that flows northward along the West Coast of Greenland, a branch of which turns westward and crosses the northern Labrador Sea forming the northern section of the Northwest Atlantic subpolar gyre.

Further south, near the northern Grand Bank, the Coastal Labrador Current becomes broader and less defined. In this region, most of the inshore flow combines with the offshore branch and flows eastward, with a portion of the combined flow following the bathymetry southward around the southeast Grand Bank, and the remainder continuing east and southward around the Flemish Cap (Figure 37). A smaller inshore component flows through the Avalon Channel and around the Avalon Peninsula, and then westward along the Newfoundland south coast. Off the southern Grand Bank the offshore branch flows westward along the continental slope, some of which flows into the Laurentian Channel and eventually onto the Scotian shelf. This extension of the Labrador Current on the Scotian shelf is referred to as the Scotian shelf break current. Additionally, there are strong interactions between the offshore branch of the Labrador Current and large-scale circulation. A significant portion of the offshore branch combines with the North Atlantic Current and forms the southern section of the subpolar gyre. Further east, the Flemish Cap is located in the confluence zone of subpolar and subtropical western boundary currents of the North Atlantic. Labrador Current water flows to the east along the northern slopes of the Cap and south around the eastern slopes of the Cap. In the eastern Flemish Pass, warmer high salinity North Atlantic Current water flows northward contributing to a topographically induced anticyclonic gyre over the central portion of the Cap.

Satellite altimetry data are used over a large spatial area to calculate the annual-mean anomalies of the Labrador Current transport (Han et al., 2014). A total of nine cross-slope satellite altimetry tracks are used to cover the Labrador Current on the NL shelf break from approximately 47°N to 58°N latitude (Figure 37). Similarly, five tracks from approximately 55°W to 65°W longitude are used for the Scotian shelf break current. The nominal cross-slope depth ranges used for calculating the transport are from 200 to 3,000 m isobaths over the NL shelf break and from 200 to 2,000 m isobaths over the Scotian shelf break.

An empirical orthogonal function (EOF) analysis of the annual-mean transport anomalies was carried out. An index was developed from the time series of the first EOF mode and normalized by dividing the time series by its SD. The mean transport values are provided based on ocean circulation model output along the NL shelf break (Han et al., 2008) and over the Scotian shelf break (Han et al., 1997). The mean transport of the Labrador Current along the NL shelf break is 13 Sv ( $1 \text{ Sv} = 10^6 \text{ m}^3 \text{ s}^{-1}$ ) with a SD of 1.4 Sv, and the mean transport of the Scotian shelf break current is 0.6 Sv with a SD of 0.3 Sv. The mean transport values will be updated as new model output becomes available. The SD values will be updated as knowledge on nominal depth improves.

The Labrador Current transport along the NL shelf break was out of phase with that of the Scotian shelf break current for most of the years over 1993–2022 (Figure 38). The transport over the NL shelf break

was strong in the early- and mid-1990s, weak in the mid-2000s and early-2010s, and became strong again in late 2010s. In contrast, the transport over the Scotian shelf break fluctuated in a nearly opposite way. The Labrador Current transport index was positively and negatively correlated with the winter NAO index over the NL and Scotian shelves breaks, respectively.

In 2022 the annual-mean transport of the Labrador Current over the Labrador and northeastern Newfoundland Slope ceased the weakening trend that began in 2019 and became over one standard deviation above normal. The transport on the Scotian Slope in 2022 was normal only for the second time since 2014 (the other being 2019). All years since 2014 were negative.

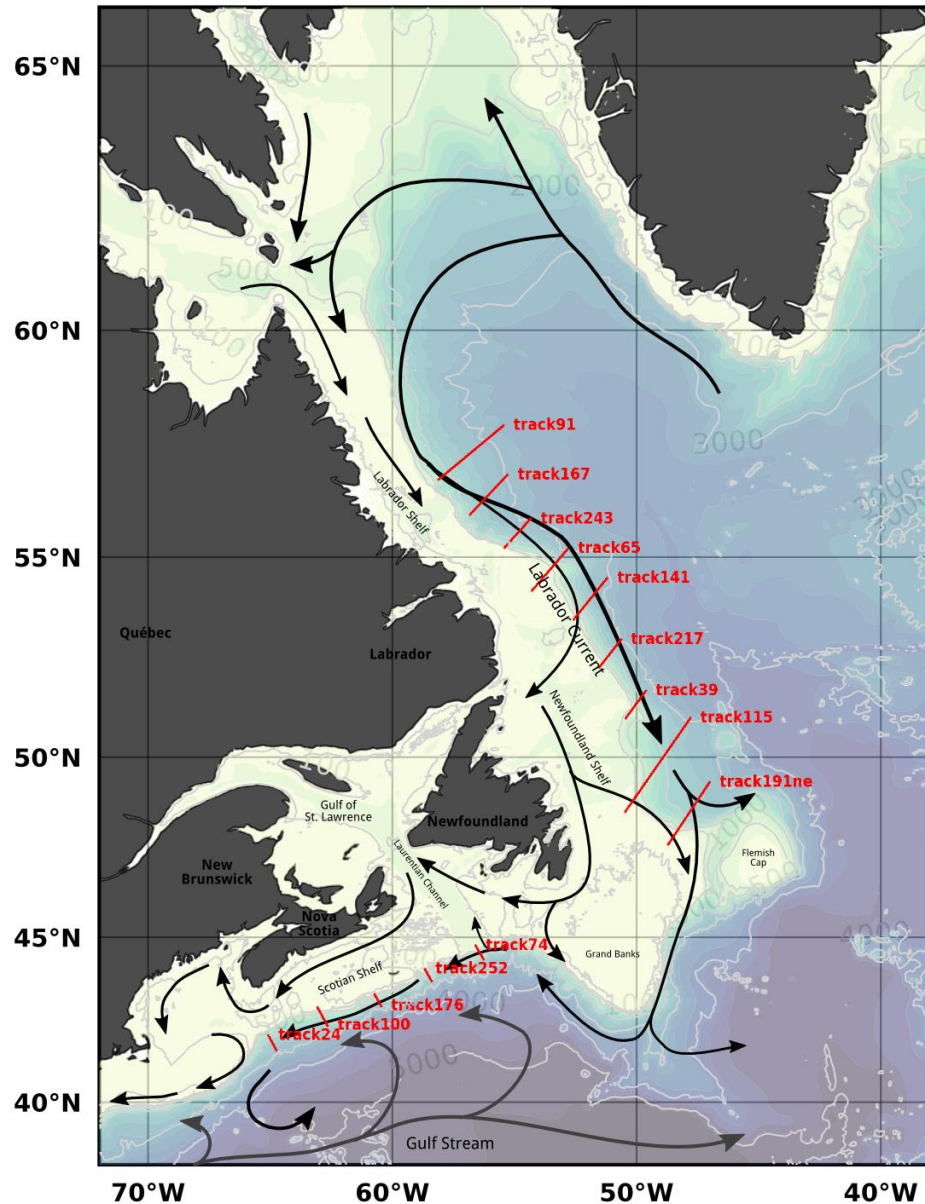


*Figure 37: Map showing the Northwest Atlantic bottom topography (depth contour values in light gray) and schematic flow patterns (arrows). The transport is calculated across the cross-slope sections (red lines) identified by their satellite ground tracks numbers. The series of northern tracks are used for the Labrador Current calculation on the NL shelf, while the series of tracks in the south are used for the Scotian shelf break current transport.*

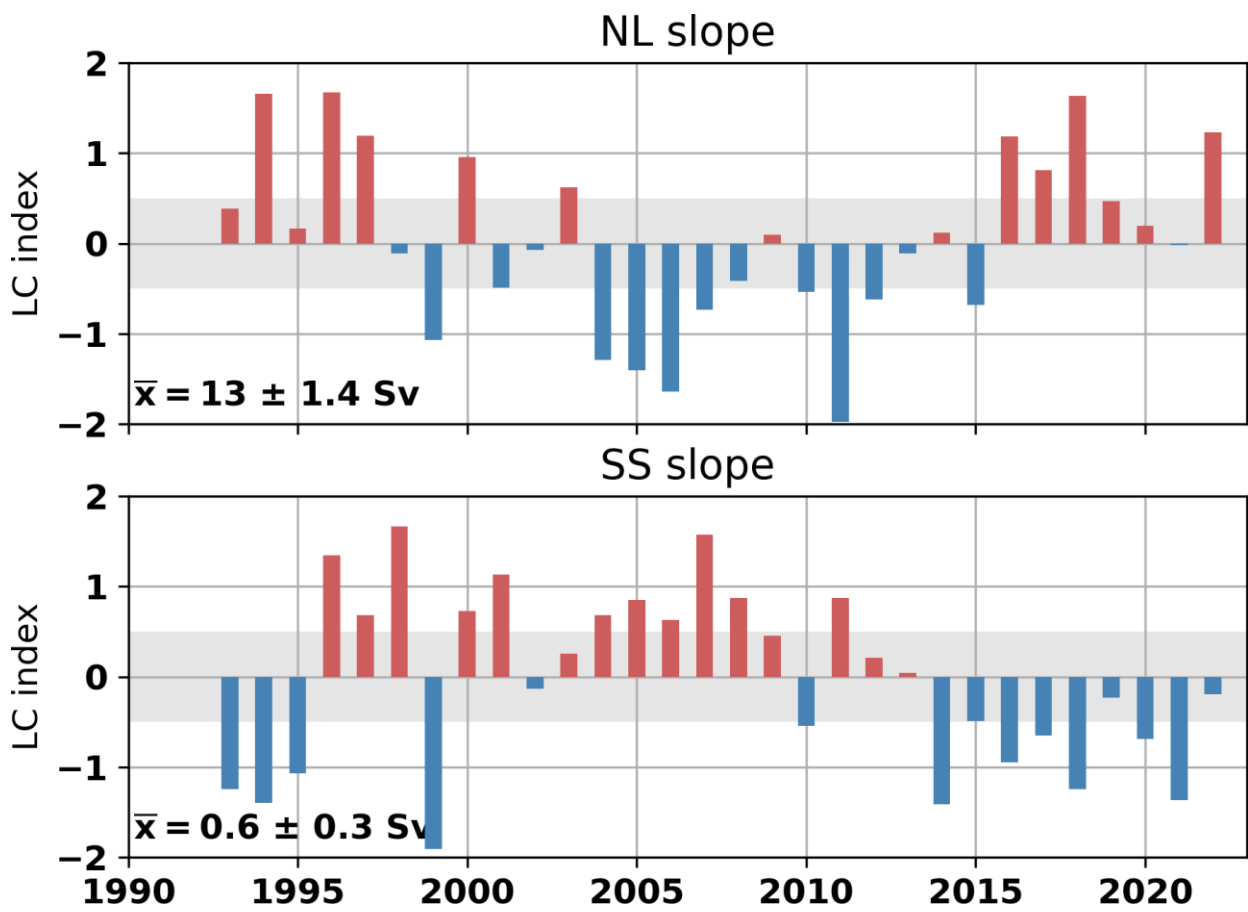


Figure 38: Normalized index of the annual-mean transport of the Labrador Current on the NL shelf break (top) and Scotian shelf break (bottom). Long-term averages over 1993–2022 (with standard deviation) are  $13 \pm 1.4 \text{ Sv}$  for the Labrador Current and  $0.6 \pm 0.3 \text{ Sv}$  for the Scotian shelf break current. Shaded gray areas represent the  $\pm 0.5 \text{ SD}$  range considered “normal”.

# 8 Summary

The NL climate index (NLCI; Cyr & Galbraith, 2021), summarizes selected time series discussed throughout this report (Figure 39). The NLCI runs between 1951 to present, and is updated annually. This index is presented here in the form of a scorecard followed by a stacked bar plot of 10 equally weighted time series:

- Winter NAO index (starts in 1951; see Figure 3);
- Air temperatures at five sites (starts in 1950; see Figure 6);
- Sea ice season duration and maximum area for the northern Labrador, southern Labrador and Newfoundland shelves (starts in 1969; see Figure 12)
- Number of icebergs crossing 48°N (starts in 1950; see Figure 13);
- SSTs in NAFO Division 2GHJ3KLNOP (starts in 1982; see Figure 15);
- Vertically averaged temperature at Station 27 (starts in 1951; see Figure 18);
- Vertically averaged salinity at Station 27 (starts in 1951; see Figure 18);
- CIL core temperature at Station 27 (starts in 1951; see Figure 20);
- Summer CIL areas on the hydrographic sections Seal Island, Bonavista Bay and Flemish Cap (starts in 1950; see Figure 29); and
- Spring and fall bottom temperature in NAFO Divisions 3LNOPs and 2HJ3KLNO, respectively (starts in 1980; see Figure 36).

The NLCI can be interpreted as a measure of the overall state of the climate system with positive values representing warm and fresh conditions with less sea-ice and conversely negative values representing cold and salty conditions. It replaces the *Composite Environmental Index* (CEI) presented in similar reports on NL physical conditions until recently (e.g., Cyr et al., 2019).

The NLCI highlights the different climate regimes prevailing since the early 1950s. For example, the relatively warm 1960s were followed by cold conditions in the early 1970s and most importantly from the mid-1980s to the mid-1990s which was the coldest decade on record. The warming trend from the early 1990s that peaked in 2010 was followed by recent cooling that culminated in 2015. While the NLCI for years 2016 to 2019 were normal (with a certain spread between positive and negative anomalies), the NLCI has been positive since 2020, including the warmest year on record in 2021 (+1.5). In 2022, the NLCI was at +0.7. The NLCI and its subindices are available at <https://doi.org/10.20383/101.0301> [consulted 2023-10-04] (Cyr & Galbraith, 2020).

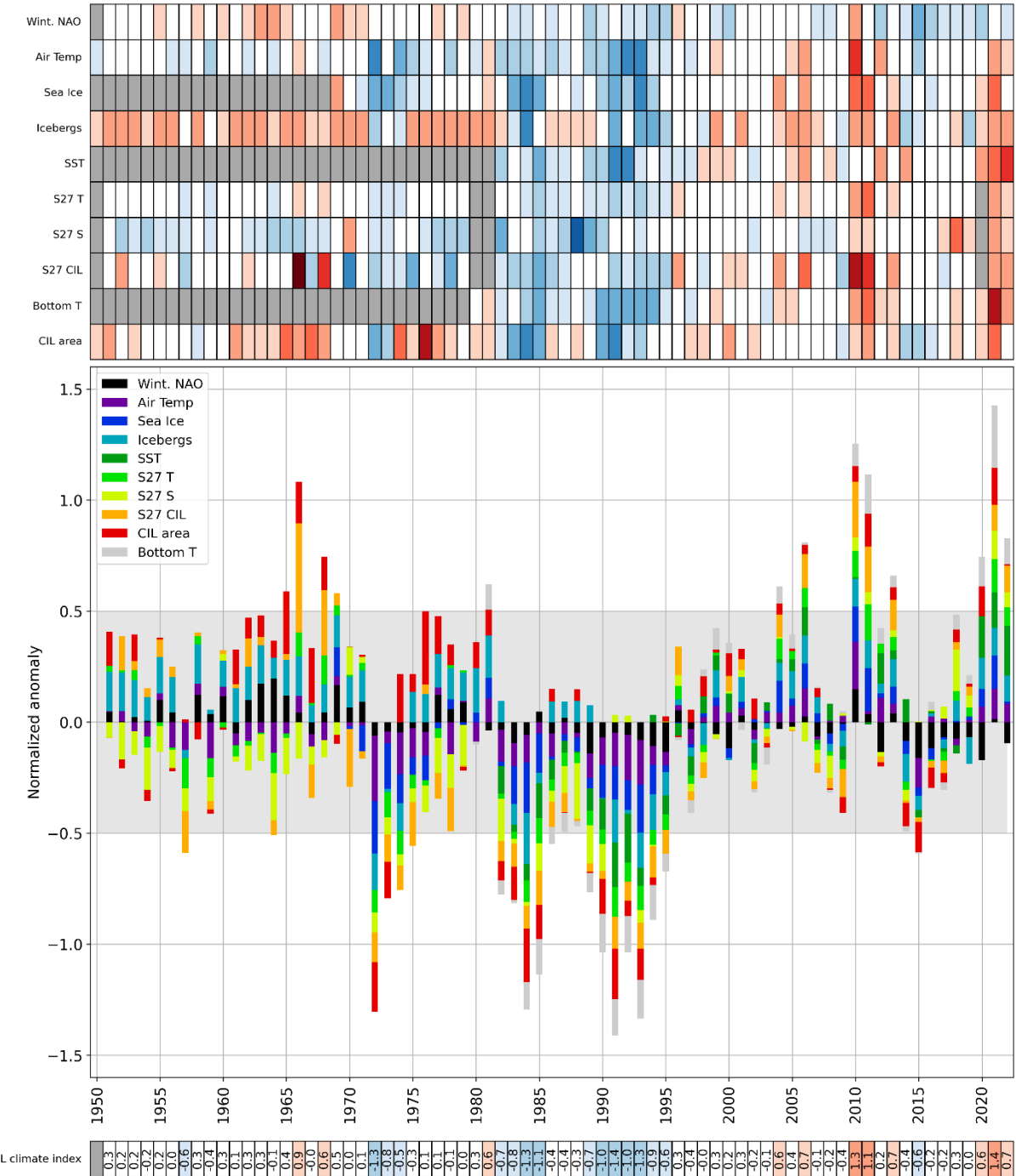


Figure 39: Newfoundland and Labrador climate index derived by averaging the normalized anomalies of various time series presented in this report. The scorecard in the top panel represents the 10 subindices used to construct the climate index, color-coded according to their value (blue negative, red positive, white neutral). The sign of some indices (NAO, ice, icebergs, salinity and CIL volume) has been reversed when positive anomalies are generally indicative of colder conditions. Grey cells in the scorecards indicate the absence of data. The central panel represents the climate index in a stacked-bar fashion, in which the total length of the bar is the average of the respective subindices and in which their relative contribution to the average is adjusted proportionally. The scorecard at the bottom of the figure shows the color-coded numerical values of the climate index.

## **8.1 Highlights of 2022**

- Based on the NL climate index, 2022 was overall warm at +0.7.
- Except for winter NAO (positive, thus indicative of colder conditions), sea ice (normal) and CIL area (normal), all sub-indices of the NLCI showed warm anomalies.
- Sea surface temperatures were at record-warm values over the zone (beating 2021), also establishing new monthly and seasonal records across the different NAFO divisions.
- The bottom temperatures averaged over the spring (3LNOPs) and fall (3KLNO) were the third warmest of the time series after 2021 and 2011 (series started in 1980), although with some uncertainties due to incomplete surveys.
- The transport on the Scotian Slope was normal for the second time only since 2014 (last time was in 2019). On the NL slope, the transport was back to positive anomalies after three years being normal.

## **9 Acknowledgements**

This work is a contribution to the scientific program of the Atlantic Zone Monitoring Program. We thank the many scientists and technicians at the Northwest Atlantic Fisheries Centre for collecting and providing much of the data contained in this analysis and the Marine Environment Data Section of Fisheries and Oceans Canada in Ottawa for providing most of the historical data. We also thank the captain and crew of the RV Atlantis and RRS James Cook for oceanographic data collection during the spring and fall of 2022, respectively. We thank Heather Andres and David Hebert for reviewing the document.

# References

- Colbourne, E., Holden, J., Craig, J., Senciall, D., Bailey, W., Stead, P., & Fitzpatrick, C. (2015). Physical Oceanographic Conditions on the Newfoundland and Labrador Shelf During 2014. *DFO Can. Sci. Advis. Sec. Res. Doc.*, 2015/053, v + 37 p.
- Colbourne, E., Narayanan, S., & Prinsenberg, S. (1994). Climatic changes and environmental conditions in the Northwest Atlantic, 1970-1993. *ICES Journal of Marine Science Symposia*, 198, 311–322.
- Coyne, J., Cyr, F., Donnet, S., Galbraith, P. S., Geoffroy, M., Hebert, D., Layton, C., Ratsimandresy, A., Snook, S., Soontiens, N., & Walkusz, W. (2023). Canadian Atlantic Shelf Temperature-Salinity (CASTS). *Federated Research Data Repository*. <https://doi.org/10.20383/102.0739>
- Cyr, F., Bourgault, D., & Galbraith, P. S. (2011). Interior versus boundary mixing of a cold intermediate layer. *Journal of Geophysical Research, in Press*. <https://doi.org/10.1029/2011JC007359>
- Cyr, F., Colbourne, E., Holden, J., Snook, S., Han, G., Chen, N., Bailey, W., Higdon, J., Lewis, S., Pye, B., & Senciall, D. (2019). Physical Oceanographic Conditions on the Newfoundland and Labrador Shelf during 2017. *DFO Can. Sci. Advis. Sec. Res. Doc.*, 2019/051, iv + 58 pp. <http://waves-vagues.dfo-mpo.gc.ca/Library/362068.pdf>
- Cyr, F., & Galbraith, P. S. (2020). Newfoundland and Labrador climate index. In *Federated Research Data Repository*. <https://doi.org/10.20383/101.0301>
- Cyr, F., & Galbraith, P. S. (2021). A climate index for the Newfoundland and Labrador shelf. *Earth System Science Data*, 13(5), 1807–1828. <https://doi.org/10.5194/essd-13-1807-2021>
- Cyr, F., & Galbraith, P. S. (2022). Newfoundland-Labrador Shelf. Ch. 4.3. In C. González-Pola, K. M. H. Larsen, P. Fratantoni, & A. Beszczynska-Möller (Eds.), *ICES Report on Ocean Climate 2020* (p. 121 pp.). ICES Cooperative Research Reports No. 356.
- Cyr, F., Snook, S., Bishop, C., Galbraith, P. S., Chen, N., & Han, G. (2022). Physical Oceanographic Conditions on the Newfoundland and Labrador Shelf during 2021. *DFO Can. Sci. Advis. Sec. Res. Doc.*, 2022/040, iv + 48 p. [http://www.dfo-mpo.gc.ca/csas-sccs/Publications/ResDocs-DocRech/2016/2016\\_079-eng.html](http://www.dfo-mpo.gc.ca/csas-sccs/Publications/ResDocs-DocRech/2016/2016_079-eng.html)
- Cyr, F., Snook, S., Bishop, C., Galbraith, P. S., Pye, B., Chen, N., & Han, G. (2021). Physical Oceanographic Conditions on the Newfoundland and Labrador Shelf during 2019. *DFO Can. Sci. Advis. Sec. Res. Doc.*, 2021/017, iv + 52 pp. <http://waves-vagues.dfo-mpo.gc.ca/Library/362068.pdf>
- Dickson, R. R., Meincke, J., Malmberg, S. A., & Lee, A. J. (1988). The “great salinity anomaly” in the northern North Atlantic 1968–1982. *Progress in Oceanography*, 20(2), 103–151.
- Doubleday, W. G. (1981). Manual on groundfish surveys in the Northwest Atlantic. In *NAFC*

*Sco. Coun. Studies* 2 (p. 56 p.).

- Drinkwater, K. F., Myers, R. A., Pettipas, R. G., & Wright, T. L. (1994). Climatic data for the Northwest Atlantic: the position of the shelf/slope front and the northern boundary of the Gulf Stream between 50°W and 75°W, 1973–1992. *Canadian Data Report of Fisheries and Ocean Sciences*, 125, iv +103 p.
- Florindo-López, C., Bacon, S., Aksenov, Y., Chafik, L., Colbourne, E., & Penny Holliday, N. (2020). Arctic ocean and hudson bay freshwater exports: New estimates from seven decades of hydrographic surveys on the Labrador shelf. *Journal of Climate*, 33(20), 8849–8868. <https://doi.org/10.1175/JCLI-D-19-0083.1>
- Galbraith, P. S., Chassé, J., Shaw, J., Dumas, J., Lefaivre, D., & Bourassa, M. (2023). Physical Oceanographic Conditions in the Gulf of St . Lawrence during 2022. *Canadian Technical Report of Hydrography and Ocean Sciences*, 354, v+88p.
- Galbraith, P. S., Larouche, P., Caverhill, C., Galbraith, P. S., Larouche, P., & Sea-surface, C. C. A. (2021). A Sea-Surface Temperature Homogenization Blend for the Northwest Atlantic A Sea-Surface Temperature Homogenization Blend for the. *Canadian Journal of Remote Sensing*, 47(4), 554–568. <https://doi.org/10.1080/07038992.2021.1924645>
- Han, G., Chen, N., & Ma, Z. (2014). Is there a north-south phase shift in the surface Labrador Current transport on the interannual-to-decadal scale? *Journal of Geophysical Research: Oceans*, 119(1), 276–287. <https://doi.org/10.1002/2013JC009102>
- Han, G., Hannah, C. G., Loder, J. W., & Smith, P. C. (1997). Seasonal variation of the three-dimensional mean circulation over the Scotian Shelf. *Journal of Geophysical Research: Oceans*, 102(1), 1011–1025. <https://doi.org/10.1029/96jc03285>
- Han, G., Lu, Z., Wang, Z., Helbig, J., Chen, N., & de Young, B. (2008). Seasonal variability of the Labrador Current and shelf circulation off Newfoundland. *Journal of Geophysical Research*, 113(C10), C10013. <https://doi.org/10.1029/2007JC004376>
- Hebert, D., Layton, C., Brickman, D., & Galbraith, P. S. (2023). Physical Oceanographic Conditions on the Scotian Shelf and in the Gulf of Maine during 2022. *Canadian Technical Report of Hydrography and Ocean Sciences*, 359, vi + 81 p. <http://www.dfo-mpo.gc.ca/csas-sccs/csas-sccs@dfo-mpo.gc.ca>
- ICNAF. (1978). List of ICNAF Standard Oceanographic Sections and Stations. *ICNAF Selected Papers Number 3*, 109–117. <https://doi.org/10.1111/j.1949-8594.1914.tb16026.x>
- International Ice Patrol. (2020). *International Ice Patrol Annual Count of Icebergs South of 48 Degrees North, 1900 to Present, Version 1*. <https://doi.org/10.7265/z6e8-3027>
- Kerr, R. A. (2000). A North Atlantic Climate Pacemaker for the Centuries. *Science*, 288(5473), 1984–1985.
- McDougall, T. J., & Barker, P. M. (2011). *Getting started with TEOS-10 and the Gibbs Seawater (GSW) Oceanographic Toolbox* (Issue May). SCOR/IAPSO WG127.

- Petrie, B., Akenhead, S. A., Lazier, S. A., & Loder, J. (1988). The cold intermediate layer on the Labrador and Northeast Newfoundland Shelves, 1978–86. *NAFO Science Council Studies*, 12, 57–69.
- Petrie, B., Pettipas, R. G., & Petrie, W. M. (2007). An Overview of Meteorological, Sea Ice and Sea-Surface Temperature Conditions off Eastern Canada during 2006. *Canadian Science Advisory Secretariat, 2007/022*, iv + 38pp.
- Theriault, J. C., Petrie, B., Pepin, P., Gagnon, J., Gregory, D., Helbig, J., Herman, A., Lefavre, D., Mitchell, M., Pelchat, B., Runge, J., & Sameoto, D. (1998). Proposal for a northwest zonal monitoring program. *Canadian Technical Report of Hydrographic and Ocean Sciences*, 194, vii + 57 p.
- Thyng, K. M., Greene, C. A., Hetland, R. D., Zimmerle, H. M., & DiMarco, S. F. (2016). True colors of oceanography: Guidelines for effective and accurate colormap selection. *Oceanography*, 29(3), 9–13. <https://doi.org/10.5670/oceanog.2016.66>
- Vincent, L. A., Wang, X. L., Milewska, E. J., Wan, H., Yang, F., & Swail, V. (2012). A second generation of homogenized Canadian monthly surface air temperature for climate trend analysis. *Journal of Geophysical Research*, 117(D18110). <https://doi.org/10.1029/2012JD017859>